

DISSERTATION ZUR ERLANGUNG DES DOKTORGRADES
DER FAKULTÄT FÜR BIOLOGIE
DER LUDWIG-MAXIMILIANS-UNIVERSITÄT MÜNCHEN

**A systematic analysis of Epstein-Barr virus genes and their
individual contribution to virus production and composition
reveals critical downstream functions**



Yen-Fu Adam Chen

Datum der Einreichung: 23.02.2021

Datum der mündlichen Prüfung: 10.11.2021

Erstgutachter: Prof. Dr. Bettina Kempkes

Zweitgutachter: Prof. Dr. Heinrich Leonhardt

Eidesstattliche Versicherung

Hiermit erkläre ich an Eides statt, dass die vorliegende Arbeit mit dem Titel

„A systematic analysis of Epstein-Barr virus genes and their individual contribution to virus production and composition reveals critical downstream functions“

von mir selbstständig und ohne unerlaubte Hilfsmittel angefertigt wurde, und ich mich dabei nur der ausdrücklich bezeichneten Quellen und Hilfsmittel bedient habe. Die Arbeit wurde weder in der jetzigen noch in einer abgewandelten Form einer anderen Prüfungskommission vorgelegt.

München, 23.02.2021

Yen-Fu Adam Chen

Some of my results in this thesis have been published or are available as pre-print

1. Manuel Albanese*, **Yen-Fu Adam Chen***, Corinna Hüls, Kathrin Gärtner, Takanobu Tagawa, Ernesto Mejias-Perez, Oliver T. Keppler, Christine Göbel, Reinhard Zeidler, Mikhail Shein, Anne K. Schütz, Wolfgang Hammerschmidt. Micro RNAs are minor constituents of extracellular vesicles and are hardly delivered to target cells. *bioRxiv* 2020.05.20.106393; <https://doi.org/10.1101/2020.05.20.106393>
2. Mickaël Bouvet, Stefanie Voigt, Takanobu Tagawa, Manuel Albanese, **Yen-Fu Adam Chen**, Yan Chen, Devin N. Fachko, Dagmar Pich, Christine Göbel, Rebecca L. Skalsky, Wolfgang Hammerschmidt. Multiple viral microRNAs regulate interferon release and signaling early during infection with Epstein-Barr virus. *mBio*, in press, *bioRxiv* 2020.12.03.393306; <https://doi.org/10.1101/2020.12.03.393306>
3. S. Danisch, C. Slabik, A. Cornelius, M. Albanese, T. Tagawa, **Y.A. Chen**, N. Krönke, B. Eiz-Vesper, S. Lienenklaus, A. Bleich, et al. Spatiotemporally skewed activation of programmed cell death receptor 1-positive T cells after Epstein-Barr virus infection and tumor development in long-term fully humanized mice. *Am. J. Pathol.*, 189 (2019), pp. 521-539. <https://doi.org/10.1016/j.ajpath.2018.11.014>

* shared first authorship

Table of Contents

<i>Abstract</i>	4
<i>Introduction</i>	5
Epstein-Barr virus and its characteristics	5
The EBV genome, its replication and steps that lead to virus synthesis	6
Medical need of a preventive EBV vaccine	7
Different strategies of designing an EBV vaccines	8
Studying EBV protein functions can contribute to EBV vaccine development.....	9
Scope and aim of my thesis.....	10
<i>Results</i>	12
A prophylactic EBV vaccine candidate under development and the question of its optimized production.	12
EBV expression plasmids library with 78 individual viral genes.....	14
Effects of individual EBV genes on virus titers	18
Certain viral genes increase or decrease virus titers	20
Measuring viral bioparticle concentrations using Elijah cells	21
Subgroups of viral genes increase or decrease the concentration of bioparticles upon ectopic expression.....	24
Physical particle concentration of virus stocks.....	24
Certain viral genes increase or decrease particles numbers	27
Statistical analysis and correlation of three parameters characterizing functional virus release, bioparticles and physical particles.....	28
Expression timing of viral genes does not affect the three analyzed parameters of virus stocks	32
Only one out of ten selected viral genes associated with elevated bioparticle numbers improves infectivity of viral stocks together with BALF4.....	32
Selection of 24 viral genes that elevate or repress bioparticle concentration.....	33
Design and validation of 78 shRNA candidates targeting 24 viral and control genes.....	34
Validation of knockdown efficacies of 24 transcript mimics representing viral targets in stably shRNA-transduced 2089 EBV producer cells	38
Analysis of virus titers in supernatants from 2089 EBV producer cell lines stably transduced with 24 sets of shRNAs directed against selected EBV transcripts.....	38

Changes of virus titers in supernatants from EBV producer cell lines stably transduced with shRNAs directed against ‘high bin’ and ‘low bin’ viral transcripts	41
Ectopic expression and shRNA knockdown of viral genes and transcripts – comparing bioparticle concentration of 24 viral targets.....	42
Analysis of the fusogenic activity of 24 virus stocks upon ectopic expression of individual viral genes from the ‘high bin’ and ‘low bin’ groups	44
Incorporation of CD63:Blam slightly improves the virus titer.....	48
A novel assay to detect and quantify cellular fusion of extracellular particles with primary human cells and various established cell lines.....	48
Subpopulations of peripheral blood mononuclear cells differ in their uptake of the CD63:Blam reporter protein delivered by engineered EVs.....	49
Without VSV glycoprotein, EVs can barely deliver the CD63:Blam reporter protein to 17 different cell lines	50
<i>Discussion</i>	53
The problem of EBV yield and virus quality	53
The impact of individual EBV genes on virus yield and virus quality	53
76 EBV genes and their contribution to virus titers.....	55
Bioparticle concentration profiles after ectopic expression of 76 single EBV genes.....	56
Quantification of physical particle concentration of the 76 EB virus stocks	56
High correlation between the three characteristic parameters of virus stocks	57
No distinct category of protein function contributes significantly to virus titer, bioparticle concentration or number of physical particles.	57
Expression of BALF4 together with selected viral genes does not enhance virus titers with one exception	58
shRNA mediated knockdown of 24 selected viral transcripts identifies essential and dispensable viral genes	58
The shRNA strategy directed against genes of the ‘low bin’ group fails to identify a viral gene with regulatory functions controlling EBV’s lytic phase	60
Comparison of bioparticle concentration of virus stocks generated by ectopic expression of viral genes and stocks from shRNA expressing EBV producer cells.....	61
Quantitation of the fusogenic activity of EBV virions.....	61
Alternative application of the CD63:Blam fusion assay	63
<i>Materials and Methods</i>	64

References 73
Appendix 82
Curriculum Vitae110
Acknowledgements.....111
Epilogue.....113

Abstract

A vaccine to prevent infectious diseases associated with Epstein-Barr virus (EBV) has been put forward decades ago but has not made it to the clinic yet. EBV is a very complex herpes virus and its complexity, uncertainties about viral antigenic targets and technical difficulties to establish and mass-produce viral mutants are major obstacles. To mimic the complexity of the virus which encompasses more than 80 proteins, virus-like particles (VLPs) have a high potential as a vaccine prototype. To explore conditions to optimize and improve virus production, I established and tested an EBV gene library with 78 expression plasmids and a set of designed shRNAs investigating the functions of individual viral genes in the context of virus synthesis. Engineered virus stocks were then systematically characterized with respect to virus titers, bioparticle and physical particle concentration and virus uptake by primary human B cells, EBV's target cells *in vivo*. To quantitate virus uptake by these cells, I developed a novel β -lactamase-based assay that can monitor fusion events of the viral envelope with membranes of recipient cells at the level of single cells by flow cytometry. Together, my results identified several EBV genes such as BALF4, BVLF1 and BKRF4, encoding a viral glycoprotein, a regulator of transcription of late viral genes, and a possible tegument protein, respectively, that improve virus production regarding virus yield, virus composition and quality and virus uptake. My experiments also indicated that EBV does not encode a master gene that governs EBV synthesis dampening virus production, contrary to my initial working hypothesis. Conditional expression of viral genes that improve EBV production as identified in my work will likely enhance and improve yield, assembly and important functional parameters of VLPs (such as their efficient uptake by antigen presenting immune cells, for example) supporting the development of a much improved EB-VLP based vaccine candidate to be used for clinical development and testing.

Introduction

Epstein-Barr virus and its characteristics

Epstein-Barr virus (EBV) was discovered by Michael Anthony Epstein, Bert Geoffrey Achong and Yvonne Barr in samples of Burkitt's lymphoma biopsies in 1964 (Epstein et al., 1964). EBV belongs to the large of herpesviruses and is also known as human herpesvirus 4 (HHV4) (Albà et al., 2001). Together with EBV, human herpesviruses encompass 9 members including herpes simplex 1 (HHV-1), herpes simplex 2 (HHV-2), varizella-zoster virus (VZV, HHV-3), human cytomegalovirus (HCMV, HHV-5), human herpesvirus 6A, 6B, (HHV-6A, HHV-6B), human herpesvirus 7 (HHV-7) and Kaposi sarcoma-associated herpesvirus (KSHV, HHV-8) besides EBV, which are further classified into three subfamilies, alpha, beta and gamma. These pathogens can cause a wide range of different infectious diseases, but many infections in early childhood go unnoticed (Davison, 2007). A hallmark of all herpesviruses is their 'lifestyle' characterized by predominantly latent infections *in vivo* and *in vitro*. Latency means that the infected target cells carry viral genome copies, which are epigenetically repressed such that no or only a very restricted set of viral genes is expressed preventing immune recognition as well as virus *de novo* synthesis. Only upon reactivation, the latently infected cells turn into virus factories which release progeny.

Since its discovery, EBV has been implicated in several life-threatening malignancies, which include Burkitt's lymphoma, Hodgkin's lymphoma and nasopharyngeal carcinoma, among others. Primary infection with EBV usually takes place in early childhood and is asymptomatic. In industrialized countries, first encounter with EBV is often delayed until adolescence and young adulthood, but then infection with EBV can lead to Infectious Mononucleosis (IM) in up to 50 % of all individuals (Faulkner et al., 2000). EBV targets mainly mature human B cells and epithelial cells. The virus enters via a viral glycoprotein complex consisting of three members, gH/gL/gp42, which bind to HLA class II molecules after viral adhesion to the prevalent CD21 surface receptor on B cells via gp350, a very abundant glycoprotein on the viral envelope. Paradoxically, entry of EBV into epithelial cells, which lack HLA class II molecules is hampered by gp42 and the expression of only gH/gL provides the tropism for epithelial cells (Möhl et al., 2016; Sathiyamoorthy et al., 2016).

EBV's canonical infection route starts with EB virions in the oropharynx that make their way through the mucosal layers of epithelial cells to infect B cells present in lymphoid tissues such as lymphnodes and tonsils. How EBV traverses the epithelial layer is controversial. The newly infected B cells express an incomplete set of lytic

and latent genes but are incapable of releasing infectious virions. This phase is termed pre-latent phase (Faulkner et al., 2000; Taylor et al., 2015; Buschle and Hammerschmidt, 2020) and leads to a stable latent infection in B cells, preferentially memory B cells with a long lifespan, eventually. Stable latent infection is supported by a very much reduced expression of viral antigens to evade immune recognition. In B cells, EBV persists lifelong in its human host. Only upon terminal differentiation of latently infected B cells to plasma cells, which can ensue upon antigen encounter, plasma cells turn into virus producing cells releasing infectious virions.

The EBV genome, its replication and steps that lead to virus synthesis

In latently infected B cells, several copies of the EBV genome are maintained as extrachromosomal plasmids or mini-chromosomes. The plasmid copies replicate in synchrony with the host cell in S phase. DNA replication of the EBV genomic copies initiates at the origin of DNA synthesis recognized as *oriP* which governs viral replication of the entire genome during latency (Aiyar et al., 1998). In this phase, the expression of viral genes is strictly limited. When the virus reactivates from latency and the lytic phase of infection initiates, viral genes such as BZLF1 and BRLF1 (also known as Zta and Rta, respectively) are expressed to start the expression of the early class of viral genes. Thus, BZLF1 and BRLF1 are categorized as immediate early genes (Murata and Tsurumi, 2014) and both gene products are able to switch on the lytic phase of EBV's life cycle (Feederle et al., 2000). BZLF1 is a very interesting virally encoded transcription factor, which has properties of a pioneer factor (Zaret and Mango, 2016) and can revert epigenetic repression of EBV DNA fostering expression of viral lytic genes (Buschle et al., 2019; Schaeffner et al., 2019). Upon initial expression of BZLF1 and BRLF1, mainly BZLF1 induces the expression of the class of early viral genes, which are essential for autonomous viral DNA replication during EBV's lytic phase. These genes include the viral DNA polymerase encoded by BALF5, a single-stranded DNA-binding protein encoded by BALF2, a DNA polymerase processivity factor encoded by BMRF1 and a primase-helicase complex, formed by three viral proteins encoded by BSLF1, BBLF4 and BBLF2/3 (Fixman et al., 1992; Sugimoto et al., 2019). Together with BZLF1 (Schepers et al., 1993), this group of replication factors initiates lytic DNA replication at *oriLyt*, the lytic origin of DNA replication (Hammerschmidt and Sugden, 1988) in an asynchronous manner to yield massive concatemers of newly replicated viral DNA, which serve as templates for transcription of late viral genes and are cleaved and subsequently packaged into preformed viral capsids in the nucleus.

To support the following wave of late viral genes, which encompass mainly viral structural and tegument proteins, the viral BcRF1 gene product is essential. It

encodes a viral TATA-box like DNA binding protein, which binds to promoters of late viral genes to enable efficient expression of all late proteins (Wyrwicz and Rychlewski, 2007). Additionally, BGLF3, BDLF4, BVLF1, BDLF3.5 and BFRF2 are essential for supporting lytic gene expression (Aubry et al., 2014). The EBV structural proteins are critical for synthesizing viral components that sustain the integrity of virion morphogenesis. A complex, which comprises the major capsid protein (BcLF1), the minor capsid protein (BFRF3), a scaffold protein (BdRF1), a protease (BVRF2) together with two minor capsid proteins (BDLF1 and BORF1) was found to be essential for nucleocapsid assembly and maturation (Henson et al., 2009; Wang et al., 2011, 2015).

Although many viral structural proteins are known, there are still multiple unsolved questions. Virus formation, nuclear export of DNA-filled capsids, their first and second envelopment at nuclear and cytoplasmic membranes, respectively, and the release and egress of mature virions from cells require many prior steps such as viral DNA packing and capsid assembly in the nucleus of lytically infected cells. BBRF1 acts as a portal protein, which guides the amplified viral DNA into preformed, but empty capsids in the nucleus. In the absence of BBRF1 and BMRF1 viral DNA cannot be delivered and packaged (Pavlova et al., 2013; Sugimoto et al., 2019). Moreover, BFRF1A, BGRF1 and BVRF1 are directly or indirectly linked to viral DNA packing (Visalli et al., 2019) and BFLF2, BFRF1, BSRF1 and BBRF2 have been identified to be necessary for viral DNA loading and processing to unit length genomes (Farina et al., 2005; Granato et al., 2008; Masud et al., 2019; Yanagi et al., 2019). Overall, the EBV genome encodes more than 80 proteins, which can be classified into different categories based on various criteria. Certain functions have been discovered and are known but the functions of many more viral gene products are still vague, hypothetical or completely unknown.

Medical need of a preventive EBV vaccine

Primary infection of EBV in childhood is mostly asymptomatic, but if primary infection takes place later during adulthood and adolescence, it can cause Infectious Mononucleosis (IM), leading to fever, fatigue and lymphadenopathy with a low rate of acute complications such as spleen rupture and airway obstructions. In addition, IM increases the risk of developing Burkitt's lymphoma, Hodgkin's lymphoma and multiple sclerosis later in life (Faulkner et al., 2000) and IM is also involved in progression of gastric cancer and nasopharyngeal carcinoma (Li et al., 2018). The post-transplant lymphoproliferative disease (PTLD) is a major problem as EBV-negative organ transplant patients are vulnerable to PTLD because they are immunosuppressed and thus lack an efficient cellular immunity to control EBV infected B

cells. Clearly, the call for a prophylactic EBV vaccine to prevent IM and its sequelae and other EBV-associated consequences of infection is becoming more and more important.

Different strategies of designing an EBV vaccines

The glycoproteins of EBV play critical roles during virus infection and are interesting targets of virus-neutralizing antibodies. The major gp350 glycoprotein binds to CD21 on B cells to promote cell adhesion and the trimeric gH/gL/gp42 complex interacts with MHC class II molecules initiating uptake of the virus into endosomes prior to membrane fusion. Moreover, gp42 has been identified to support infection of epithelial cells. Another glycoprotein encoded by the BALF4 gene is a gB homologue (Neuhierl et al., 2009) and promotes viral fusion. As the main target of a subunit vaccine, gp350 has been utilized as antigen and vaccine drug substance. Clinical studies showed that the recombinant gp350 vaccine can reduce the rate of IM, if the vaccine was applied prior to first infection with EBV. The recombinant gp350 vaccine proceeded to a phase 2 clinical trial by Glaxo Smith Kline (Cohen, 2015). Although the vaccine was found capable of reducing the incidence of IM, its lacking potency to prevent EBV infection led to a halt of its further clinical development (Sokal et al., 2007). So far, there have been many other approaches targeting different antigens of EBV. An EBNA3A epitope vaccine was found to be able to induce CD8⁺ T-cell response and is in a phase 1 trial (Elliott et al., 2008). Our group is currently in the process of developing an EBV vaccine with the primary indication to prevent IM. Its drug substance is virus-like particles (VLPs) that lack viral DNA and EBV oncogenes such that they cannot propagate infection and cellular transformation. EB-VLPs are morphologically and biochemically identical to EB virions and thus encompass about 50 different viral proteins and potential antigens (Johannsen et al., 2004). In a pre-clinical mouse model, VLPs could elicit strong CD4⁺ and CD8⁺ T-cell responses besides antibodies reactive against a broad spectrum of viral proteins (Ruiss et al., 2011). These EB-VLPs were engineered by deleting essential packaging signal sequences on genomic viral DNA together with viral oncogenes that pose a risk. An alternative approach to generate EB-VLPs is the deletion of BFLF1/BFRF1A, which encode DNA packaging functions and gB to prevent infection together with enhanced BNRF1 expression. This experimental VLP vaccine demonstrated protection against EBV infection in a humanized mouse model (Zyl et al., 2018; van Zyl et al., 2019).

Studying EBV protein functions can contribute to EBV vaccine development

Several approaches have been proposed to develop vaccines against EBV associated disease on the basis of virus-like particles (VLPs), but the key question of their efficient production has not been addressed and their practical availability and efficacy are uncertain. It is in particular unclear if the cellular host, the HEK293 cell line established a long time ago (Russell et al., 1977) optimally supports expression of all lytic EBV genes as well as morphogenesis and egress of viral particles as these cells are very distant to EBV's genuine host cell. In an EBV infected human host, EBV infects resting B cells in a latent manner. Only upon terminal differentiation of latently infected B cells, plasma cells are thought to be the source of infectious virus (Laichalk and Thorley-Lawson, 2005). The selection of HEK293 cells as an EBV host and EBV synthesis *in vitro* dates back to pioneering work by my laboratory in 1998, when the entire EBV genome was cloned onto a bacterial artificial chromosome, a BACmid, which is also called maxi-EBV (Delecluse et al., 1998). Cloning of EBV as a BACmid was a technical achievement, but it was more challenging to identify a cell that would support virus synthesis upon induction of EBV's lytic cycle. Among the many established cell lines tested, only HEK293 cells turned out to support virus *de novo* synthesis (personal communication). In fact, the search for a better suited cell that promotes efficient virus synthesis has failed so far (unpublished data).

Moreover, the functions of most EBV genes and their products with respect to virus *de novo* synthesis and the biology of the host cell are not known or unclear. Consequently, my thesis is designed to study individual viral functions using a plasmid library of >75 EBV genes cloned into an expression plasmid. Single viral genes are tested upon their ectopic expression in the established 2089 EBV producer cell line and concomitant with induction of EBV's lytic phase followed by detailed analyses of the resulting composition of viral particles and their functionality. Knowing the contribution of single EBV genes might open opportunities to enhance and improve virus yield and the quality of viral particles with respect to their function, fusion and antigenicity.

Regarding one aspect of functional virions, their fusion with target cells is a critical and potentially limiting step. Thus, I devoted some of my PhD work developing means to monitor membrane fusion between the viral envelope and cellular membranes and adapted such an assay. Its principle was shown in the field of HIV research in 2002 (Cavrois et al., 2002; Jones and Padilla-Parra, 2016), but it has not been introduced into the field of herpesviruses. I developed this assay further to quantify EBV fusion events at the level of single cells as a new parameter of analysis.

Clearly, vaccine preparations containing infectious EB virion are unsuitable as

vaccine candidates, but synthesis of intact, fully infectious EBV, its morphogenesis, egress and basic viral functions are proxies for VLP production. This is because production of both infectious virions and virus-like particles follow identical technical, cellular and viral principles. In contrast to infectious EB virions, studying VLPs is a rather cumbersome endeavor because a detailed investigation of their numbers, their biochemical composition and their uptake by target cells require sophisticated and very time-consuming assays.

Scope and aim of my thesis

For more than 20 years now HEK293 cells have been instrumental to produce recombinant EBV stocks. The identification of this cell line as a source of infectious EB virions was pure serendipity since the cells are very distant to cells that produce EBV progeny *in vivo*. Nevertheless, HEK293 cells have remained the only usable source to generate recombinant EBV stocks so far. No systematic analysis has addressed the fundamental question whether virus yield with respect to virus concentration, virion composition and functionality can be improved while using these EBV producer cells. It was my task to tackle this question and to apply and establish (novel) assays to characterize these important parameters in the field of herpesvirology.

Practically, I generated EB virus stocks from the 2089 EBV producer cells line 2089 after ectopic expression of single EBV genes. They stem from an expression plasmid library that I curated for my particular needs here in this project. Alternatively, I adopted an shRNA technology to repress selected viral transcripts in the cells to knockdown specific viral genes of interest. The virus stocks were further characterized (**Figure 1**) regarding their physical particle concentration using a nanoparticle tracking analysis (NTA) instrument. The bioparticle concentrations were measured in an Elijah cell binding assay quantitating bound virion particles on the cell surface. Human primary B cells were incubated with engineered, CD63:β-lactamase-equipped EB virions and their fusogenic activities were subsequently analyzed by flow cytometry. Raji cells were utilized as a tool to determine the virus titer of the EB virus stocks. Flow cytometry detected the fraction of cells that express green fluorescence protein (GFP) encoded by recombinant EBV derivatives indicative of viral infection, the endpoint of the infectious route. Information derived from this PhD work is potentially useful to unravel the contributions of single viral genes and their encoded EBV proteins to efficient virus production. This information is also crucial to optimize EBV as well as VLP yield and the composition of infectious virions and non-infectious virus-like particles for further studies or applications.

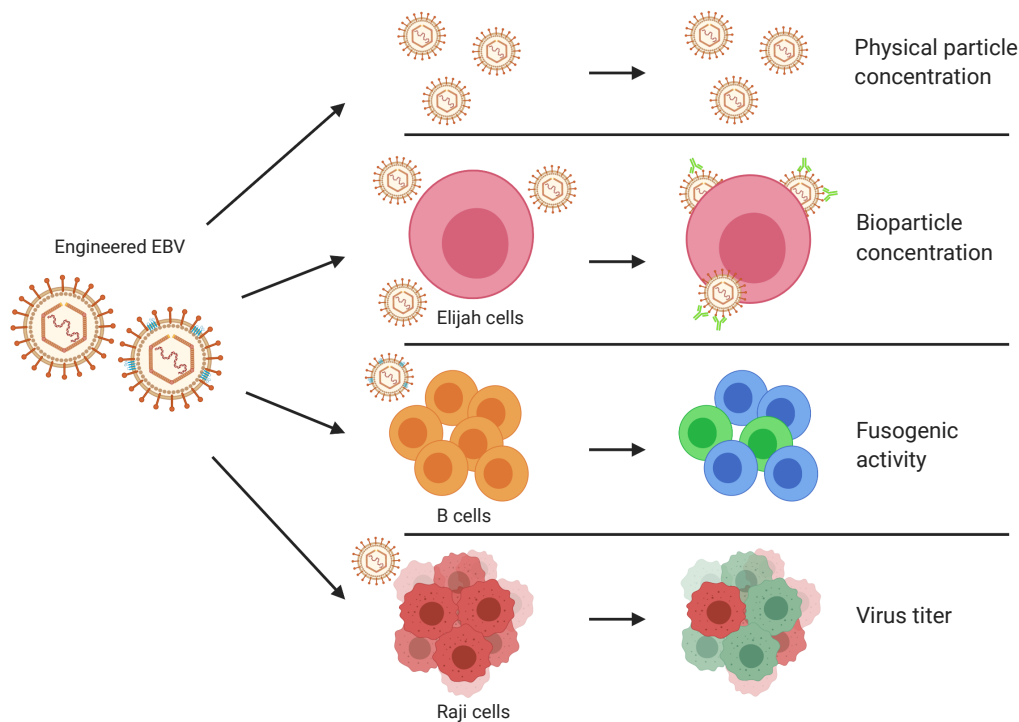


Figure 1. Overview of the experimental strategy of analyzing the composition of engineered EBV stocks and their virus-cell interactions.

EBV stocks are obtained from the stable EBV producer cell line 2089 after transient transfection of an expression plasmid encoding the viral activator BZLF1. Supernatants of the cells containing infectious virus were collected after three days. Engineered EB viruses were obtained by co-transfection of BZLF1 together with an individual expression plasmid from a panel of 76 different EBV genes to study their effects on quality and quantity of the ensuing EBV stocks. Alternatively, the EBV producer cell line was transfected with a plasmid encoding a reporter gene, CD63:β-lactamase, to equip virus particles with an enzyme to study viral fusion with target cells. In yet another setting the EBV producer cell line was stably transduced with shRNAs to control certain selected viral transcripts and study the effects of their knockdown on virus production and composition. Different individual virus stocks were analyzed with the aid of three different target cells (Elijah cells, primary B cells, Raji cells) and their *physical particle concentration* was quantified using nanoparticle tracking analysis (NTA) instrument, ZetaView PMX110. Elijah cells were used to assess *bioparticle concentration* in the virus stocks via cell surface binding and subsequent analysis of bound particles by flow cytometry. Virus particles engineered to contain the CD63:β-lactamase reporter protein were analyzed for their *fusogenic activity* with human primary B cells as targets again by flow cytometry. Finally, Raji cells were incubated with virus stocks to measure the *virus titer*, i.e., the concentration of infectious virus particles which confer expression of green fluorescence protein gene (GFP) in the infected cells as measured by flow cytometry. The four read-outs form the core of my analytics and address the main aims of my PhD thesis.

Results

A prophylactic EBV vaccine candidate under development and the question of its optimized production.

Since the first recombinant BLLF1 (gp350) subunit vaccine was developed to prevent EBV infection and EBV-associated diseases, there have been several attempts to develop alternative vaccines (Epstein et al., 1985). The most advanced vaccine development by Glaxo Smith Kline (GSK), also based on an adjuvanted gp350 protein formulation, reached phase II clinical testing with a medium efficacy preventing Infectious Mononucleosis. The trial was abandoned for unknown reasons in 2007, but several academic and commercial initiatives are known, which have announced pre-clinical and clinical testing of diverse candidate EBV vaccines (Moutschen et al., 2007; Sokal et al., 2007; Cohen et al., 2013). All of them are based on subunit vaccines and many are centered on viral glycoproteins with the idea to evoke EBV-neutralizing antibodies in the vaccinees. One of the most advanced vaccine candidates is probably by Moderna, Inc. and builds on this company's mRNA technology according to a recent press release¹.

My laboratory and the laboratory of Henri-Jacques Delecluse put forward a very different idea of a preventive EBV vaccine that relies on virus-like particles (VLPs) of Epstein-Barr virus as the drug substance (Ruiss et al., 2011; van Zyl et al., 2019). EB-VLPs mimic the composition of EB virions and their complexity which encompasses more than 50 viral proteins (Johannsen et al., 2004). In pre-clinical assays, formulations with EB-VLPs as a complex antigen cocktail induced both humoral and cellular immune responses directed against a multitude of viral antigens and epitopes (Ruiss et al., 2011).

The generation of EB-VLPs is based on stable HEK293 cell-derived clones that carry an engineered EBV genome in a latent fashion. The cells can be propagated and expanded at will and can be induced to produce and release VLPs into the cells' supernatant. Since the VLPs must not propagate viral infection, EBV genomes contained in such EB-VLP producer cells need to be genetically modified to meet this mandatory criterion. The genetic modifications are achieved by targeted genetic alterations in *E. coli* cells that carry a recombinant EBV genome as a bacterial artificial chromosome. The BACmid, which is also termed 'maxi-EBV' is maintained as a single copy plasmid per *E. coli* cell. My laboratory pioneered this approach

¹ <https://investors.modernatx.com/news-releases/news-release-details/moderna-announces-progress-prophylactic-vaccines-modality-cmv/>

(Delecluse et al., 1998), established the first EB-VLPs (Delecluse et al., 1999) and improved the recombinering technology (Pich et al., 2019) based on two genetic approaches in *E. coli* (Wang et al., 2009; Warming et al., 2005).

With this technology at hand (Delecluse et al., 2008; Feederle et al., 2010) it is possible to alter the genetic composition of the EBV genome in *E. coli* such that it encodes all components of EB-VLPs but is non-infectious after its reconstitution in HEK293 cells. For example, the cis-acting packing signals of viral DNA can be deleted or essential viral genes that encode packaging functions can be disabled to achieve this aim (Hettich et al., 2006; Delecluse et al., 1999; Pavlova et al., 2013). The alterations of EBV's genetic composition ensure that EB-VLPs will be devoid of viral genomic DNA (among other modifications that contribute to safety and immunogenicity) when reconstituted in the next step. The maxi-EBV DNA is then isolated and purified from *E. coli* and stably introduced into HEK293 cells, which give rise to EB-VLPs upon induction of EBV's lytic phase. Lytic induction is generally achieved by transient transfection of an expression plasmid that encodes BZLF1, a viral gene and genetic switch that induces virus production in latently EBV infected cells upon its induced expression (Hammerschmidt and Sugden, 1988; Delecluse et al., 1998).

Virus-like particles are ideal candidates for an EBV vaccine and are a promising strategy for EBV vaccine development (Hellebrand et al., 2006; Ruiss et al., 2011; Pavlova et al., 2013) because EB-VLPs likely induce robust immune responses against many EBV components and are capable of establishing antiviral effector T cells. To optimize VLP production, i.e., to increase their yield, improve their composition and uptake by EBV's target cells and immune cells, it would be helpful to understand viral gene regulation, virion assembly, morphogenesis and egress during virus production. It is not clear, for example, if the process of EBV production is efficient or can be further improved because HEK293 cells are not the genuine viral host cells in a human organism. Therefore, my aim and plan were to identify possible means to improve EBV and VLP production in HEK293 cells. EBV as a fully infectious agent is clearly easier to trace and to quantify than EB-VLPs that lack the genetic information of the virus. Once identified in the EBV model working with infectious virus, means and measures to improve virus yield could similarly be applied to HEK293 cells that support EB-VLP production. This is because both EBV and EB-VLP production follow identical viral principles.

My basic approach was first to test all known single EBV genes in a HEK293 cell line termed 2089 that carries the B95-8 strain of EBV as published earlier (Delecluse et al., 1998). Subsequently, I validated and refined my results using different read-outs as shown in **Figure 1** to characterize the functions of selected individual genes

further. Lastly, I adapted a fusion assay to the needs of my PhD work. Together with Manuel Albanese, I invented this general approach in a different project while working with extracellular vesicles (EVs) (Albanese et al., 2020). The source of all individual EBV genes cloned into a basic expression plasmid backbone was a library and repository of expression plasmids established by Dr. Josef Mautner. I used this library, modified the open reading frames to ensure proper expression of their unmodified viral genes and studied the consequences of introducing 78 individual expression plasmids in the platform cell line 2089 concomitantly with inducing EBV's lytic cycle. I generated and tested the virus stocks to monitor the consequences of ectopic expression of all individual viral genes on the production of particles, concentration of infectious virions and viral characteristics using different functional analytical parameters as shown in **Figure 1**.

EBV expression plasmids library with 78 individual viral genes

The 78 individual viral genes in the EBV expression library were provided by Dr. Josef Mautner (**Table 1**). Certain viral genes have attracted much interest by virologists and colleagues from the EBV field. For example, BZLF1, BALF4 and BLLF1 have been studied intensively and their biological functions have been documented in detail (Janz et al., 2000; Neuhierl et al., 2002; Busse et al., 2010; Schaeffner et al., 2019). Besides these very well-known and almost famous viral genes, there are still many EBV genes with unsettled, even enigmatic functions.

With this EBV expression plasmid library, I was able to investigate potential functions of these genes using single gene expression plasmids. Since the plasmid library was established to express and purify single viral proteins from HEK293 cells after transient DNA transfection, all proteins are fused to epitope tags in the original plasmid library. This means that I had to remove these additional epitope tags, namely 6xHis and EBNA1 antibody tags, at the C-terminus of the open reading frames of all 76 expression plasmids as described in Materials and Methods in more detail. The purpose of this step was to express the original and unmodified viral proteins because several viral fusion proteins with compromised functions are known.

Table 1. Overview of 78 EBV genes regarding their identity, classification in five functional classes and their expression timing

Gene	Identity	Related Function	Early/Late phase ¹
A73	Protein A73	Unknown	TBD
BALF1	Apoptosis regulator BALF1	Non-structural protein	E
BALF2	Single-stranded DNA-binding protein	DNA or Capsid associated	E
BALF3	DNA packaging terminase subunit 2	DNA or Capsid associated	L
BALF4	Envelope glycoprotein B	Membrane protein	L
BALF5	DNA polymerase catalytic subunit	DNA or Capsid associated	E
BARF1	Homolog of the human proto-oncogene c-fms	Membrane protein	E
BaRF1	Ribonucleotide reductase subunit 2	Non-structural protein	E
BBLF1	Myristylated tegument protein	Tegument	L
BBLF2/BBLF3	Helicase-primase subunit	DNA or Capsid associated	E
BBLF4	Helicase-primase helicase subunit	DNA or Capsid associated	E
BBRF1	Capsid portal protein	DNA or Capsid associated	L
BBRF2	Tegument protein UL7	Tegument	L
BBRF3	Envelope glycoprotein M	Membrane protein	L
BcLF1	Major capsid protein	DNA or Capsid associated	L
BCRF1	Interleukin-10	Non-structural protein	TBD
BcRF1	Viral TATA box binding protein	DNA or Capsid associated	L
BDLF1	Capsid triplex subunit 2	DNA or Capsid associated	L
BDLF2	Envelope glycoprotein 48	Membrane protein	L
BDLF3	Envelope glycoprotein 150	Membrane protein	L
BDLF3.5	Protein UL91	Unknown	TBD
BDLF4	Protein UL92	Non-structural protein	TBD
BdRF1	Capsid scaffold protein	DNA or Capsid associated	L
BFLF1	DNA packaging protein UL32	DNA or Capsid associated	TBD
BFLF2	Nuclear egress lamina protein	DNA or Capsid associated	TBD
BFRF1	Nuclear egress membrane protein	DNA or Capsid associated	E
BFRF1A	DNA packaging protein UL33	DNA or Capsid associated	TBD
BFRF2	Protein UL49	Unknown	TBD
BFRF3	Small capsid protein	DNA or Capsid associated	L
BGLF1	DNA packaging tegument protein UL17	DNA or Capsid associated	L
BGLF2	Tegument protein UL16	Tegument	L
BGLF3	Protein UL95	Tegument	TBD
BGLF3.5	Tegument protein UL14	Tegument	TBD

Gene	Identity	Related Function	Early/Late phase ¹
BGLF4	Tegument serine/threonine protein kinase	DNA or Capsid associated	E
BGLF5	Deoxyribonuclease	DNA or Capsid associated	E
BGRF1/BDRF1	DNA packaging terminase subunit 1	DNA or Capsid associated	TBD
BHLF1	Protein BHLF1	DNA or Capsid associated	E
BHRF1	Apoptosis regulator BHRF1	Non-structural protein	E
BILF1	Membrane protein BILF1	Membrane protein	L
BILF2	Membrane protein BILF2	Membrane protein	L
BKRF2	Envelope glycoprotein L	Membrane protein	L
BKRF3	Uracil-DNA glycosylase	Non-structural protein	E
BKRF4	Tegument protein G45	Tegument	L
BLLF1	Glycoprotein 350	Membrane protein	L
BLLF2	Protein BLLF2	Unknown	TBD
BLLF3	Deoxyuridine triphosphatase	Non-structural protein	E
BLRF1	Envelope glycoprotein N	Membrane protein	L
BLRF2	Virion protein G52	Tegument	L
BLRF3	Unknown	Unknown	TBD
BMLF1	EB2	DNA or Capsid associated	E
BMRF1	DNA polymerase processivity subunit	DNA or Capsid associated	E
BMRF2	Envelope protein UL43	Membrane protein	L
BNLF2a	Protein BNLF2a	Non-structural protein	E
BNLF2b	Protein BNLF2b	Unknown	TBD
BNRF1	Tegument protein G75	Tegument	L
BOLF1	Tegument protein UL37	Tegument	L
BORF1	Capsid triplex subunit 1	DNA or Capsid associated	L
BORF2	Ribonucleotide reductase subunit 1	Non-structural protein	E
BPLF1	Large tegument protein	Tegument	L
BRLF1	Protein Rta	DNA or Capsid associated	IE
BRRF1	Protein G49	DNA or Capsid associated	E
BRRF2	Tegument protein G48	Tegument	TBD
BSLF1	Helicase-primase primase subunit	DNA or Capsid associated	E
BSLF2/BMLF1	Multifunctional expression regulator	DNA or Capsid associated	E
BSRF1	Tegument protein UL51	Tegument	L
BTRF1	Tegument protein UL88	Tegument	TBD
BVLF1	Protein UL79	Unknown	TBD
BVRF1	DNA packaging tegument protein UL25	DNA or Capsid associated	L
BVRF2	Capsid maturation protease	DNA or Capsid associated	L

Gene	Identity	Related Function	Early/Late phase ¹
BXLF1	Thymidine kinase	Non-structural protein	E
BXLF2	Envelope glycoprotein H	Membrane protein	L
BXRF1	Nuclear protein UL24	Unknown	TBD
BZLF1	Protein Zta	DNA or Capsid associated	IE
BZLF2	Envelope glycoprotein 42	Membrane protein	L
LF1	Protein G10	Non-structural protein	TBD
LF2	Virion protein G11	Non-structural protein	TBD
RPMS1	Protein RPMS1	Unknown	TBD
sLF3	Protein LF3	Unknown	TBD

¹: E, early; IE, immediate early; L, late; TBD: to be determined.

The table was adapted according to overviews published in (Cai et al., 2017; Johannsen et al., 2004; Young et al., 2007)

Effects of individual EBV genes on virus titers

After restoring the integrity of 76 viral genes in the expression plasmid library, each plasmid was assigned a distinctive number in the institute's database (Appendix, **Table 6**). To test all members of this plasmid library, 6.5×10^5 EBV producer cells of the 2089 cell line carrying a recombinant EBV B95-8 strain genome with a green fluorescence protein gene were seeded in 6-well cluster plates (Delecluse et al., 1998). After overnight cultivation, the medium was exchanged with 2 ml fresh exosome-depleted (ex⁻) medium (see Materials and Methods for its preparation and formulation). The cells were transiently co-transfected with 0.5 μ g p509 plasmid DNA encoding the BZLF1 gene together with 0.5 μ g plasmid DNA encoding one of the 76 individual viral genes. 0.5 μ g p509 and 0.5 μ g pCMV vector DNAs, the 'empty' expression vector plasmid were co-transfected as control and reference for subsequent normalization. BZLF1 serves as the fundamental gene to induce EBV's lytic cycle in the 2089 EBV producer cells. BALF4 encoded by the plasmid p6515 is the viral gB (glycoprotein B) homologue, which is found in all herpesviruses and was used as a positive control (Neuhierl et al., 2002). The standard protocol to produce virus stocks with the 2089 EBV producer cell line builds on transient transfection of the BZLF1 encoding expression plasmid p509, an approach which was established in my laboratory (Delecluse et al., 1998). After three days, the virus supernatants were harvested and partially purified using filters with 1.2 μ m mesh size. 1×10^5 Raji cells, a human Burkitt's lymphoma cell line, were incubated with 5 μ l EBV virus stocks for 3 days. EBV infected Raji cells were identified by green fluorescence protein expression and quantified by flow cytometry. All experiments were done in triplicates. The results from infection experiments with three independent sets of virus stocks were normalized to the respective controls, which were set to one. The ratios of the 76 tested combinations plus the two controls were arranged in descending order (**Fig. 2**). The viral BALF4 gene, which encodes the gB glycoprotein of EBV was co-transfected with BZLF1 served as a positive control. BALF4 has been shown previously to generate highly infectious virus stocks in a similar experimental setup (Neuhierl et al., 2002). As shown in **Figure 2A** the genes contained in the plasmid library were sub-grouped according to viral functional classes as in **Table 1** and color-coded as follows – green: DNA or capsid-associated protein; red: membrane protein; brown: tegument protein; blue: non-structural protein; grey: protein with unknown functions (**Fig. 2A**). To relate the results to expression timing of the individual genes, the readouts were color-coded according to three criteria as follows – red: early viral gene; blue: late viral gene; grey: viral gene with unknown temporal expression kinetics (**Fig. 2B**).

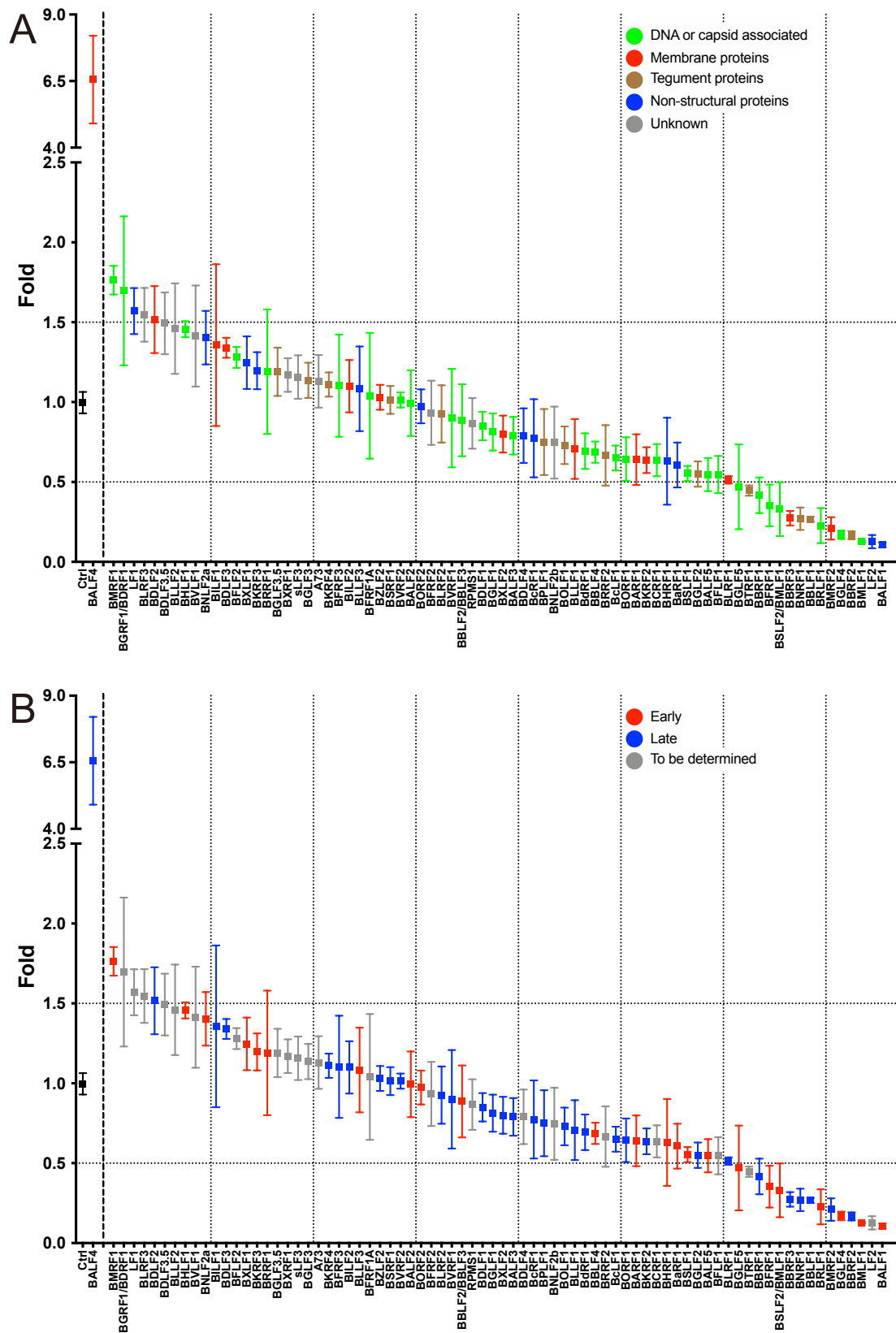


Fig. 2 Comparison of the virus titer of samples generated by co-transfection of BZLF1 together with expression plasmids from a panel of 76 EBV genes plus two controls.

6.5x10⁵ EBV producer cells (2089) were seeded in 6-well cluster plates. After overnight cultivation, the

cell medium was exchanged with 2 ml exosome-depleted (ex) medium (see Materials and Methods) followed by transient transfection of the cells with the BZLF1 expression plasmid p509 in combination with single expression plasmids from a panel of 76 individual EBV genes cloned into the pCMV plasmid backbone. The virus supernatants were harvested 3 days after transfection and filtrated using 1.2-micron filters. 1×10^5 Raji cells were incubated with 5 μ l harvested virus supernatants. After three days, the infected Raji cells were investigated by flow cytometry (BD FACSCanto™) analyzing the expression of green fluorescence protein. The x-axes list the individual EBV genes transfected in combination with BZLF1. The BZLF1 (p509) expression plasmid co-transfected with p6816, an empty pCMV vector plasmid served as reference and control (Ctrl). The titers of infectious EBV stocks according to the percentage of GFP-positive Raji cells (GRU) were normalized to the reference sample (Ctrl), which was set to 1. The results are listed in descending order. **(A)** EBV genes are color-coded according to five functional groups. (i) green: DNA or capsid-associated proteins, (ii) red: membrane proteins, (iii) brown: tegument proteins, (iv) blue: non-structural proteins, and (v) grey: proteins with unknown functions. **(B)** The EBV genes are marked according to their early or late expression characteristics. (i) red: early, (ii) blue: late, and (iii) grey: viral genes with unknown expression timing. Mean and standard deviation of three biological replicates are shown. Horizontal 0.5- and 1.5-fold line are indicated. Dotted vertical lines indicate groups of 10 viral genes for better visualization.

Certain viral genes increase or decrease virus titers

The results in **Figure 2** indicated that co-transfection of BMRF1, BGRF1/BDRF1, LF1, BLRF3, BDLF2 or BDLF3.5 together with BZLF1 yielded mean virus titers, which were at or exceeding a factor of 1.5 indicating that only six genes yielded slightly higher virus titers than the negative control. Two genes encode DNA or capsid-associated proteins, one is a membrane protein, one is a non-structural protein, and two genes have unknown functions. No tegument protein encoding gene is among this list. According to expression timing among the six proteins that enhanced virus titers one is expressed early, one is expressed late and four have no known expression timing. It seems as if there is no clear attributable functional role nor a discrete expression timing within this group of six viral genes that led to higher virus infectivity of the virus stocks. The majority of viral genes tested, about 60 in total, are in a neutral zone with little variations to virus titers at around control level. In contrast, the last 15 plasmids co-transfected with BZLF1 and encoding BGLF5, BTRF1, BBRF1, BFRF1, BSLF2/BMLF1, BBRF3, BNRF1, BBLF1, BRLF1, BMRF2, BGLF4, BBRF2, BMLF1, LF2, and BALF1 led to virus titers lower than the control and reduced by a factor of 2 and more (**Fig. 2**). Seven genes in this group of viral factors with repressive functionality encode DNA or capsid-associated proteins, two are membrane proteins, four are tegument proteins and two are non-structural proteins suggesting that their presumably higher expression is contra-productive. Seven genes are expressed in the

early phase, whereas six genes are expressed in the late phase and two have no known expression timing. Again, there is no clear attributable functionality nor does expression timing seem to be a notable criterion.

Taken together, ectopic expression of the 76 individual viral genes resulted in small differences in the concentration of the virus stocks, only. The positive control BALF4 is clearly superior compared to the remaining tested viral genes and increases the infectivity of the virus stocks by a factor of 6.5. The viral BMRF1, BGRF1/BDRF1, LF1, BLRF3, and BDLF2 genes also support infectivity but only between 1.5- to 1.8-fold (**Fig. 2**). Remarkably, the B95-8 laboratory strain lacks the viral LF1 gene suggesting that it contributes a previously unknown but supportive functions during virus synthesis or enhances viral infectivity. A larger group of genes (n=15) exhibits repressive functions and shows a clear negative impact on virus synthesis or virus infectivity in this set of experiments.

Measuring viral bioparticle concentrations using Elijah cells

Viral infectivity as measured in **Figure 2** is the successful endpoint of the infectious route, which initiates with virus binding to target cells as the very first step. I measured this key function using a cellular binding assay as shown schematically in **Figure 1** using Elijah cells, a human B cell line derived from a case of Burkitt's lymphoma (Rowe et al., 1985).

The previously tested 76 EBV virus stocks plus appropriate controls were analyzed for viral particles binding to the surface of Elijah cells followed by flow cytometry using a fluorochrome-coupled monoclonal antibody with a superior specificity against gp350, the abundant glycoprotein in the viral envelope (obtained from Helmholtz Zentrum Muenchen antibody core facility; unpublished). The data expressed as mean fluorescence intensity (MFI) values were calculated and normalized to the control and standard reference and termed 'bioparticle concentration' as illustrated in **Figure 1**. Elijah cells and individual virus stocks were incubated for a limited time at low temperature to allow rigid viral binding to the cells via glycoproteins on the viral envelope and Elijah cell surface receptors. Virus binding was detected with an gp350-specific, fluorochrome-coupled monoclonal antibody on live cells. Practically, 2×10^5 Elijah cells were incubated with 20 μ l virus stocks at 4 °C for 3 h. The fluorochrome-coupled gp350-specific antibody was added and the cells were analyzed by flow cytometry after appropriate washing steps. The raw values of MFI were recorded. Virus stocks generated with the 2089 EBV producer cells after co-transfection of an empty vector plasmid together with BZLF1 (p509) served as the reference control (Ctrl) and standard for calculating the ratios of MFI values as shown in **Figure 3A**. Virus stocks generated by co-transfection of the BALF4 encoding

Virus production and generation of samples were identical as described in Figure 2. The number of viral particles bound to Elijah cells was determined, which is an indirect measure of bound virions. The read-out is based on the binding of EBV particles to Elijah cells, a cancerous human B cell line, and the quantification of bound virus using a gp350-specific, fluorochrome-coupled monoclonal antibody by flow cytometry as described in Materials and Methods. The ratios of mean fluorescence intensity (MFI) values of individual samples versus the MFI value of the reference sample (Ctrl) were calculated and are provided on the y-axes. The x-axes list the transfected individual EBV genes in combination with BZLF1. An empty pCMV vector plasmid co-transfected with the BZLF1 plasmid p509 served as reference (Ctrl). Ratios are arranged in descending order. An expression plasmid encoding BALF4 served as a positive control. Shaded areas on the left and right flanks highlight groups of viral genes termed 'high bin' and 'low bin', respectively, encompassing 12 and 14 group members. Three singly highlighted genes (BPLF1, BBRF1, BGLF4) were randomly picked as further candidates tested later. **(A)** EBV genes are classified according to five functional groups and are color-coded. (i) green: DNA or capsid-associated proteins, (ii) red: membrane proteins, (iii) brown: tegument proteins, (iv) blue: non-structural proteins, and (v) grey: proteins with unknown function. **(B)** EBV genes are color-coded according to their early or late expression characteristics. (i) red: early, (ii) blue: late, and (iii) grey: viral genes with unknown expression timing. Mean and standard deviation of three biological replicates are shown. The horizontal lines indicate 0.5- and 1.5-fold ratios. Dotted vertical lines indicate groups of 10 viral genes for better visualization.

The most interesting result is the finding with a virus stock produced by co-transfection of BALF4 and BZLF1, which showed absolutely no difference in this assay **(Fig. 3)** in contrast to the previous set of experiments in **Figure 2**, when this virus stock revealed a substantially higher virus infectivity. The results prove that BALF4 is limiting in virions when virus synthesis is induced by transient expression of BZLF1, only, in 2089 EBV producer cells. The results also documented that BALF4 increased the quality of EBV virions but did not contribute to virion quantity. As I will show later, BALF4, which is EBV's glycoprotein B (gB) homologue present in all herpesviruses, is the essential fusogenic viral protein that promotes fusion of the virus envelope with membranes of the target cells.

The other virus stocks showed a very similar trend as already seen in **Figure 2**. Variances between differently produced virus stocks were detectable and ranged from about a factor of 1.5 to 0.5. Only a small group of 13 virus stocks (BSLF1 -> BMLF1) showed a reduction below a factor of 0.5. Identical to **Figure 2**, the color codes in **Figure 3A** illustrate the five functional groups of viral proteins. Again, no discrete functional characteristics was obvious suggesting that various gene functions contribute to viral bioparticles synthesis. When the results were color-coded according to gene expression timing regarding early, late genes or genes with

unknown timing, no special contribution of the three different classes could be found (**Fig. 3B**). This result suggests that various viral genes expressed throughout the entire lytic phase of virus production contribute to viral bioparticles biosynthesis. Certain viral genes can even reduce and repress bioparticle production.

Subgroups of viral genes increase or decrease the concentration of bioparticles upon ectopic expression

After data normalization, 60 virus stocks locate within a broad middle range in between factors of 0.5 to 1.5 with subtle differences among the different virus stocks (**Fig. 3**). BKRF4, BVLF1 and BNLF2a, which represent a tegument protein, a protein with unknown function and a non-structural protein, respectively, are top candidates here and are part of the 'high bin' group. BKRF4, BVLF1 and BNLF2a all belong to different groups regarding expression timing (**Fig. 3B**), but the three genes show a similar effect and increase bioparticle production by about 50 % compared to the control. Thirteen viral genes that decrease bioparticle concentration by a factor of 0.5 encompass BSLF1, BTRF1, LF1, BSLF2/BMLF1, BMRF2, BBRF3, BNRF1, BBLF1, BRLF1, BALF1, BBRF2, LF2 and BMLF1. Four genes among this class belong to DNA or capsid-associated proteins, two are membrane proteins, four are tegument proteins and three belong to the group of non-structural proteins. Based on expression timing, five genes are expressed early, five are expressed late and three have no known expression timing. Remarkably, virus stocks generated by ectopic expression of BALF1, BBRF2, LF2 and BMLF1 genes have a considerably reduced viral bioparticle concentrations in the order of 0.1, only, and lead the 'low bin' group of viral genes (**Figure 3**).

Physical particle concentration of virus stocks

The same virus stocks analyzed in **Figure 2** and **3** were investigated for their absolute number of physical particles by nanoparticle tracking analysis (NTA) using a ZetaView PMX110 instrument. All virus supernatant stocks were first diluted 50-fold with PBS to obtain a concentration in between 10^7 and 10^8 particles per ml. During analysis of the particles their movement by diffusion was recorded within 11 distinct spots in the chamber. Particle concentration of virus supernatant stocks was recorded and normalized to the control generated by co-transfection of BZLF1 and DNA of an empty plasmid vector (**Fig. 4**). Particle concentration in supernatants obtained after expression of the 76 viral genes plus two controls are arranged in descending order and the results are separated by vertical lines to obtain bins of 10 genes each for better visualization.

Remarkably and in accordance with results shown in **Figure 3** (bioparticle

concentration), virus stocks obtained after co-transfection of BALF4 and BZLF1 contained identical numbers of physical particles (**Fig. 4**). Particle concentration in the different virus stocks varied in between factors of 1.3 to 0.3. Certain virus stocks showed an inconsistent number of physical particles from one experiment to the next documented by their standard deviation (e.g., BcLF1, BVRF1, BGLF3.5, LF1 among others) for unknown reasons. At the low end of the data, reduction of physical particle concentration was moderate, only, very much in contrast to the results obtained in **Figures 2 and 3**, which depict viral infectivity and bioparticle concentration, respectively. It thus appears as if physical particle concentration and viral functions correlate moderately, only.

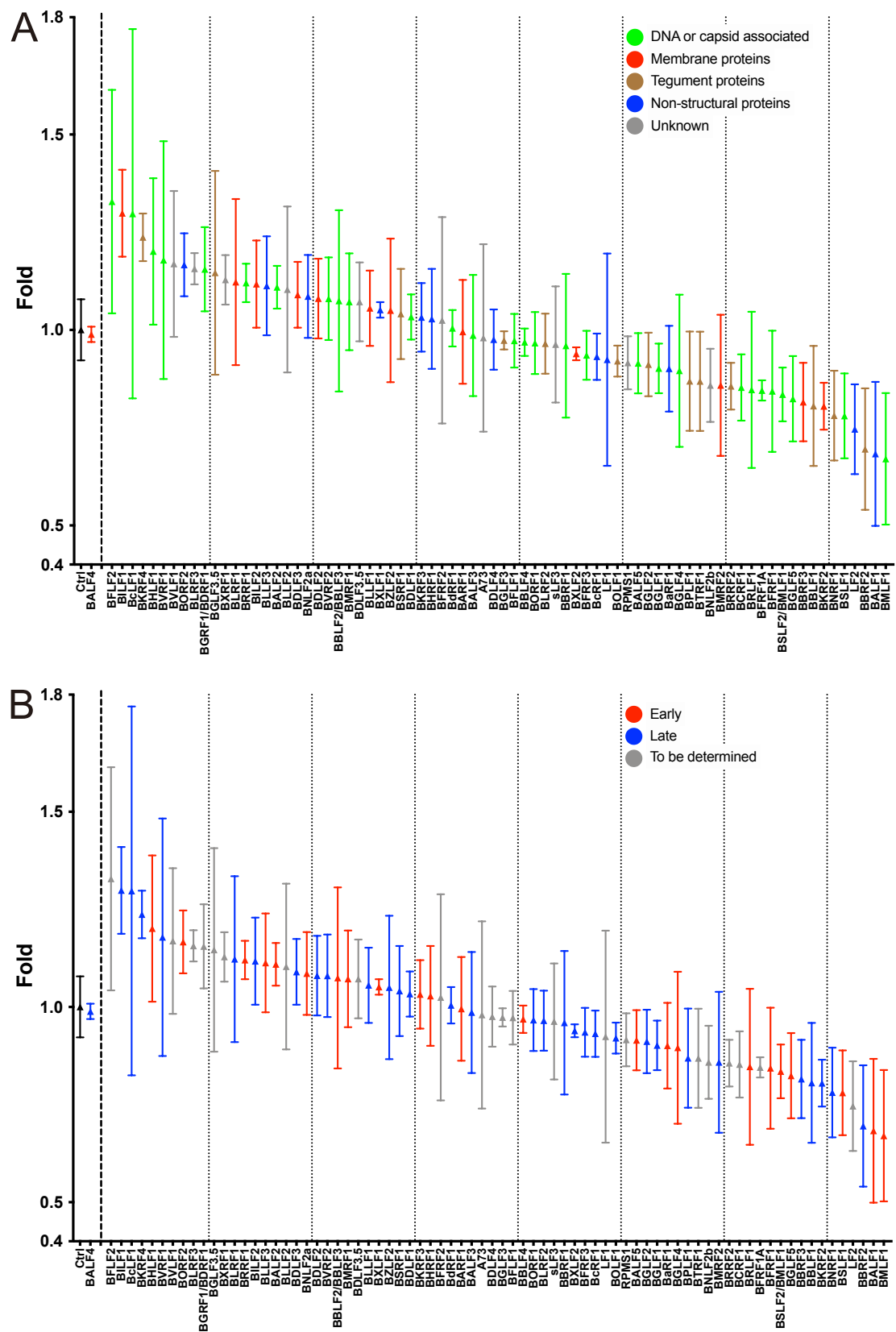


Fig. 4 Comparison of physical particle concentrations in virus samples generated by co-transfection of BZLF1 together with expression plasmids from a panel of 76 EBV genes including two controls.

Samples investigated in Figure 2 and 3 were analyzed here for their physical particle concentration by nanoparticle tracking analysis (NTA). NTA was performed with the ZetaView PMX110 instrument and the images were analyzed with the ZetaView 8.04.02 software. Standard calibration beads (102.7±1.3 nm) were used to confirm the range of linearity. 1 ml diluted supernatant samples were injected for analysis. Particle concentration and size were measured and documented. The x-axes list the transfected individual EBV genes in combination with BZLF1. An empty pCMV vector plasmid (p6816) plus the BZLF1 plasmid (p509) were co-transfected as reference (Ctrl). The positive control encompasses supernatants obtained after co-transfection of both BZLF1 and BALF4 expression plasmids. The number of physical particles in the range of 100 – 200 nm contained in the supernatants of cells were analyzed and normalized to the reference sample. The readouts are arranged in descending order. **(A)** EBV genes are classified according to five functional groups and color-coded. (i) green: DNA or capsid-associated proteins, (ii) red: membrane proteins, (iii) brown: tegument proteins, (iv) blue: non-structural proteins, and (v) grey: proteins with unknown functions. **(B)** EBV genes are marked according to their early or late expression characteristics. (i) red: early, (ii) blue: late, and (iii) grey: viral genes with unknown expression timing. Mean and standard deviation of three biological replicates are shown. The 0.5- and 1.5-fold line are indicated. Dotted vertical lines indicate groups of 10 viral genes for better visualization.

Notably, the virus stocks contained not only virus particles but also cell debris, sizeable protein aggregates as well as an unknown fraction of extracellular vesicles (EVs), all of which potentially contribute to physical particle numbers in this analysis. The instrument cannot distinguish real virus particles from other particle within the same size range and its dynamic range of measuring is limited to 10^7 to 10^8 particles/ml.

Certain viral genes increase or decrease particles numbers

The read-outs in the two panels of **Figure 4** are color-coded as in **Figures 2** and **3**. Ten genes are at the high end, five of which are associated with DNA or capsid functions, one is a membrane protein, one gene is a tegument protein, one is a non-structural protein and two have unknown functions. At the low end are 16 genes, eight of which are associated with DNA or capsid functions, two give rise to membrane proteins, four encode tegument proteins and two are non-structural proteins. Regarding expression timing, within the top 10 genes, 2 are expressed early, 4 are expressed late and the remaining have no known expression timing (**Fig. 4B**). In the group of 16 virus stocks, which have the lowest number of physical particles 7 are expressed early, 5 are expressed late and the expression timing of the remaining genes is unknown. No particular function appears to cluster in the virus stocks arranged in descending order. Also, expression timing does not yield an obvious color pattern suggesting that various viral genes expressed throughout the entire lytic

phase of virus production and egress can modulate the biosynthesis of physical particles as measured by the NTA instrument.

Statistical analysis and correlation of three parameters characterizing functional virus release, bioparticles and physical particles

The finding so far shown in **Figures 2 to 4** document the characteristics of three distinctive parameters obtained from 76 individual EBV stocks plus two controls. **Figure 2** shows infectious virus titers of stocks after co-transfection of BZLF1 and 76 individual EBV gene expression plasmids. **Figure 3** demonstrates the bioparticle concentration of these virus stocks whereas **Figure 4** indicates their physical particle concentration.

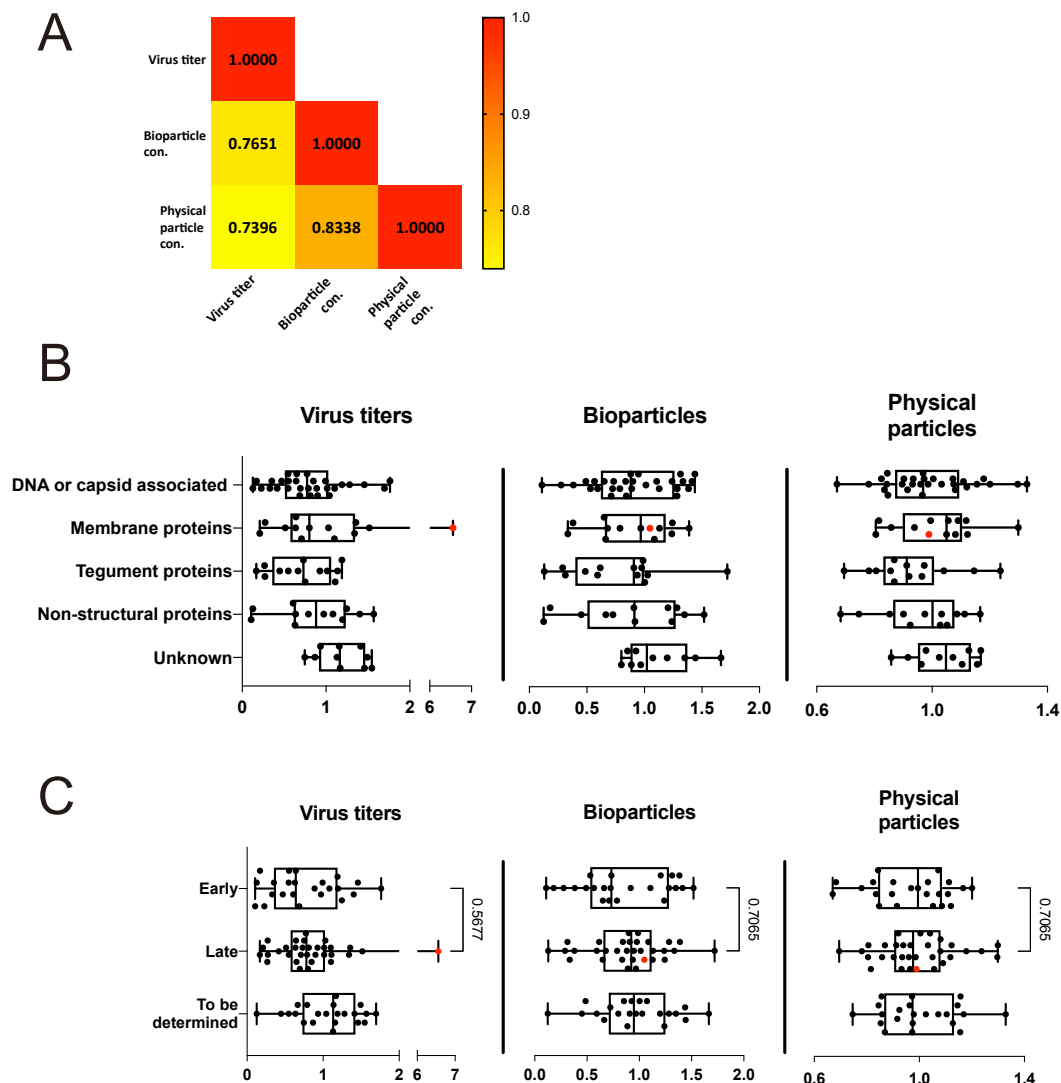


Fig. 5 Statistical analysis and comparison of individual virus supernatants according to their virus titer, bioparticle concentration, physical particle concentration, functional group category and expressing timing classification.

Three characteristic measurements of 76 harvested individual virus supernatants plus two controls are shown summarizing the data in Figures 2-4: (i) virus titer (green Raji units, GRU, Figure 2); (ii) bioparticle concentration (Elijah ratios, Figure 3); and (iii) physical particle concentration (ZetaView, Figure 4). Possible overall correlation of the data and their statistical significance are provided in panel A together with specific correlation within functional groups and expression timing shown in panel B and C. **(A)** Mean values of the three functional tests (virus titer, bioparticle concentration, and the physical particle concentration data) were set as rank order and the statistical correlation was assessed using the Spearman rank correlation method. Correlations between two groups were analyzed and the correlation coefficients (R^2) are shown in the grids of the heatmap. (i) bioparticle concentration versus virus titer: 0.7651; (ii) physical particle concentration versus virus titer: 0.7396; (iii) physical particle concentration versus bioparticle concentration: 0.8338. The color scale bar on the right indicates the intensity of the value. 1.0 is red and 0.7 is set to yellow. **(B)** Virus samples generated by individual co-expression of 76 expression plasmids encoding viral genes together with BZLF1 (Figure 2A) were parted according to their functional groups (DNA or capsid-associated proteins, membrane proteins, tegument proteins, non-structural proteins and unknown). The x-axes show the fold changes compared to the references. The left, middle and right panel show the results of the three assays as indicated. The data are provided as box plots and each point represents the mean value of individual virus samples. The single red dots indicate the mean value of the virus sample generated by co-transfection of BZLF1 with BALF4. The statistical numerical results are presented in Table 2. **(C)** Results obtained with 76 virus supernatants are displayed according to their expression timing: early, late, and 'to be determined' and arranged as in panel B. The x-axes indicate the fold change. The red dots indicate BALF4. The unpaired Wilcoxon rank sum test was conducted in the statistical analysis between the early and late groups, the group labeled 'to be determined' was excluded from the statistical test. The median of the different populations is shown and the p-values are provided.

The mean values of three measurements of the 76 virus stocks were taken and set as rank order to investigate a possible (and likely) correlation of these measurements. I assessed the mutual relationship using the Spearman rank correlation method. The values are provided in a heatmap shown in **Figure 5A**. The parameters are placed on the x- and y-axis of the grids of the heatmap. The color scale on the right indicates the intensity and the correlativity between two parameters ranging from 0.7 to 1.0. The correlativity of bioparticle concentration versus virus titer was found to be 0.7651 (dark yellow) the physical particle concentration versus virus titer was slightly lower at 0.7396 (light yellow) while the correlation between physical particle concentration and bioparticle concentration was highest at 0.8338 (orange).

To look for correlative details in my data, mean values derived from the three quantitative parameters (virus infectious titers, bioparticle and physical particle

concentration) were sorted according to functional groups or grouped according to expression timing criteria. To analyze the data from the three quantitative parameters, the data of **Figures 2 to 4** were transformed into three box plots (**Fig. 5B**). The y-axis denotes functional groups (DNA or capsid-associated proteins, membrane proteins, tegument proteins, non-structural proteins and unknown) and the x-axes show the fold change of each parameter (left: virus titer [GRU]; middle: bioparticle concentration [Elijah]; right: physical particle concentration [Zetaview]). The dots represent the mean values of the corresponding individual measurements and the single red dot in each panel indicates the results obtained with the BALF4 gene encoding the viral glycoprotein gB. The statistics are summarized in **Table 2**. The means of virus titers, bioparticle concentration and physical particle concentration of the EBV virus stocks were grouped by biological functions and genes encoding viral proteins of unknown functionality were excluded from the test. The Kruskal Wallis rank sum test of one-way ANOVA was applied. The p-value adjustment method by Benjamini-Hochberg was applied to calculate the statistical significance between two functional groups in a pair-wise comparison. For example, the p-value of the Kruskal-Wallis rank sum test is 0.7328 for the parameter of infectious viral titers (GRU in **Table. 2**) showing the statistical significance that prevent rejecting the null hypothesis of the overall test. This result indicated that all protein functions contribute to the GRU parameter as they do not significantly differ. The same statistical test was applied to the two remaining parameters as shown in **Table 2**. The p-value of the Kruskal-Wallis rank sum test is 0.7519 of bioparticle concentration among functional groups. P-values between groups are shown in the second part of the table. Additionally, 0.4194 is the p-value of the Kruskal-Wallis rank sum test of physical particle concentration and other p-values are also given. Again, no statistically significant contribution of proteins with different functions was found to contribute to the values of bioparticle concentration (Elijah) or physical particle concentration (ZetaView).

Table 2. Statistical analysis of the correlation of the three read-out categories

Virus titers

Kruskal-Wallis rank sum test Kruskal-Wallis chi-squared = 1.2844, df = 3, p-value = 0.7328			
Pairwise comparisons using Wilcoxon rank sum test P value adjustment method: BH			
	DNA or capsid associated proteins	Membrane proteins	Non-structural proteins
Membrane proteins	0.74	-	-
Non-structural proteins	0.74	0.74	-
Tegument proteins	0.74	0.74	0.74

Bioparticles

Kruskal-Wallis rank sum test Kruskal-Wallis chi-squared = 1.2047, df = 3, p-value = 0.7519			
Pairwise comparisons using Wilcoxon rank sum test P value adjustment method: BH			
	DNA or capsid associated proteins	Membrane proteins	Non-structural proteins
Membrane proteins	0.96	-	-
Non-structural proteins	0.96	0.96	-
Tegument proteins	0.96	0.96	0.96

Physical particles

Kruskal-Wallis rank sum test Kruskal-Wallis chi-squared = 2.825, df = 3, p-value = 0.4194			
Pairwise comparisons using Wilcoxon rank sum test P value adjustment method: BH			
	DNA or capsid associated proteins	Membrane proteins	Non-structural proteins
Membrane proteins	0.60	-	-
Non-structural proteins	0.87	0.60	-
Tegument proteins	0.60	0.60	0.60

BH: Benjamini-Hochberg (p-value adjustment method)

Expression timing of viral genes does not affect the three analyzed parameters of virus stocks

Mean values of the three measured parameters (virus titer [GRU]; bioparticle concentration [Elijah]; physical particle concentration [Zetaview]) were transformed into dots and displayed according to the criterion 'expression timing' of the viral genes, which are known to be expressed early or late or which have no known expression time (**Fig. 5C**). The left panel shows box plots of mean values of virus titer versus expression timing derived from **Figure 2B**. The middle panel transforms data shown in **Figure 3B** into box plots of bioparticle concentration versus expression timing. The right panel of box plots states physical particle concentration versus expression timing as in **Figure 4B**. The y-axes mark the groups of expression timing and the x-axes display the ratios of mean values of the three parameters. The red dot in each panel points to the mean value of virus stocks obtained by ectopic expression of BALF4. I used the unpaired Wilcoxon rank sum statistical test to analyze expression timing versus the three parameters. Data obtained with genes of unknown expression timing were excluded from the analysis. The two classes of viral genes with early or late expression timing had p-values of 0.5677, 0.7065 and 0.7065 from the left to the right panel documenting that expression timing of viral genes is also not a criterion that contributes significantly to the three analyzed parameters.

Only one out of ten selected viral genes associated with elevated bioparticle numbers improves infectivity of viral stocks together with BALF4

In this and in the next chapters, I concentrated on subgroups of selected viral genes that enhance (or reduce) mean values of certain parameters.

BALF4 is the only viral gene that boosts viral infectivity (**Fig. 2**) but it does not affect bioparticle concentration (**Fig. 3**) nor the concentration of physical particles in virus stocks generated by co-transfection of BALF4 and BZLF1 (**Fig. 4**). On the contrary, certain viral genes seem to increase the concentration of bioparticles as shown in **Figure 3** but in the order of 1.5-fold, only. In this chapter I asked if these single viral genes associated with higher bioparticle concentration could yield better virus stocks when co-expressed with together BALF4 than virus stocks obtained by co-transfection of BALF4 and BZLF1, only.

Ten EBV gene expression plasmids, BKRF4, BVLF1, BNLF2a, BXRF1, BFLF2, BMRF1, BHLF1, BXLF1, BVRF2 and BALF2, were chosen based primarily on their elevated viral bioparticle concentration as shown in the left grey block in **Figure 3**, which encompasses members of the 'high bin' group. In this ranking, the ten genes caused a higher bioparticle concentration in the supernatants.

To investigate a possible additive or synergistic effect, I co-transfected the individual ten expression plasmids together with p509 and p6515, which encode BZLF1 and BALF4, respectively, into 2089 EBV producer cells. The virus supernatant stocks were collected and 5 μ l was used to infect Raji cells to determine the virus titers as in **Figure 2**. An empty pCMV vector was co-transfected with BZLF1 and BALF4 as a control (Ctrl) and used as standard for normalization (**Fig. 6**). The results showed that only in case of the BVL1 expression plasmid an additive effect could be observed in the range of 1.5-fold, which was also observed with BVL1 in experiments shown in **Figure 3**. Co-transfection of BKRF4, BVRF2 or BALF2 seemed to reduce the virus titer and BNLF2a, BXRF1, BFLF2, BMRF1, BHLF1 and BXLF1 did not influence the virus titers.

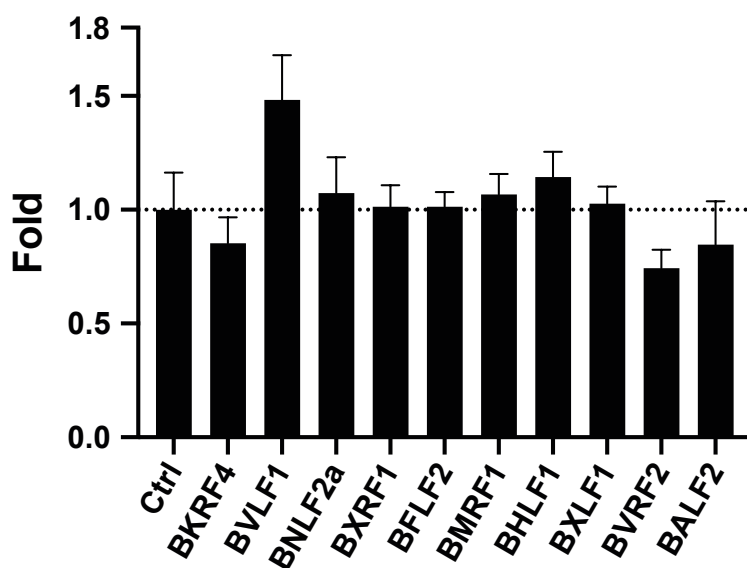


Fig. 6 Comparison of viral titers in virus stocks generated by co-transfection of the EBV genes BZLF1, BALF4 and 10 single expression plasmids encoding selected viral genes of the ‘high bin’ group.

The 2089 EBV producer cells were seeded and transiently transfected with 0.25 μ g BZLF1 (p509), 0.25 μ g BALF4 (p6515) and 0.5 μ g of 10 selected EBV expression plasmids as indicated and described in Figure 2 and Materials and Methods. The virus supernatants were harvested 3 days after transfection and partially purified using 1.2-micron filters. 1×10^5 Raji cells were incubated with 5 μ l of the harvested virus supernatants. After three days, the infected Raji cells were investigated by flow cytometry (BD FACSCanto™) analyzing the fraction of cells expressing green fluorescence protein. Mean and standard deviation of three biological replicates are shown.

Selection of 24 viral genes that elevate or repress bioparticle concentration

To concentrate my subsequent studies on potentially interesting viral genes, I

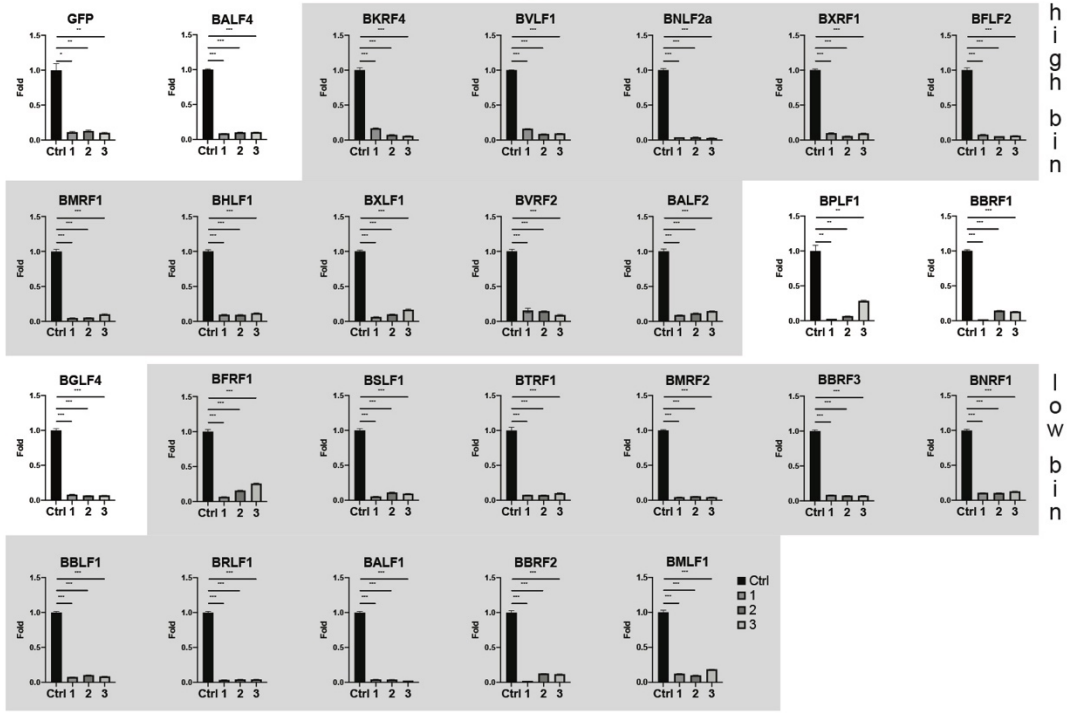
chose candidates from the high and low ends of genes identified in the experiments in **Figure 3** in which I studied bioparticle concentration in Elijah cell binding assays. I asked if members of the top group of genes are essential for virus production as measured in infection experiments with Raji cells in **Figure 2**. On the contrary I asked if members of the bottom group of viral genes might regulate virus synthesis negatively and hence repress virus infectious titers, because some could act as master regulators controlling and thus limiting virus production.

To investigate these scenarios, the top 10 genes and the bottom 11 genes in the ranking order in **Figure 3** were selected and termed 'high bin' and 'low bin' genes, respectively. Certain genes were excluded for various reasons. LF1 and LF2 were excluded since the B95-8 EBV strain, which is contained in the 2089 EBV producer cell line does not encompass these two genes. Their ectopic expression in the 2089 producer cells was informative but their lack precludes a knockdown strategy as explained below. BSLF2/BMLF1 was excluded because BMLF1 was also in the 'low bin' group and could be the cause of low bioparticle number. BLLF1 (gp350) ectopic expression directly affected the read-out since the gp350-specific antibody was utilized to detect bioparticles. Therefore, BLLF1 (gp350) was excluded as well. Also, BLRF3 was excluded from the 'high bin' group as it is part of EBNA3 and likely not directly involved in virus production. Eventually, the 'high bin' group contains BKRF4, BVLF1, BNLF2a, BXRF1, BFLF2, BMRF1, BHLF1, BXLF1, BVRF2 and BALF2 and genes of the 'low bin' group encompass BFRF1, BSLF1, BTRF1, BMRF2, BBRF3, BNRF1, BBLF1, BRLF1, BALF1, BBRF2 and BMLF1. Additionally, I randomly selected three genes BPLF1, BBRF1 and BGLF4 from the large middle group as shown in **Figure 3**. The rank order of bioparticle concentrations was copied from **Figure 3** and is summarized in **Figure 8A**. The color codes of functional groups in this figure panel and in **Figure 3B** are identical. 11 genes encode DNA or capsid-associated proteins (green), 2 genes encode membrane proteins (red), 6 genes give rise to tegument proteins (brown), 3 genes code for non-structural proteins (blue) and 2 gene have unknown functions (grey).

Design and validation of 78 shRNA candidates targeting 24 viral and control genes

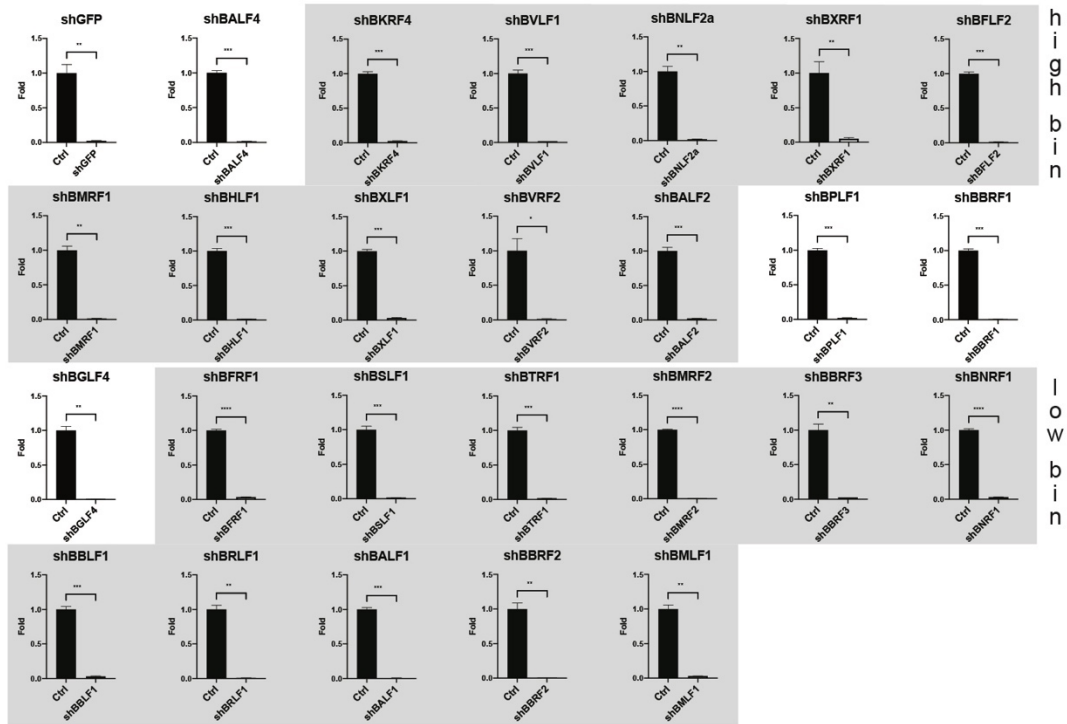
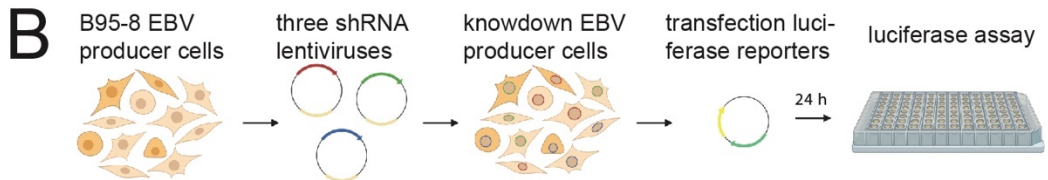
To test the 24 selected viral genes for their possible essential or regulatory roles in EBV's lytic phase, I developed an shRNA knockdown strategy to repress individual viral genes and to study their contribution during virus production. Towards this end, the DNA sequences of the 24 viral genes in FASTA format were used as input for splashRNA, a search and design tool website for shRNA sequence candidates (<http://splashrna.mskcc.org>) (Pelossof et al., 2017). Several candidates with their

predicted efficiency scores were obtained for all 24 selected viral genes. Three promising shRNA antisense guides were chosen for each EBV gene target to establish a knockdown shRNA pool for all selected genes and controls. Altogether, 72 individual synthetic sequences (plus 6 for additional control shRNAs) were cloned into the miR-3G frame shRNA construct (Watanabe et al., 2016). Subsequently, the miR-3G frames were introduced into the lentivirus pCDH vector plasmid (p6924), which also encodes puromycin resistance to allow selecting the lentivirally transduced 2089 EBV producer cells. Six control shRNA were also introduced into this vector to target GFP and BALF4 as positive controls. In total, I constructed 78 shRNA expression vectors to establish 26 shRNA knockdown pools with three shRNAs each. To pretest the many shRNA expression vectors, I also cloned the three sequences of the three shRNAs per target gene in complementary strand orientation into psiCHECK2, a standard dual luciferase reporter (p5264) that expresses *firefly* and *Renilla* luciferase proteins. To evaluate shRNA knockdown efficiencies, 293T cells were co-transfected with the 78 single shRNA vector plasmids to express the shRNAs together with one of the 26 corresponding luciferase reporter plasmids. The experimental setup is shown schematically in **Figure 7A**. After 24 h, the luciferase activities were measured. An 'empty' lentiviral pCDH vector (p6924) was co-transfected with the luciferase reporter as a negative control. Using *firefly* and *Renilla* luciferase measurements for internal data correction, the *Renilla* luciferase ratios were normalized to the negative control and the results are shown in **Figure 7A**. Every shRNA expression vector demonstrated excellent knockdown efficiency of at least 90 % of the luciferase target. An unpaired two-tailed t tests proved the potent knockdown of luciferase activity in this assay (**Fig. 7B**).



high bin

low bin



high bin

low bin

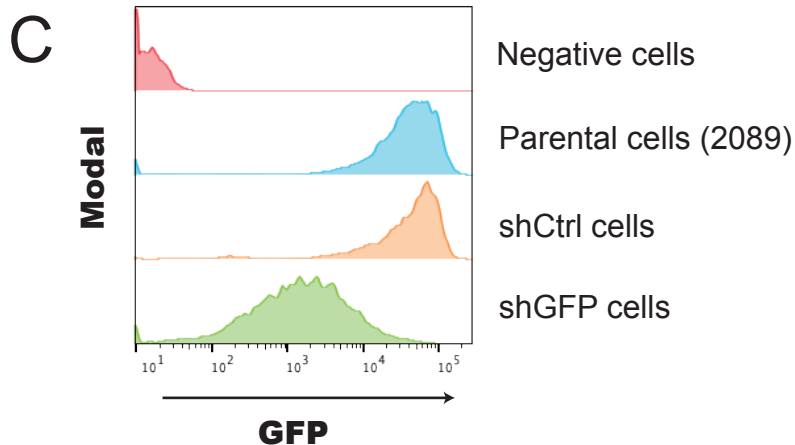


Fig. 7 Functional analysis of 72 shRNA constructs directed against 24 selected viral transcripts plus controls.

Based on results obtained from bioparticle quantification (Elijah cell binding assay) in Figure 3, two groups of viral genes termed ‘high bin’ and ‘low bin’ encompassing 10 and 11 members (shaded areas), respectively, were selected that profoundly increased or decreased the number of EBV particles in viral supernatants. shRNA antisense guides for each EBV gene were generated (<http://splashrna.mskcc.org>) and three shRNA sequences per EBV target gene were individually cloned into the miR-3G frame of the basic shRNA vector (pCDH; p6924) that also encodes resistance against puromycin. A set of corresponding EBV target genes cloned into the psiCHECK2 dual luciferase reporter allows functional testing. **(A)** The flow chart depicts the experimental setup of the reporter assay shown in this panel. Transient reporter assays were conducted in 24-well cluster plates seeded with 2×10^5 293T cells, which were co-transfected with the individual reporter plasmids (26 in total including controls) together with single matching lentiviral shRNA expression plasmids. As reference and control, an empty pCDH lentiviral plasmid (p6924) was co-transfected with the indicated luciferase reporter (Ctrl). As additional controls, luciferase reporter plasmid with GFP and BALF4 as target genes were used in combination with three individual lentiviral vectors encoding GFP- and BALF4-specific shRNAs. After 24 h, luciferase activities were recorded and normalized to the reference. ‘High bin’ and ‘low bin’ samples are indicated. **(B)** The flow chart shows the experimental setup of introducing sets of three shRNA encoding lentiviruses into the 2089 EBV producer cell line and the selection with puromycin. The individual cell lines stably transduced with three shRNA vectors each were analyzed by transient transfection with matching dual luciferase reporter plasmids encoding corresponding viral targets as in panel A. Mean and standard deviation of three biological replicates are shown. Asterisks indicate statistical significance as determined by using the unpaired two-tailed t test with Welch’s correction (** $P \leq 0.01$; *** $P \leq 0.001$). **(C)** The effect of three shRNAs stably introduced into the 2089 EBV producer cell line and directed against GFP was analyzed by flow cytometry. GFP-negative cells were used as control. GFP expression of parental 2089 EBV producer cells (2089) and a derivative stably transduced with an empty pCDH lentiviral plasmid (p6924) as an shRNA control (shCtrl) are shown. The x-axis denotes intensity of GFP fluorescence.

Validation of knockdown efficacies of 24 transcript mimics representing viral targets in stably shRNA-transduced 2089 EBV producer cells

2089 EBV producer cells were stably transduced with the set of 24 shRNA expressing lentiviral vectors. In addition, two control vectors encoding shRNAs directed against GFP (the viral genome in 2089 EBV producer cells expresses GFP stably) and BALF4 transcripts were included. Lentiviral vector stocks were generated by transfecting packaging and envelope plasmids (p4502 and p5451) together with discrete pools of three shRNA encoding lentiviral vector plasmids directed against one viral transcript target. The EBV producer cells were incubated with the lentivirus-containing medium for 3 days (schematic diagram in **Fig. 7B**). The transduced cells were further expanded and 10 µg/ml puromycin was added for the initial selection of the transduced cells. To test the knockdown efficacies, the 24 stably transduced 2089 EBV producer cell lines together with two control cell lines transduced with shRNAs against GFP and BALF4 were transiently transfected with the matching luciferase reporter plasmids or an empty luciferase reporter (p5264) as a negative control. After 24 h, the luciferase activities were measured, and the efficacies were calculated and depicted in **Figure 7B**. Overall, the 26 transduced cell lines, including the two controls indicated a very convincing knockdown efficacy and documented high functional levels of shRNAs constitutively expressed in the different cell lines including the shRNA mediated knockdown of GFP expression at protein level (**Fig. 7C**). Convincingly, a statistical analysis using the unpaired two-tailed t test supported the almost complete repression of the luciferase reporter activities (**Fig. 7A,B**).

Analysis of virus titers in supernatants from 2089 EBV producer cell lines stably transduced with 24 sets of shRNAs directed against selected EBV transcripts

The EBV producer cell lines each stably transduced with a set of three shRNA vectors were expanded under co-selection using 3 µg/ml puromycin and 100 µg/ml hygromycin B to ensure shRNA expression and maintenance of the EBV genome 2089, respectively. Controls included 2089 EBV producer cells transduced with the empty lentivirus pCDH shRNA vector backbone (p6924), only, as well as cells encoding triple set of shRNAs directed against GFP and BALF4 transcripts as tested in **Figure 7**. The 24 shRNA specific viral targets were selected, including the 'high bin' and 'low bin' groups of genes identified in previous Elijah assays monitoring bioparticle concentration marked with grey shaded areas in **Figure 3**. The 10 candidate genes in the 'high bin' group have higher bioparticle concentration whereas in the 'low bin' group ectopic expression of 11 viral genes reduced bioparticle concentration considerably (**Fig. 3**). The two panels in **Figure 8A** recapitulate these previous findings. In

addition, I randomly selected three targets from the large group of viral genes with no discrete functionality to include BPLF1, BBRF1 and BGLF4 in my study (**Fig. 8A**). Virus stocks from the different 2089 EBV producer cell lines were generated by transient transfection of BZLF1 (p509) followed by infecting Raji cells and quantifying virus titers by flow cytometry. The results were separated according to the 'high bin' and 'low bin' groups of candidates in **Figure 8B** (black columns). To allow a comparison also with supernatants from cells co-transfected with both BZLF1 (p509) and BALF4 (p6515) plasmids, I repeated the experiments measuring virus infectivity. **Figure 8B** also depicts the analysis of virus titers obtained from these experiments (white columns).

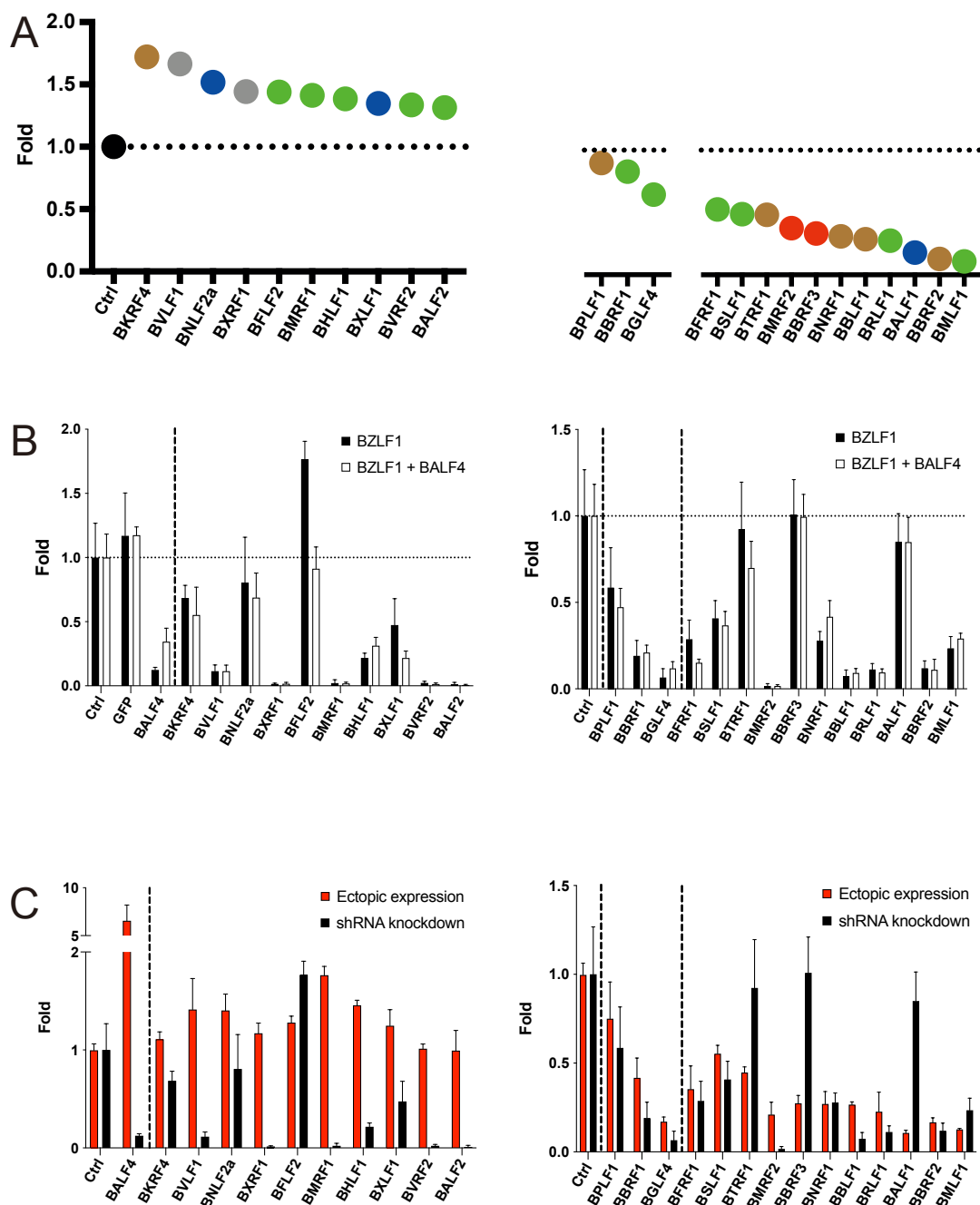


Fig. 8 Analysis of viral titers in supernatants generated with 2089 EBV producer cell lines stably transduced with sets of three shRNAs directed against 24 individual viral transcripts plus controls.

(A) Recapitulation of selected data shown in Figure 3. Three groups of viral genes are shown that increased ('high bin' group, left panel) or decreased ('high bin' group, right panel) the yield of bioparticles (viral particles). In addition, three genes were randomly selected as measured in the Elijah cell binding assay (single grey columns in Fig. 3) when co-transfected together with BZLF1 into the EBV producer cell line 2089. The EBV genes are arranged in descending order and the color codes depict the different functions of viral proteins as in Figure 3. The color codes indicate (i) green: DNA or capsid-associated proteins, (ii) red: membrane proteins, (iii) brown: tegument proteins, (iv) blue: non-structural proteins, and (v) grey: proteins with unknown functions. **(B)** Newly established EBV producer cell lines based on the parental producer cells 2089 were stably transduced with 24 sets of three shRNAs each, together with matching control cell lines. Controls encompass the EBV producer cell line 2089 stably transduced with the empty pCDH shRNA expression vector (Ctrl) or two sets of three shRNAs each directed against GFP or BALF4. The viral genes termed 'high bin' and 'low bin' groups are shown in the left and right panels, respectively. The individual cell lines were transiently transfected with the p509 expression plasmid coding for BZLF1 alone or in combination with the p6515 expression plasmid coding for BALF4 as indicated. The virus supernatants were harvested 3 days after transfection, filtered (1.2 μm pore size) and 10 μl were used to infect 1×10^5 Raji cells for three days. The Raji cells were analyzed for the fraction of GFP-positive cells by flow cytometry and their virus titers (GRU titers) were calculated. Supernatants harvested from the control cell lines are shown on the left side of the graph with the 'high bin' group of genes separated by a vertical dotted line from the test samples. The 'low bin' group is shown on the right separated from the control and the other three genes by dotted lines. **(C)** Virus titers of supernatants obtained from the 24 individual shRNA expressing EBV producer cell lines (black columns; shRNA knockdown) analyzed in panel B are compared with virus titers found in supernatants from the parental EBV producer cell line 2089 upon transient expression of viral genes (red columns; ectopic expression). The latter data are selected and copied from Fig. 2. Mean and standard deviation of three biological replicates are shown.

Controls included 2089 EBV producer cells transduced with the empty lentiviral vector (Ctrl) and cells transduced with the triple set of shRNA directed against GFP transcripts. The two controls revealed that this manipulation did not change virus titers in the supernatants of 2089 EBV producer cells induced with BZLF1 alone or in conjunction with BALF4 as expected (data not shown). The data from the two sets of experiments were normalized (black and white columns) and set to one (**Fig. 8B**). The horizontal dotted lines indicate the virus titer of the reference (Ctrl). All virus titers were normalized to this control, which stems from supernatants of 2089 EBV producer cells transduced with the empty shRNA expression vector pCDH (p6924). The vertical line separates the controls and remaining genes are arranged in the

same order as **Figure 8A**.

Virus titers obtained after BZLF1 transfection of shBALF4 transduced EBV producer cells showed considerable reduction of infectivity as expected but co-transfection of both BZLF1 and BALF4 partially rescued the loss of virus titer from the shBALF4 transduced cells (**Fig. 8B**, left panel) when BALF4 was re-introduced. This experiment demonstrated that shRNA pools can successfully repress lytic viral genes causing a substantial phenotype indicative of functional repression.

Changes of virus titers in supernatants from EBV producer cell lines stably transduced with shRNAs directed against 'high bin' and 'low bin' viral transcripts

As expected, certain shRNA sets decreased virus titers dramatically but not all shRNA sets caused a serious phenotype (**Fig. 8B**). Basically, shRNAs directed against transcripts of BXRf1, BMRF1, BVRF2 and BALF2 (left panel) and BMRF2 (right panel) induced a complete or almost complete failure to produce infectious EBV stocks. Other shRNAs had a weak repressive phenotype (BKRF4, BHLF1, BXLF1, BFRF1, BSLF1, BNRF1, BMLF1) or did not or did hardly affect production of infectious virus (BNLF2a, BPLF1, BTRF1, BBRF3 and BALF1). Others showed in-between phenotypes (**Fig. 8B**). Remarkably, the shRNA mediated knockdown of BFLF2 seemed to induce virus titers to some degree (**Fig. 8B**, left panel). Induction of the 2089 EBV producer cell lines carrying the different shRNA sets with both BZLF1 and BALF4 did not reveal a convincing function or contribution of BALF4 in this series of experiments (white columns in **Fig. 8B**), which is in line with results presented in **Figure 3**.

The results obtained so far support the conclusion that certain viral genes seem to be absolutely essential (BXRf1, BMRF1, BVRF2, BALF2, BMRF2) or, conversely, are entirely dispensable (BNLF2a, BFLF2, BTRF1, BBRF3 and BALF1) for the production of infectious virus stocks. Importantly, the results did not support my hypothesis that EBV encodes a gene that controls production of infectious virus. This is because the knockdown of any of the 11 transcript candidates in the 'low bin' group did not increase virus production as I had hoped (right panel in **Fig. 8B**). In this set of experimentation, only the shRNA knockdown of BFLF2 seemed to yield elevated virus titers (**Fig. 8B**) in a range similar to the gene's ectopic expression in **Figure 2** and **Figure 3** experiments, which appears contradictory.

I also compared virus titers obtained in experiments shown in **Figure 2** (ectopic expression of single viral genes in BZLF1 induced 2089 EBV producer cells) with virus titers of the 24 selected shRNA knockdown EBV producer cell lines (also induced by BZLF1 transduction) as in **Figure 8B**. The direct comparison is provided in **Figure 8C**. Normalized virus titers obtained after ectopic expression of the 24 single viral genes

are marked in red and the corresponding virus titers from the shRNA knockdown producer cells are depicted in black (**Fig. 8C**). BALF4 expression yielded maximal virus titers but its knockdown repressed virus titers to about 10 % compared to the normalized control value. These results also validate the shRNA knockdown strategy and confirm BALF4's role as an essential gene that boost viral infectivity upon ectopic expression (**Fig. 8C**) (Neuhierl et al., 2002). In the 'high bin' group, the majority of viral genes that yielded higher virus titers upon ectopic expression of viral genes provides critical lytic products because their shRNA mediated knockdown repressed virus titers considerably (BVLF1, BXRf1, BMRF1, BVRF2, BALF2) or moderately (BXLf1, for example). The knockdown of BFLF2 is an exception because it increased the virus titer slightly. In the 'low bin' group (**Fig. 8C**, right panel), the knockdown of certain viral transcripts reduced virus titers even further (BGLF4, BMRF2, BBLF1 and BRLF1) indicating their regulatory function, which is disturbed upon overexpression of these genes as well as upon their repression. Their proper function seems to require a certain homeostatic or fine-tuned level of expression. A similar interpretation might apply for BTRF1, BBRF3 and BALF1. Their ectopic expression or their shRNA mediated knockdown reduced or restored virus titers, respectively, as seen in **Figure 8C**.

Ectopic expression and shRNA knockdown of viral genes and transcripts – comparing bioparticle concentration of 24 viral targets

Virus stocks from experiments in which I tested the virus stocks for their infectivity in Raji cells in **Figure 8B** were also analyzed for their bioparticle concentrations using the Elijah cell binding assay as in shown in **Figure 3**. Virus stocks were added to Elijah cells and bound bioparticles were quantified. The results are summarized in **Figure 9A**.

The 2089 producer cell line transduced with the set of three shRNA directed against the GFP transcript did not affect bioparticle concentration much (**Fig. 9A**, left panel). The shRNA mediated knockdown of BALF4 showed a minor decrease of bioparticle concentration, which was partially rescued when BALF4 was transfected into this shRNA knockdown producer cell line (**Fig. 9A**, left panel). The bioparticle concentrations of BVLF1 and BALF2 indicated a substantial reduction in the shRNA expressing EBV producer cell lines which is in agreement with their low virus titers in **Figure 9B** and **C**. In the right panel of **Figure 9A**, BBRF3 and BALF1 had equivalent bioparticle concentrations comparable with their virus titers in **Figure 8B**. Moreover, the concentration of bioparticles was considerably low in supernatants from BGLF4, BBLF1 and BRLF1 knockdown cells reminiscent of their virus titers (**Fig. 8C**). Interestingly, expression of BALF4 upon lytic induction of the 24 shRNAs carrying EBV

producer cell lines did not lead to considerable deviations regarding bioparticle concentration in the supernatants (**Fig. 9A**).

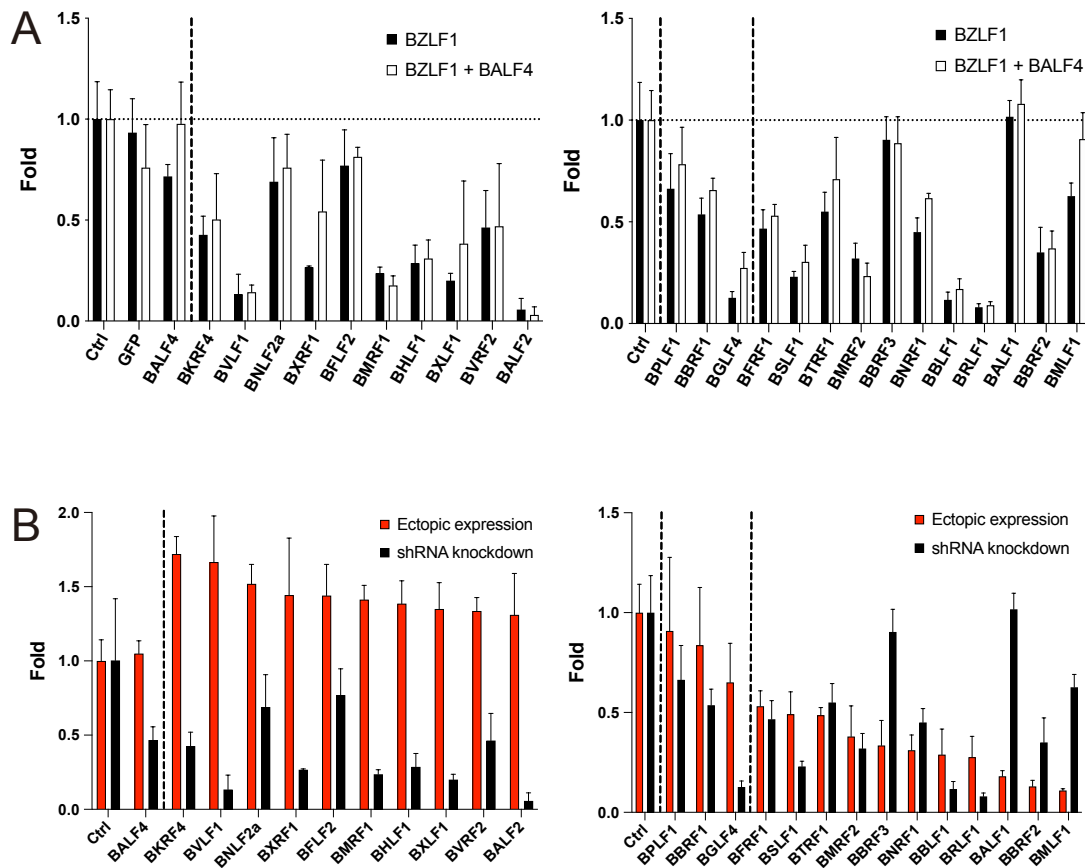


Fig. 9 Analysis and comparison of bioparticles in supernatants from the 2089 EBV producer cell line stably transduced with sets of three shRNAs directed against 24 viral transcripts in the Elijah cell binding assay.

Supernatants analyzed in Figure 8 were tested for their bioparticle concentration in the Elijah cell binding assay. **(A)** Following the setup in panel B of Figure 8, 20 μ l supernatants from the 24 EBV producer cell lines stably transduced with 24 sets of three shRNAs together with matching controls were analyzed for bioparticle concentration after transfection of only BZLF1 (p509) or after co-transfection with both p509 and BALF4 (p6515) expression plasmids. **(B)** Bioparticle concentrations found in supernatants from 2089 EBV producer cells upon expression of single viral genes as analyzed in Figure 3 (red columns; ectopic expression) are compared with results shown in panel A of this figure (black columns; shRNA knockdown). Mean and standard deviation of three biological replicates are shown.

Finally, I compared supernatants obtained after ectopic expression of single viral genes analyzed in **Figure 3** with corresponding supernatants from the 24 shRNA expressing EBV producer cell lines for their bioparticle concentration in the Elijah cell binding assay after BZLF1 mediated lytic induction (**Fig. 9B**). Results from ectopic

expression of single viral genes and the matching shRNA knockdown experiments are shown in red and black, respectively (**Fig. 9B**). Bioparticle concentration declined to about 50% upon knockdown of BALF4 suggesting that BALF4 might also be involved in bioparticle generation. Bioparticle concentration from supernatants of shRNA knockdown cells of the 'high bin' group were severely or moderately reduced (**Fig. 9B**, left panel). In the right panel of **Figure 9B**, ectopic expression of single viral genes showed lower bioparticle concentrations initially. The majority of supernatants from shRNA expressing EBV producer cell lines did not show very different bioparticle concentrations (BBRF1, BFRF1, BTRF1, BMRF2, BNRF1) whereas some had reduced numbers of bioparticles (BGLF4, BSLF1, BBLF1, BRLF1). The shRNA mediated knockdown of BBRF3, BALF1, BBRF2 and BMLF1 transcripts increased bioparticle production reaching levels similar with or identical to the control (**Fig. 9B**, right panel).

Analysis of the fusogenic activity of 24 virus stocks upon ectopic expression of individual viral genes from the 'high bin' and 'low bin' groups

Together with my colleague Manuel Albanese, I developed a novel assay to measure the fusogenic activity of engineered extracellular vesicles (EVs) (Albanese et al., 2020). Here I adapted the principle of this assay to analyze the fusogenicity of EB virions using primary human B cells, EBV's primary target cells.

The enzyme β -lactamase (BlaM) is utilized by bacteria to cleave the β -lactam ring of antibiotics of the penicillin group, e.g., ampicillin, such that the bacteria become resistant. The principle was employed to synthesize a compound, termed CCF4 with a β -lactam ring in its center, which links two separate fluorochromes, hydroxycoumarin and fluorescein, located at opposite ends. The concept is based on fluorescence (or Förster) resonance energy transfer (FRET). When light of 409 nm wavelength excites hydroxycoumarin in the compound, the energy is transferred to fluorescein, which emits light with a wavelength of 520 nm. If the β -lactam ring is cleaved, excitation causes hydroxycoumarin to emit light with 447 nm wavelength directly without an energy transfer because the hydroxycoumarin moiety is absent. The difference between the two wavelengths and their intensities can be detected and differentiated by flow cytometry. The β -lactamase (BlaM) assay has been developed in the HIV field to detect fusion of HIV particles with T cells (Cavrois et al., 2002; Jones and Padilla-Parra, 2016). In the BlaM assay, β -lactamase enzyme is introduced into recipient cells by virus-mediated transfer and then the modified substrate CCF4-AM is added to cells. After the substrate is taken up by cells, it is cut by endogenous cytoplasmic esterases to the negatively charged CCF4 product

locking it in the cytoplasm of the CCF4-loaded cell. Once BlaM is also introduced into the cells, the enzyme cuts the β -lactam ring of CCF4 and altering its emission wavelength. The protocol has been constantly improved (Cavrois et al., 2014) and it is applicable to detect transduction of BlaM linked to viruses or other entities.

As demonstrated in a pre-print with Manuel Albanese and me as shared first authors (Albanese et al., 2020), we investigated extracellular vesicles (EVs) also termed exosomes, which range in size from 30 nm to 1000 nm and which could play an essential role in signal transduction. Many papers claim that EVs contribute to cell-to-cell communication and deliver cargos from donor to recipient cells. It is believed that four major routes deliver messengers to target cells, e.g., receptor binding and activation, fusion, endocytosis and ligand cleavage from extracellular vesicles (Meckes and Raab-Traub, 2011). In their lumen and on their surface EVs can contain many proteins and DNA and RNA molecules that originate from donor cells. Viral proteins such as the EBV encoded LMP1 protein, cytoskeletal proteins, myosin and tetraspanin protein CD63 can be found incorporated and enriched in EVs. Based on this knowledge, a codon-optimized β -lactamase gene was fused to the carboxy terminus of the human CD63 protein, which is enriched in EVs, via a conventional G₄S linker (Albanese et al., 2020). Subsequently, the fusion protein was cloned into a pcDNA3.1(+) (p5267) expression vector, which was transiently introduced into different cell types. They readily gave rise to EVs that contain CD63: β -lactamase (subsequently termed CD63:BlaM) in their vesicle membrane. Upon EV delivery to CCF4-loaded cells the BlaM assay is an easy method to evaluate a successful EV-mediated transfer of CD63:BlaM to target cells (Albanese et al., 2020).

To evaluate EBV fusion with the virus' genuine target cells, human primary B cells, I developed this novel assay shown schematically in **Figure 10A**. The aim was to study virus fusion separately and independent of viral infectivity (**Fig. 1**). The latter summarizes the entire infection process including *de novo* gene expression of infectious EBV particles (detecting GFP expression in Raji cells as shown in **Figure 2**).

2089 EBV producer cells were co-transfected with an expression plasmid encoding CD63:BlaM (p7200) together with BZLF1 (p509) and single expression plasmids that encode the 21 individual viral genes of the 'high bin' and 'low bin' groups plus controls as defined in **Figure 8A**. Human primary B cells isolated from adenoid tissue (nasal polyps biopsies) were incubated with 20 μ l CD63:BlaM-containing virus stocks for 4 h. Subsequently, the cells were loaded with the CCF4-AM substrate and incubated at room temperature for 16 h. During this period, the cytoplasmic CCF4 substrate is cleaved in infected but not in non-infected cells. The fraction of cells with emission light shift was determined by flow cytometry. The same virus stocks were used to infect Raji cells and the virus titers were recorded as

in my experiments shown in **Figure 2**. A virus stock generated by transient transfection of the 2089 EBV producer cells with BZLF1 (p509), only, served as control. Yet another control was a virus stock generated by co-transfection of BZLF1, an empty expression vector plasmid and CD63:Blam to normalize the data depicted in **Figure 10B**.

The left panel shows the fusogenic activities of 10 EBV stocks obtained by ectopic expression of viral genes of the 'high bin' group. With the prominent exception of the single virus stock generated by ectopic expression of BALF4 all other virus stocks did not show changes in their fusogenicity activity. The BALF4 virus stock showed a four-fold increase in this assay and another virus stock generated with BMRF1 had a somewhat improved fusogenic activity, probably because this virus stock also scored better with respect to its bioparticle concentration (**Fig. 3**). Within the members of the 'low bin' group of genes, all virus stocks showed medium (BFRF1, BSLF1, BTRF1) or much reduced fusogenic activities probably following a similarly reduced bioparticle concentration (**Fig. 3**) in this group of genes. Interestingly, while the fusogenicity of the BGLF4 virus stock was clearly compromised, the two virus stocks belonging to the 'middle bin' group, BPLF1 and BBRF1, had comparable fusion activity at the level of the control stock (**Fig. 10B**, right panel). The BBRF1 virus stock is interesting, because its infectivity is reduced by more than 50 % (**Fig. 2**) while its fusogenic activity is wild-type.

Taken together, the assay demonstrates that BALF4 is the driver of viral fusion with target cells as thought previously (Neuhierl et al., 2002). In addition, the assay unveils that virus stocks generated by ectopic expression of certain viral genes such as BBRF1 are not compromised with respect to virus fusion (**Fig. 10B**, right panel) but impaired in their infectivity (**Fig. 8C**). This observation shows that measuring virus fusion independent of virus infectivity can be a valuable new parameter in the herpesvirus field. BBRF1 is a prime example, because it encodes the capsid portal protein (**Table 1**) indispensable for loading EBV DNA into viral capsids. Upon BBRF1 knockdown, the virus stocks probably contain fewer infectious virions (they lack the viral DNA genome), but the virus stocks nevertheless show the identical fusogenic activity compared with wildtype virus indicating that fusion and viral gene expression are non-linked, independent steps in the multifaceted process of viral infection.

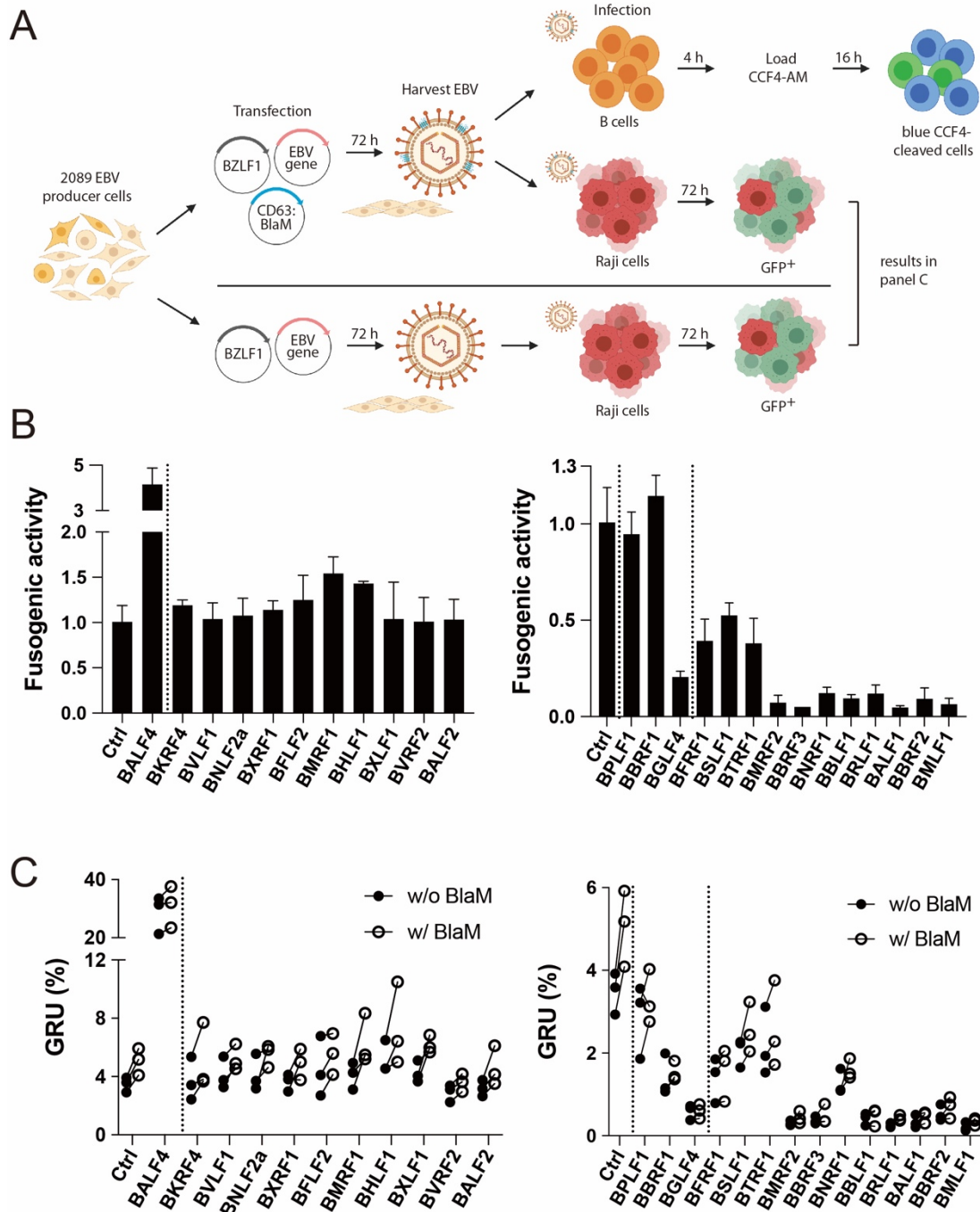


Fig. 10 Analysis of engineered EBVs obtained from 2089 EBV producer cells transiently transfected with 24 individual expression plasmids and their fusion with primary human B cells using the novel β -lactamase fusion assay.

(A) The flow chart depicts the experimental steps of the fusion assay (top pathway) and its comparison with the Raji cell-based test for infectivity (below). **(B)** Results of the β -lactamase fusion assay with supernatants of the 2089 EBV producer cell line transiently transfected with 24 individual expression plasmids encoding viral genes of the 'high bin', 'low bin' groups and three control genes. The cells were co-transfected with three plasmids as shown in panel A (plasmids encode BZLF1 [p509], CD63: β -lactamase [p7200] and one of the 24 selected EBV genes or controls) and the supernatants were tested

on primary human B cells as targets. The read-outs are based on determining the fraction of 'blue' B cells with cleaved CCF4 substrate by flow cytometry. Shown are the results from the 'high bin', 'low bin' groups and three controls separated by vertical dotted lines. **(C)** The supernatants analyzed in panel B were also tested for their infectivity of Raji cells using GFP expression as indicator of viral infection as schematically shown in panel A. For comparison, the 2089 EBV producer cell line was transiently transfected with 24 individual expression plasmids encoding viral genes of the 'high bin', 'low bin' groups and three control genes together with BZLF1 p509, only, omitting the CD63:β-lactamase expression plasmid p7200. The pairwise comparison of supernatants generated with and without CD63:β-lactamase (BlaM) is shown and the results from the 'high bin' and 'low bin' groups in the left and right graphs, respectively, are provided as in panel B.

Incorporation of CD63:BlaM slightly improves the virus titer

To study possible consequences of CD63:BlaM expression during EBV's lytic phase or upon incorporation of the fusion protein into EBV particles I compared two sets of virus stocks in Raji cell infection experiments. One set of virus stocks was generated by co-transfection of individual expression plasmids encoding the 21 members of 'high bin' and 'low bin' groups of viral genes (plus controls) with BZLF1 and CD63:BlaM into 2089 EBV producer cells. For comparison, the same set of plasmids excluding CD63:BlaM was co-transfected in parallel. The infectivity of the two sets of virus stocks was analyzed by infecting Raji cells. The fraction of infected Raji cells shown in **Figure 10C** followed my previous results depicted in **Figures 2 and 8C**. As shown in **Figure 2**, virus stocks generated with BALF4 had the highest virus titer. Other ectopically expressed viral genes of the 'high bin' group had moderately higher virus titers in terms of infectivity comparable with my findings in **Figure 2**. Similarly, virus stocks generated with individual members of the 'low bin' group showed considerably lower infectious virus titers (**Fig. 10C**, right panel). Virus stocks generated by the concomitant expression of the CD63:BlaM fusion proteins had a slight tendency to higher virus titers (**Fig. 10C**). This was a very consistent observation suggesting that the incorporation of CD63:BlaM is somewhat advantageous and can enhance virus titer but to a rather limited degree, only. More importantly, this results indicates that CD63:BlaM does not interfere or even compromise infectivity of EBV particles.

A novel assay to detect and quantify cellular fusion of extracellular particles with primary human cells and various established cell lines

The novel assay, which I introduced in the previous chapter is based on viral fusion events with targets cells and the reporter protein CD63:BlaM with which viral particles can be equipped. Examples such as BALF4 and BBRF1 demonstrate that viral

fusion can be monitored directly. The examples also show that viral fusion and viral infectivity are independent parameters that both contribute to viral success.

This opportunity allowed me to address a very related question in the field of extracellular vesicles (EVs). They are continuously released from probably all cells and EVs are believed to be messengers between cells supporting cell-to-cell communication. Moreover, there is strong belief that EVs can fuse with recipient cells (similar to viruses) such that the content of EVs, their cargos, can be physically delivered to recipient cells. The content can be microRNAs (miRNAs), for example, which could regulate gene expression in recipient cells. This hypothesis has never been convincingly demonstrated directly. Hence, I used my novel assay to prove (or refute) this long-standing hypothesis. Towards this end, I prepared generic EVs equipped with CD63:Blam as effectors from supernatants of 293T cells and incubated various types of recipient cells with these EVs to test this hypothesis.

Subpopulations of peripheral blood mononuclear cells differ in their uptake of the CD63:Blam reporter protein delivered by engineered EVs

293T cells were transfected either with CD63:Blam (p7200) or co-transfected with CD63:Blam and an expression plasmid encoding VSV-G (p5451). VSV-G is a glycoprotein of vesicular stomatitis virus (VSV) with a broad, almost universal fusogenic, cell-targeting function reflecting VSV's broad tropism. Consequently, VSV-G is widely used in combination with lentiviral or retroviral vectors to ensure their efficient fusion with target cells and delivery of the vector's genetic information. Here, I co-transfected VSV-G together with CD63:Blam to generate fusogenic EVs as a positive control to demonstrate the reliable delivery of the CD63:Blam reporter protein.

One day after transfecting 293T cells with expression plasmid DNAs, the medium was changed to plain DMEM (without FBS) and the cells were cultivated for three more days. The cell supernatants were harvested and purified by two times low speed centrifugation to remove cell debris and apoptotic bodies. Human peripheral blood mononuclear cells (PBMCs) were purified from blood donor and the cells were incubated with EV containing supernatants at 37 °C for 4 h. CCF4-AM substrate was added to the cells, which were incubated at room temperature for 16 h. Prior to their analysis by flow cytometry, the cells were stained with antibodies to specify subpopulation of cells using conventional cell markers to identify T cells, B cells, monocytes, dendritic cells (DC) and plasmacytoid dendritic cells (pDCs) (**Fig. 11A**). Supernatants with EV equipped with CD63:Blam, only, barely delivered the reporter protein to recipient cells (**Fig. 11A**). However, EVs equipped with both CD63:Blam and VSV-G are able to deliver the reporter protein very efficiently to up

to 10 % PBMCs (**Fig. 11A**). VSV-G decorated EVs led to 8 % positive T cells and about 2 % of all B cells were targeted. Monocytes showed the highest rate of fusion reaching almost 100 %, DCs showed 55 % and, lastly, pDCs showed 5 % to 10 % positive cells.

Without VSV glycoprotein, EVs can barely deliver the CD63:BlaM reporter protein to 17 different cell lines

I wanted to clarify whether my initial results with PBMCs also applied to other cells. Towards this end, two classes of EVs equipped with only CD63:BlaM or equipped with both CD63:BlaM and VSV-G were generated from supernatants of 293T, Calu-3, Caco-2, HepG2 and Huh7 donor cells by transient transfection of the respective expression plasmids. As recipient cells I employed 293T, Caco-2, A549, Calu-3, MDA-MB-231, HepG2, Huh7, LN-18, U-251MG, HEL, Mono-mac-6, THP-1, BJAB, DG-75, Elijah, Raji and lymphoblastoid cells (LCL) reflecting a broad spectrum of diverse cell types. Identical volumes of EV preparations collected from the 5 different donor cells were used to incubate the 17 recipient cell types. After addition of the CCF4-AM substrate the fractions of BlaM positive recipient cells were quantified by flow cytometry. The results are presented in five panels in **Figure 11B** summarizing results with EVs from the five different donor cells. Compared to the extremely low or mostly undetectable uptake of EVs equipped with CD63:BlaM, only, (white columns), EVs equipped with both CD63:BlaM and VSV-G led to medium and high BlaM signals (black columns) in almost all donor-recipient combinations. Supernatants from 293T and HepG2 donor cells performed very well in this assay. Caco-2 derived EVs showed a moderate ability of delivering the CD63:BlaM reporter. As recipients, U-251MG cells had the highest rate of uptake among all cells tested whereas Caco-2, A549, Calu-3, HepG2, Huh7 and LCL showed lower fractions of BlaM-positive cells (**Fig. 11B**).

Taken together, my results provide a convincing example of applying this novel fusion assay not only to virus stocks but also to physiological extracellular vesicles which all cells release. Virus-like particles, which share aspects of both types of particles, i.e., infectious EBV and EBV-derived EVs, can be investigated for their fusogenic activities and delivery of their antigenic components to immune cells demonstrating their efficacy of antigen presentation.

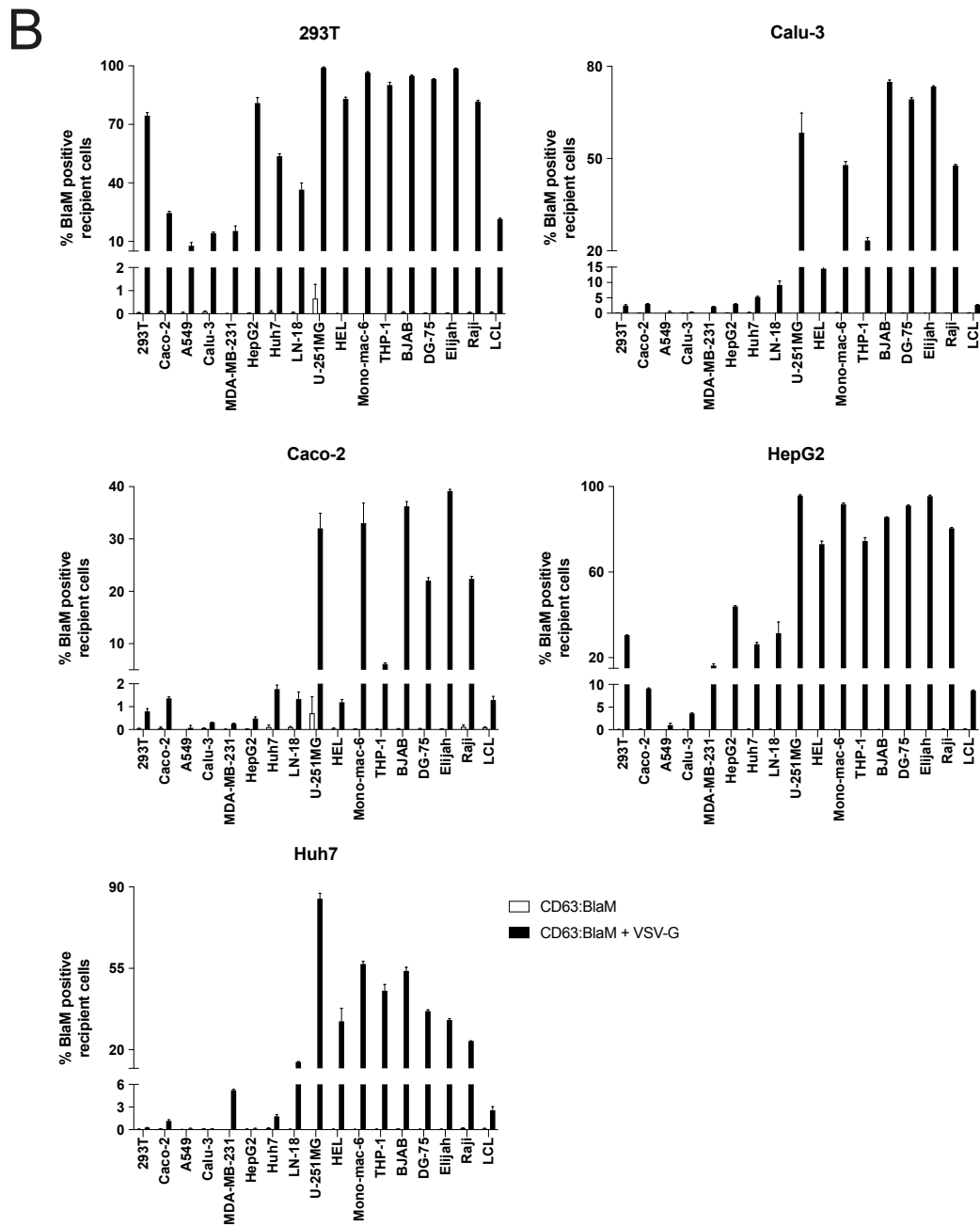
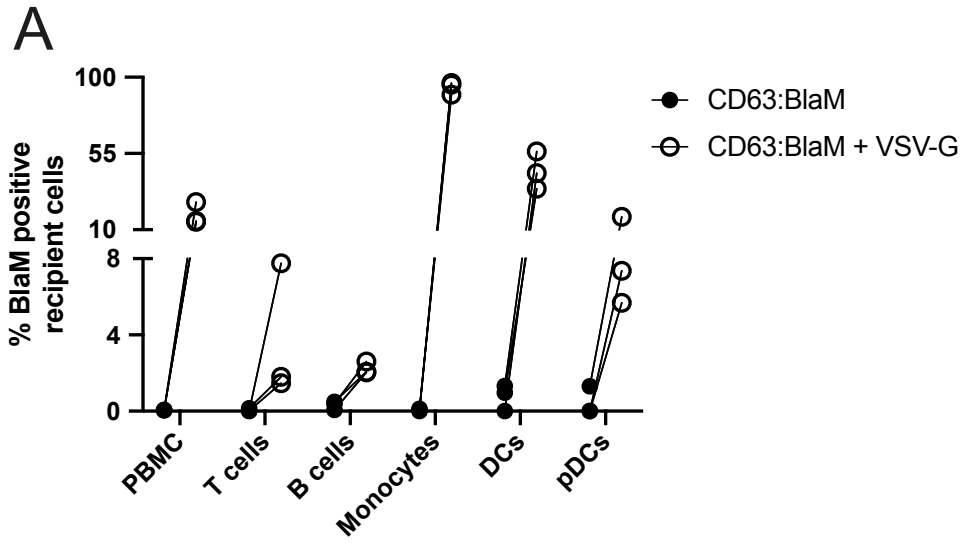


Fig. 11 A novel assay for measuring the fusogenic activity of β -lactamase-containing extracellular vesicles (EVs) generated from five different types of cells.

293T cells were transiently transfected with 12 μ g expression plasmid p7200 encoding CD63: β -lactamase with or without 8 μ g expression plasmid p5451 encoding VSV-G, a glycoprotein of vesicular stomatitis virus. One day after transfection, the medium was exchanged with plain DMEM without FBS. The conditioned medium was harvested after 3 days as described in Materials and Methods. **(A)** 500 μ l conditioned medium containing CD63: β -lactamase with or without VSV-G was incubated with 2×10^5 peripheral blood mononuclear cells (PBMCs) for 4 h. The incubated medium was removed and cells were incubated with CO_2 -independent medium containing CCF4-AM substrate at room temperature in the dark for 16 h. Antigen-specific antibodies to identify T cells, B cells, monocytes, DCs or pDCs contained in PBMCs were added and the cells were analyzed by flow cytometry. Upon β -lactamase cleavage positive cells emit light of 447 nm wavelength. Conditioned medium, which contained CD63: β -lactamase equipped EVs, only, was used as control. The percentage of β -lactamase positive cells is indicated as BlaM positive recipient cells (%). **(B)** 293T, Calu-3, Caco-2, HepG2 and Huh7 cells were used to generate supernatants with EVs containing CD63: β -lactamase with or without VSV-G. 500 μ l conditioned medium obtained from the five donor cells was incubated with recipient cells as indicated for 4 h. The conditioned medium was subsequently removed and CCF4-AM substrate was added. After 16 h, the percentage of β -lactamase-positive recipient cells was determined by flow cytometry (black columns). β -lactamase-positive cells incubated with CD63:BlaM containing EVs without VSV-G is shown (white columns).

Discussion

The problem of EBV yield and virus quality

EBV is a member of the γ -herpes virus family, which typically does not give yield to progeny when these viruses are amplified via traditional techniques. In fact, EBV (and its closest relative Kaposi sarcoma-associated herpes virus, KSHV) cannot be simply propagated in cell culture. Instead, cell lines latently infected with EBV are the source of infectious virus, which the cells produce spontaneously at low level or after induction of EBV's lytic productive phase. In many cell lines, the lytic phase can be induced upon ectopic expression of BZLF1, an immediate-early EBV gene and molecular switch (Buschle and Hammerschmidt, 2020). Almost all latently EBV infected cell lines are B cells established from Burkitt's lymphoma biopsies. Induced expression of BZLF1 in these cells is often inefficient, which results in low titer EBV stocks and inconsistent yields.

Another hurdle while working with EBV (as well as KSHV) has been the lack of viral genetics. Genetic manipulation of EBV's genomic DNA has not been possible for decades after its discovery in the sixties (Epstein et al., 1964) very much in contrast to other herpes virus such as herpes simplex virus 1. Its genetic era started more than 40 years ago in the Roizman lab using forward selection in virus infected cell cultures (Mocarski et al., 1980).

Pioneering work of my laboratory introduced a very different technology of cloning the entire EBV genome of 172 kbp in size in *E. coli* onto a single copy mini-F-factor plasmid backbone to gain access to recombinant EBVs and genetically modified EBV mutant derivatives (Delecluse et al., 1998). Genetic manipulation is done in *E. coli* using homologous recombination techniques. From *E. coli* cells, mutated genomic EBV DNA is prepared and introduced into HEK293 cells in which the virus adopts a state reminiscent of latent infection. Virus synthesis is induced in these cells by transfecting an expression plasmid coding for BZLF1 (also known as Zta, Z or EB1) and progeny is harvested from the supernatant of induced cells. This is a practical and breakthrough approach, but one obstacle of this technology was and still is suboptimal virus yield.

The impact of individual EBV genes on virus yield and virus quality

Using this system, Delecluse et al. obtained the first recombinant EBV stock from the supernatant of a HEK293 cell line derivative later termed 2089 EBV producer cells (Delecluse et al., 1998). EB virus supernatants were generated by transiently transfecting an expression plasmid (p509) encoding BZLF1. I used this cell

line throughout my work, because it yields more than 5×10^6 infectious particles per ml when Raji cells are used as EBV's target cells as I did (**Figs. 1, 2**). Infected Raji cells, which express green fluorescence protein upon infection are used to provide 'green Raji units', termed GRU, which determine the virus titer (infectivity) as indicated in my experiments. Despite this proven approach and reliable source of infectious EBV stocks, it has always been questionable, if the HEK293 cell is the ideal host to propagate the virus. The nature of these cells is probably a neuronal cell, a cell type never linked to EBV infection or synthesis. Therefore, certain viral genes might be insufficiently expressed such that virus production in HEK293 cells is suboptimal at best. Conversely, certain non-identified viral genes could exist that act as regulators of cellular or viral gene expression dampening or restricting virus production when expressed in an untimely fashion and/or at inadequately high levels. As the continuous search for another established cells that supports EBV production has not been successful, it was my task to test all available viral genes whether their single ectopic expression during virus synthesis in the 2089 EBV producer cells might yield higher yields (indicative of an insufficient expression of this particular gene of interest) or if viral genes repress virus production, which could be an indication of a negative regulator of virus production. If true, the identification of such a viral regulatory function would help to design techniques to improve virus yield from HEK293 cells. Alternatively, the identification of a viral gene that boost virus production during its enhanced expression in 2089 EBV producer cells will be another chance to improve virus yield. In case of the planned VLP-based vaccine, production of (non-infectious, harmless) virions is THE key parameter of optimal yield during the upstream GMP process of VLP manufacturing.

Interestingly, in a single study from my lab in 2002, the function of a viral glycoprotein encoded by the EBV open reading frame BALF4 was investigated. Neuhierl et al. made a genetic knockout of this gene and found that production of infectious EBV came to a full halt indicating that BALF4 is an essential gene. When Neuhierl et al. expressed BALF4 in the HEK293 cell line carrying the BALF4 knockout they observed a considerable improvement of virus titers (Neuhierl et al., 2002). They went on and found that co-transfection of BZLF1 (p509) together with BALF4 (p6515) in the parental 2089 EBV producer cell line yielded substantially higher virus titers compared to the same cells transfected with BZLF1 alone (Neuhierl et al., 2002), indicating that BALF4 is a limiting gene product during EBV production in HEK293 cells.

In my work I used this basic experimental design (with BALF4 as a proven positive control) and transfected BZLF1 together with 76 individual expression plasmids encoding single EBV genes into 2089 EBV producer cells. Supernatants from

these experiments were investigated in four different analytic schemes as shown in **Figure 1**. The results from these analyses encompassing the parameters of virus titers (**Fig. 2**), bioparticle concentration (**Fig. 3**) and physical particle concentration (**Fig. 4**) showed a very good overall correlation (**Fig. 5**). All the values obtained were arranged in descending order and the genes were color-coded based on their functional categories or, alternatively, on their expression timing (if known).

76 EBV genes and their contribution to virus titers

BALF4 scored best with regard to virus titers while the next ten top genes (BMRF1, BGRF1/BDRF1, LF1, BLRF3, BDLF2, BDLF3.5, BLLF2, BHLF1, BVLF1, BNLF2a) showed a moderate increase of virus titer, only. The role of BALF4 has been addressed previously by my laboratory and Richard Longnecker's group (Herrold et al., 1996; Neuhierl et al., 2002) and more recently by Henri-Jacques Delecluse in Heidelberg (Neuhierl et al., 2009). Together, the literature agrees on the essential role of the BALF4 encoded gB homologue of herpesviruses (also called gp110 in the EBV field) during B cell infection. My novel virus fusion assays presented in **Figure 10** demonstrates its true function as it is essential for fusion of the virus envelope with cell membranes, which commonly takes place in endosomes after receptor-mediated uptake of the virus (Chesnokova et al., 2015).

The known functions of the top ten genes down the list in **Figure 2** do not offer an immediate answer how they could contribute to the (mild) increase in virus titer. The genes fall into different functional categories and only BDLF2 and BILF1 belong to the class of membrane proteins similar to BALF4. BILF1 encodes a constitutively active G protein-coupled receptor presumably involved in signaling whereas BDLF2, one out at least 11 EBV glycoprotein is a type II envelope protein with uncertain functions (Gore and Hutt-Fletcher, 2009).

Down the lanes in **Figure 2** ectopic expression of 16 viral genes reduced virus titers by half at least with some reducing it by a factor of 10 (BLRF1, BGLF5, BTRF1, BBRF1, BFRF1, BSLF2/BMLF1, BBRF3, BNRF1, BBLF1, BRLF1, BMRF2, BGLF4, BBRF2, BMLF1, LF2 and BALF1). Infection with EBV includes several discernable steps, i.e., virus binding, endocytosis, envelope fusion, viral transcription and translation of viral proteins. The Raji cell infection assay monitors all these steps leading to the expression of green fluorescence protein, which serves as a virally encoded surrogate marker of successful infection. Therefore, virus-cell binding, virus fusion, transcription and translation could be regarded as indicators evaluating the quantity of infectious viruses in a given volume and the quality of virus stocks. Whereas quantity is an obvious feature, quality is a rather vague parameter as it describes the virus fraction of a virus stock that is fully functional, i.e., infectious, whereas the

remaining virus particles are not. This is, because they have not been properly assembled, they became damaged or essential virion components are underrepresented or entirely missing for various reasons. These particles are commonly called defective interfering particles.

It is not obvious how those EBV genes, which repress virus titer could act and, to my knowledge, there is no example in the literature that fits my experiments and data. There are seven DNA or capsid-associated early genes within the group of 16 genes that lead to a reduce virus titer. This and remaining classifications do not indicate how the viral genes could cause a trend to lower titers. Their expression could be toxic to the cell or cause problems in assembling virus components during morphogenesis as their unbalanced levels could alter protein stoichiometry (**Fig. 2**).

Bioparticle concentration profiles after ectopic expression of 76 single EBV genes

The same virus stocks were tested for their bioparticle concentrations by binding to Elijah cells. The bioparticles adhere to the Elijah cell surface and are detected using a gp350-specific antibody. The bioparticle concentrations were quantified and aligned (**Fig. 3**). BKRF4, BVLF1, BNLF2a, BXRF1, BFLF2, BMRF1, BLLF1, BHLF1, BLRF3, BXLF1, BVRF2 and BALF2 expression seemed to enhance bioparticle concentration to some degree. They are called the 'high bin' group (n=12). Expression of BFRF1, BSLF1, BTRF1, LF1, BSLF2/BMLF1, BMRF2, BBRF3, BNRF1, BBLF1, BRLF1, BALF1, BBRF2, LF2 and BMLF1, the 'low bin' group of genes (n=14) led to a reduction of bioparticle concentration. Technically, the assay measures bound particles on the surface of Elijah cells, an established human B cell line from a case of Burkitt's lymphoma (Rowe et al., 1985; Baker et al., 1998). Binding is probably mediated by the interaction of gp350 with CD21 on the cell surface, but this is speculation (Feederle et al., 2005; Pavlova et al., 2013). Operationally, I consider particle binding as a proxy for the amount of biologically active, i.e., cell binding virus particles contained in virus stocks. A functional classification of the genes of the 'high bin' and 'low bin' groups were classified according accepted criteria was not very informative nor was expression timing (**Fig. 3A,B**). Among the 26 genes, ten gene products are DNA or capsid associated, three are membrane proteins, five are tegument proteins, five are non-structural proteins and three proteins have no known function. It remains unclear which specific function might enhance or reduce the capacity of producing bioparticles as measured in the Elijah cell binding assay.

Quantification of physical particle concentration of the 76 EB virus stocks

Besides measuring virus titer and bioparticle concentration, identical virus

stocks were quantified using the NTA instrument that can detect and record the particles in a predefined size range (100 nm – 200 nm) by their zeta charges. The normalized results were arranged in rank order from highest to lowest. The top ten genes are BFLF2, BILF1, BcLF1, BKRF4, BHLF1, BVRF1, BVLF1, BORF2, BLRF3 and BGRF1/BDRF1. BRRF2, BCRF1, BRLF1, BFRF1A, BFRF1, BSLF2/BMLF1, BGLF5, BBRF3, BBLF1, BKRF2, BNRF1, BSLF1, LF2, BBRF2, BALF1 and BMLF1 have the lowest physical particle concentrations (**Fig. 4**). The quantification inevitably included cell debris, protein aggregates, cellular fragments and any sort of cellular particles such as extracellular vesicles and exosomes that fall into the same size range causing background interference. This parameter, however, can define real physical particles compared to bioparticles. Among the 26 genes selected, 13 encode DNA or capsid-associated proteins, three are membrane proteins, five are tegument proteins, three are non-structural proteins and two are proteins of unknown function (**Fig. 4A**). By the definition of expression timing, nine are expressed early, nine are expressed late and eight have unknown expression timings (**Fig. 4B**). Again, there is no obvious correlation between functional groups or expression timing versus a gain or loss of the number of physical particles.

High correlation between the three characteristic parameters of virus stocks

Since the virus titers, bioparticle concentrations and physical particle concentrations were recorded, it is worth to investigate the interrelation between each pair of characteristics and examine the reliability of the measurements. Mean values of **Figure 2-4** were transformed to rank orders and listed in parallel. The ordinal table was assessed by Spearman rank method and the result is shown as a heatmap and the correlation coefficients (R^2) were indicated in the grids (**Fig. 5A**). Bioparticle concentration vs. virus titer is 0.7651; physical particle concentration vs. virus titer is 0.7396; physical particle concentration vs. bioparticle concentration is 0.8338. The coefficients clearly point to a strong positive correlation. Similarly, the value of 0.8338 between physical particle concentration and bioparticle concentration is highest suggesting that physical particle numbers mostly reflect the number of intact virus particles that bind to the surface of Elijah cells.

No distinct category of protein function contributes significantly to virus titer, bioparticle concentration or number of physical particles.

The contributions of all genes investigated to the three measured parameters are listed in **Table 1**. Mean values of three characteristics (**Fig 2A-4A**) were extracted and provided as box plots (**Fig. 5B**). Each dot represented an EBV gene and red dots

stand for values obtained by ectopic expression of BALF4. Virus titers, bioparticle and physical particles were analyzed by the Kruskal-Wallis rank sum test (**Table 2**). The overall p values indicated that there were no significant differences among groups and also a pairwise comparisons using the Wilcoxon rank sum test suggested no statistically firm difference regarding attributed protein functions, virus titers, bioparticles and physical particles of the virus stocks. Similarly, examining a possible significant contribution by the category expression timing was not informative.

I interpret the outcome of these analyses to mean that many of the selected viral genes contribute to various aspects of virus production. Hence, there is no clear direction towards a certain group of protein function or time window of gene expression as documented here.

Expression of BALF4 together with selected viral genes does not enhance virus titers with one exception

In **Figure 2** the ectopic expression of BALF4 together with BZLF1 led to a substantial increase in virus titer but not to an increase in bioparticles or physical particle concentration (**Fig. 3** resp. **4**). Together, this finding suggests that the expression of BALF4 improved the quality of single infectious virions in the virus stock but did nothing to change the concentration of virions per se. No other EBV genes showed a similar level of superior infectivity compared with BALF4 but certain EBV genes enhanced it to a limited degree (**Figure 2**). Intriguingly, it was unclear whether co-expression of BALF4 together with these viral genes might further boost virus titers (or infectivity) beyond BALF4 levels. Among the top ten viral genes tested only BVLF1 showed a 1.5-fold increase in virus titer compared with the BALF 4 only control and the remaining nine candidates. BALF4 in combination with BVLF1 raised the virus titer 12-fold. Ectopic expression of BVLF1 led to more virus particles (**Figs. 3** and **4**) in contrast to BALF4 pointing to a combination of two different effects which together improve virion quality (BALF4) and quantity (BVLF1). Other viral genes tested in this experiment in combination with BALF4 did not have a discernable contribution suggesting that BALF4 is probably the only fusogenic EBV protein.

shRNA mediated knockdown of 24 selected viral transcripts identifies essential and dispensable viral genes

To further investigate the role of certain EBV genes during virus production, I employed the shRNA technology to knockdown selected viral transcripts (using sets of three shRNAs per target) of 10 genes that enhanced (BKRF4, BVLF1, BNLF2a, BXRf1, BFLF2, BMRF1, BHLF1, BXLF1, BVRF2, BALF2; the 'high group') or decreased bioparticle concentration (BFRF1, BSLF1, BTRF1, BMRF2, BBRF3, BNRF1, BBLF1,

BRLF1, BALF1, BBRF2, BMLF1; the 'low bin' group) together with three viral genes and controls (BPLF1, BBRF1, BGLF4, GFP, Ctrl) (**Fig. 8A**). Knockdown efficiencies as determined by co-expression of individual shRNAs together with the corresponding luciferase reporters in 293T cells were excellent (**Fig. 7A**). Contrary to expectations of lab members, the functionality of the stably expressed shRNAs was also perfect (**Fig. 7B**). Upon induction of virus production in the 24 shRNA expressing EBV producer cell lines some shRNA sets caused severe consequences with respect to virus titers (**Fig. 8B,C**) and bioparticle concentration (**Fig. 9**). The results supports the validity of this experimental approach despite the abundance of viral lytic transcripts during the productive lytic phase in 2089 EBV producer cells.

As expected, EBV production was not affected in shGFP producer cells (**Fig. 8B**) but many stably expressed shRNAs caused a severe reduction of virus titers (**Fig. 8C**) documenting anticipated consequences of the shRNA knockdown approach. Virus stocks obtained from shBALF4 cells revealed a dramatic decrease in virus titer, which is in agreement with a BALF4 knockout EBV derivative (Neuhierl et al., 2002). Ectopic expression of BALF4 in shBALF4 EBV producer cells partially restored the virus titer as expected from the essential function of EBV's gB homologue during virus fusion (**Fig. 10C**).

Noticeably, the virus stock of shBFLF2 EBV producer cells had a roughly 1.9-fold increased virus titer, but, after transfection of BALF4 the virus titer dropped to the level of the reference (**Fig. 8B**). BFLF2, which was reported to be essential for viral nuclear egress and DNA packaging interacts with BFRF1 (Granato et al., 2008; Dai et al., 2020). While both BFLF2 and BFRF1 have partially overlapping function, they have opposite effects on regulating virus titer, bioparticle concentration and physical concentration (**Figs. 8B, 9B**). Furthermore, BFLF2 was classified to belong to the 'high bin' group, while BFRF1 was found to be a member of the 'low bin' group. The results can be interpreted to mean that both genes are critical for virus production but their expression in 2089 EBV producer cells is not optimally regulated.

The shRNA mediated knockdown of BKRF4, BNLF2a, BHLF1 and BXLF1, which are members of the 'high bin' group demonstrated a similar and moderate reduction of virus titers. The Murata group found that BKRF4 is able to increase virus titers (Masud et al., 2017), which my measurement confirmed as bioparticle concentration increased upon ectopic expression of this gene (**Fig. 3**). BNLF2a was shown to be upregulated by BZLF1 and is involved in immune invasion from cytotoxic T cells (Almohammed et al., 2018), but has no reported function in virion biogenesis. Currently, a BHLF1 knockout EBV demonstrated its limited capacity of transforming B cells (Yetming et al., 2020). BXLF1 has been identified as the viral thymidine kinase and, consequently, its knockdown reduced the virus titer, supporting its supportive

role during ribonucleotide synthesis in EBV producing cells. Similarly, the knockdown of BALF2 and BMRF1, EBV's major DNA binding protein and the DNA polymerase processivity factor, respectively, repressed the function of two viral proteins that are essential during lytic DNA replication (Fixman et al., 1992). During EBV replication, BMRF1 was also found to have a role in late gene transcription (Sugimoto et al., 2013). The ectopic expression of BMRF1 increased the virus titer slightly (**Fig. 2** and **8C**), suggesting that it could limit virus production, whereas ectopic expression of BALF2 had no measurable effect in my experiments. A very similar trend was observed with BVRF2, which is involved in capsid maturation and folding (Sugimoto et al., 2019).

For EBV late genes transcription, a group of genes form the pre-initiation complex (vPIC) consisting of BVLF1, BGLF3 and BFRF2 which, together with others viral components is involved in very efficient transcription of late genes encoding structural proteins (Aubry et al., 2014; Gruffat et al., 2016; Li et al., 2019). It was therefore not surprising to note that the shRNA mediated knockdown of BVLF1 reduced the virus titer (**Fig. 8B**), which, on the contrary, was substantially higher, when BVLF1 was ectopically expressed (**Fig. 2** and **8C**). BXR1 showed the same trend as BVLF1. BXR1 is a homologue of HHV1 UL24 and a nuclear egress protein critically involved in cytoplasmic capsid export. Consequently, its knockdown was detrimental to virus titer (**Fig. 8B**), while its ectopic expression increased it (**Fig. 2** and **8C**).

The shRNA strategy directed against genes of the 'low bin' group fails to identify a viral gene with regulatory functions controlling EBV's lytic phase

In the 'low bin' group and in case of the three viral control targets (BPLF1, BBRF1, BGLF4) a knockdown of certain gene products (BBRF1, BGLF4, BFRF1, BMRF2, BBLF1, BRLF1, BBRF2, BMFL1) had an expected severe or devastating effect on virus titer and a similar but less pronounced effect on bioparticle concentration (**Figs. 8** and **9**). This loss of virus production is in line with an essential function of these eight genes, a conclusion that is supported by the known roles of some of these viral gene products. For example, the BBLF1 protein was reported to be involved in virus budding and shown to be colocalized with gp350 to *trans*-Golgi network (TGN) (Chiu et al., 2012). Another example is BBRF2, which encodes an EBV tegument protein involved in secondary envelopment with the final viral envelope (He et al., 2020). Upon the knockout of BBRF2 in EBV genomic DNA by the CRISPR/Cas9 technique, viral infectivity subsequently dropped substantially (Masud et al., 2019). A third example is BMRF2, a glycoprotein, which is reported to facilitate virion binding to β 1 family integrins on target cells contributing to EBV infection. It is somewhat surprising to observe this effect with Raji cells, a human B cell line, because BMRF2

was claimed to play this role with polarized oral epithelial cells, only (Xiao et al., 2007, 2008).

In the 'low bin' group, a knockdown of BTRF1, BBRF3 or BALF1 had no measurable effects on virus titers or bioparticle concentration suggesting that their undisturbed expression levels are concordant with optimal gene expression or that these proteins are not limiting for virus production. However, their ectopic expression was counterproductive (**Figs. 2 and 8**).

Unexpectedly, the knockdown of all 11 viral transcripts failed to reveal a phenotype compatible with a viral function that acts as a repressor or controller of virus production. This expectation was based on the ectopic, probably unphysiological expression of 11 EBV genes which reduced bioparticle concentration and, concomitantly, virus titers (**Fig. 2 and 3**). Besides adverse effects of different nature, the unadjusted, probably elevated expression of a viral repressor of lytic functions could reduce virus titers or compromise bioparticle production. Conversely, a knockdown of such a repressor should yield the opposite effect increasing virus titers along with bioparticle concentration substantially. The results in **Figure 8B and C** clearly speak against the existence of such a viral factor.

Comparison of bioparticle concentration of virus stocks generated by ectopic expression of viral genes and stocks from shRNA expressing EBV producer cells

Virus stocks generated by ectopic expression of individual genes in the parental 2089 EBV producer cells were compared with virus stocks generated from shRNA knockdown producers. Obviously, the knockdown of BALF4 produced fewer bioparticles than its ectopic expression in the parental producer cells, which showed no effect on bioparticle numbers (**Figs. 4 and 9B**). Consistently, the ability of producing bioparticles from shRNA knockdown cells was impaired in all 10 selected genes of the 'high bin' group. In the 'low bin' group, bioparticle concentrations increased after knocking down BBRF3, BALF1, and BMLF1 but declined in shBGLF4 producer cells consistent with the trend seen with virus titers (with BMLF1 as an exception regarding this parameter). Variations of virus titers and bioparticle concentrations were small in shBPLF1, shBBRF1, shBFRF1, shBTRF1, shBMRF2, shBNRF1, and shBBRF2 EBV producer cells, which indicate a co-regulation of virus titer and bioparticle concentration.

Quantitation of the fusogenic activity of EBV virions

An analysis of the fusion event that takes place when the viral membrane of an enveloped virus and membranes of the virus' target cell intersect is very difficult

because of the transient nature of the fusion event and the very local disturbance of the cellular membrane. A common surrogate model consists of two established cell lines that are co-cultivated. One of which encodes a viral fusion moiety expressed on its plasma membrane, the other cell line serves as target cell expressing the cognate receptor of the virus-encoded fusogenic protein(s) or the assembled protein complex. In this simple model cellular fusion mediated by the action of the fusogenic viral effector is believed to mimic fusion events during viral infection. Clearly, this is an artificial model that relies on syncytia formation, which can be monitored with dyes or microscopically. Often, and in particular in case of herpesviruses such as EBV, multiple viral glycoproteins contribute to the final fusion such that it is difficult to reconstruct all these viral components in their correct composition and stoichiometry in such a model.

My alternative is shown in **Figure 10A**. The technology is based on the bacterial enzyme β -lactamase (BlaM), which was introduced to detect fusion of HIV virions with CD4 T cells and other possible HIV target cells a rather long time ago (Cavrois et al., 2002). The authors used a chimeric BlaM-Vpr enzyme which targets the enzyme into the lumen of the HIV envelope as about 100 to 200 Vpr molecules associate strongly with the HIV nucleocapsid protein (Muriaux and Darlix, 2010). The enzyme, when delivered to substrate-containing target cells cleaves the β -ring of the CCF4 substrate, causing the emission wavelength shift based on fluorescence (Förster) resonance energy transfer, FRET. It has been used for analysis of viral fusion and the method has also been improved (Jones and Padilla-Parra, 2016; Cavrois et al., 2014). I adopted this technology to make it work with EBV. The diagram in panel A of **Figure 10** depicts the preparation of modified complete EBVs encompassing a protein reporter (here a fusion protein consisting of CD63 and β -lactamase assembled into the virus' envelope) to measure fusogenic activity of virions directly and quantitatively. To measure the impact of certain ectopically expressed viral genes, virus stocks were generated by co-transfecting plasmids encoding BZLF1 (p509), CD63:BlaM (p7200) and individual, selected EBV gene into 2089 EBV producer cells. The virus stocks were harvested and incubated with human primary B cells, the primary target of EBV. After loading the CCF4 substrate into recipient cells, the fusogenic activity could be measured by detecting the percentage of cleaved substrate in these cells by flow cytometry. The results are shown in panel B of **Figure 10**. In parallel, the same virus stocks were incubated with Raji cells to measure their virus titers. For comparison, the virus stocks were prepared without the CD63:BlaM expression plasmid which were quantified in parallel as well.

BALF4 has been regarded as EBV's gB homologue, which in other herpes viruses is known to mediate viral fusion. In my assay, ectopic expression of BALF4 showed

outstanding fusogenic activity compared with the control (**Fig. 10B**). Very much in contrast, co-expression of all other viral genes of the 'high bin' or 'low bin' groups did not increase viral fusion beyond control levels indicating that BALF4 is the only viral protein that mediates fusion. Its genetic deletion abrogates viral infectivity (Neuhierl et al., 2002) supporting my finding nicely.

Alternative application of the CD63:BlaM fusion assay

My colleagues and I made use of the CD63:BlaM reporter protein in a virus-related context investigating the function and transport of EBV miRNAs when contained in extracellular vesicles (EVs) (Albanese et al., 2020). The key question here differed from my work with EBV because I wanted to enumerate the rate of EV-cell fusion to learn whether EV-borne miRNAs can be delivered to recipient cells to regulate cellular transcripts. This hypothesis has been maintained in the EV field ever since a landmark publication using EVs from latently EBV infected B cell lines provided circumstantial evidence supporting this idea (Pegtel et al., 2011). To detect EV-cell fusion events and quantify them, EV donor cells were transfected with CD63:BlaM (p7200) alone or were co-transfected with CD63:BlaM and VSV-G (p5451). VSV-G is a highly fusogenic glycoprotein from vesicular stomatitis virus. EVs released into the cell supernatant were harvested and peripheral blood mononuclear cells (PBMCs) (**Fig. 11A**) were incubated and measured by flow cytometry. Cell subpopulations were identified with specific antibodies to differentiate them according to their cell surface markers. Barely any EV fusion was detected in total PBMCs or PBMC subpopulations (T cells, B cells, monocytes, dendritic cells (DCs) and plasmacytoid dendritic cells (pDCs)). On the other hand, when EVs were used from donor cells co-transfected with CD63:BlaM and VSV-G these EVs readily delivered the reporter protein to different target cells as demonstrated by flow cytometry (**Fig. 11A**). EVs generated using five different donor cell lines with or without VSV-G and tested with 17 different recipient cells showed exactly the same phenotype (**Fig. 11B**).

In conclusion, the novel fusion assay with a protein reporter that can consist of a membrane protein (such as CD63 or gp350 of cellular and viral origin, respectively) and an enzyme of prokaryotic origin (BlaM) can be broadly applied to detect fusion events between EVs or enveloped viruses with any recipient cell type such as primary or established cells from any species. Given the failure to observe any fusion of EVs with all recipient cells tested it is very likely that no cellular protein exists with fusogenic functions reminiscent of viral glycoproteins such as VSV-G or gB encoded by EBV and studied here. My work also suggests that 'fusogenic' proteins have no cellular precedent but instead have evolved together with enveloped viruses.

Materials and Methods

Cell culture and cell lines

RPMI 1640 medium supplemented with 10% FBS, 100 U/ml penicillin-streptomycin, 1 mM sodium pyruvate, 100 pM sodium selenite, and 0.04% α -thioglycerols is used as universal cell culture medium. HEK293T cells were cultivated in DMEM supplemented with 10% FBS and 100 U/ml penicillin-streptomycin. CD63:BlacM transduced-293T, Calu-3, Caco-2, HepG2 and Huh7 cells were cultivated with 10% FBS, 100 U/ml penicillin-streptomycin, and 1% non-essential amino acid (NEAA) DMEM. (1) Peripheral blood mononuclear cells (PBMCs), (2) BJAB, (3) DG-75, (4) Elijah, (5) a lymphoblastoid cell line (LCL), which was human primary B cells infected with EBV, (6) Raji, (7) Mono-mac-6, (8) THP-1, (9) HEL, (10) LN-18, (11) U-251MG, (12) A549, (13) Calu-3, (14) HepG2, (15) Huh7, (16) MDA-MB-231, and (17) Caco-2 were cultivated with supplemented RPMI 1640 culture medium. 2089 carrying HEK293 EBV producer cells were cultivated in supplemented RPMI 1640 medium containing 100 μ g/ml hygromycin B. Lentivirally transduced EBV producer cells were cultivated in supplemented RPMI cell culture medium and co-selected with 100 μ g/ml hygromycin B and 3 μ g/ml puromycin after initial selection with 10 μ g/ml puromycin for 7 days. All cells were incubated in a 5% CO₂ and water-saturated atmosphere at 37°C.

Preparation of extracellular vesicles depleted medium

500 ml RPMI 1640 medium and 100 ml fetal bovine serum (FBS) were mixed and supplemented with 5 ml penicillin-streptomycin (10,000 U/ml), 5 ml sodium pyruvate (100 mM), 500 μ l of 100 nm sodium selenite and 500 μ l of 43.3% α -thioglycerols. The medium was ultracentrifuged using a SW32 or SW28 swinging-bucket rotor (Beckman) at 100,000 g at 4°C for at least 16 h. The supernatant was collected and filtrated using a 0.22 micron filter. The EV (exosome) depleted and filtered medium was mixed 1:1 (vol/vol) with plain RPMI 1640 medium to adjust the concentration to 10% fetal bovine serum in the ready-to-use EV (exosome) depleted (ex⁻) RPMI 1640 medium.

Transient transfection of 2089 EBV producer cells

6.5×10^5 EBV producer cells (Delecluse et al., 1998) were seeded in 6-well cluster plates. After overnight incubation, the cell medium was exchanged with 2 ml EV depleted (ex⁻) medium. 0.5 μ g BZLF1 and 0.5 μ g expression plasmid DNAs were mixed in a vial with 100 μ l plain RPMI 1640. In another vial 100 μ l plain RPMI 1640

was mixed with 6 μ l PEI MAX[®] (6 μ l PEI MAX[®] per 1 μ g plasmid DNA). The content of both vials was combined rigorously mixed, the mixture was incubated at room temperature for 20 min and was added to the EBV producer cells in a single well of a six-well cluster plate.

shRNA expression vector construction and sequence design of shRNAs

The DNA sequences of selected EBV genes were obtained from the database of National Center for Biotechnology Information (NCBI). The FASTA format sequences were used for feeding the splashRNA tool (<http://splashrna.mskcc.org>) to predict potent shRNA sequences. According to the splashRNA score, the top three antisense guide sequences were chosen, ordered as synthetic oligonucleotides and inserted into the miR-3G frame of the basic shRNA construct (p6924 in our plasmid database). For each chosen EBV gene a knockdown pool of three shRNA constructs was designed and realized. The antisense guide sequences of individual EBV genes are marked in the entries shown in **Table 7**, which have compatible ends to be cloned into AvrII and EcoRI restriction sites in the basic shRNA construct p6924. The shRNA constructs contain the puromycin resistance gene as selection marker.

Virus titer measurement (infectivity)

The virus stocks were generated by transient DNA transfection of the 2089 EBV producer cells and the supernatants, harvested 3 days after transfection, were subsequently tested for infectious virus. Specifically, 5 μ l virus stocks was added to 1×10^5 Raji cells in a volume of 2 ml cell culture medium and incubated for 3 days. The infected cells which express green fluorescence protein were determined and the fraction of GFP-positive cells, termed green Raji unit (GRU), was quantified by flow cytometry (BD FACSCanto[™]).

Bioparticle quantification (Elijah cell binding assay)

2×10^5 Elijah cells were incubated with 20 μ l of the harvested virus stocks. The mix was agitated on a mixing roller at 4 °C for 3 h. The cells were pelleted at 500 g at 4 °C for 10 min and washed with 1 ml ice-cold staining buffer (1% FBS and 2 mM EDTA in PBS). The anti-gp350 antibody (6G4) coupled to Alexa647 in 50 μ l staining buffer (1:250 dilution) was added and the Elijah cells were incubated at 4 °C for 20 min. 1 ml staining buffer was added and the cells were washed and resuspended in 300 μ l staining buffer and analyzed by flow cytometry (BD FACSCanto[™]). The Elijah cells were analyzed for their fluorescence in the appropriate channel to obtain mean fluorescence intensity (MFI) data. MFI is an indirect measure of bound virus and correlates with the number of viral particles attached to the surface of Elijah cells.

Physical particles measurement (Nanoparticle tracking analysis)

The physical particle concentration was measured using the ZetaView PMX 110 instrument (Particle Metrix), which can perform nanoparticle tracking analysis (NTA). Harvested virus stocks were diluted with PBS to adjust the concentration of particles to about $10^7 - 10^8$ particles per ml. Standard calibration beads (102.7 ± 1.3 nm) (Polysciences) were used to confirm the range of linearity of the instrument. 1 ml diluted supernatant samples were injected for analysis. All samples in the chamber were recorded at 11 positions in three cycles. Pre-acquisition parameters were set to 75 sensitivity, 50 shutter speed, a frame rate of 30 frames per second and 15 trace length. The post-acquisition parameters were set to a minimum brightness of 20, a minimum size of 5 pixels and a maximum size of 1000 pixels. Particle concentration and particle size were measured and documented and the images were analyzed using the ZetaView 8.04.02 software.

Luciferase reporter construction

Three corresponding target/sense sequences were inserted into the dual luciferase reporter plasmid psiCHECK2 (p5264). The sequences were inserted downstream of the Renilla luciferase coding sequence using the restriction enzyme sites XhoI and NotI. Firefly luciferase is used as internal control. The shRNA target sequences are shown in **Table 8**.

Luciferase assay

2×10^5 293T were seeded in a 24-well cluster plate. After overnight incubation, cells were co-transfected with 100 ng psiCHECK2 luciferase reporter plasmid and 300 ng individual corresponding pCDH shRNA expression plasmids. An empty pCDH shRNA expression plasmid (p6924) was transfected as control. Cells were lysed after 24 h and luciferase activity was measured using the Orion luminometer (Berthold). To detect the knockdown efficiency of stably shRNA transduced 2089 EBV producer cells, 1×10^5 producer cells were seeded in a 24-well cluster plate. After overnight incubation, cells were transfected with 100 ng corresponding psiCHECK2 luciferase reporter plasmid. An empty psiCHECK2 luciferase (p5264) reporter plasmid was transfected as control. After 24 h, cells were lysed and the luciferase activity was measured using the Orion luminometer.

β -lactamase (BlaM) fusion assay

EBV particles equipped with CD63:BlaM were generated by co-transfecting 6×10^5 2089 producer cells with expression plasmids encoding CD63:BlaM (p7200, 0.25 μ g)

and BZLF1 (p509, 0.25 µg) together with 0.5 µg plasmid DNA encoding single EBV genes to generate virus supernatants for further testing. The open reading frame of human CD63 is C-terminally fused to a codon-optimized β-lactamase via a G₄S linker and cloned into the expression plasmid pcDNA3.1 (+) (p5267).

For large scale production of CD63:Blam equipped EVs, 1x10⁷ cells (293T, Calu-3, Caco-2, HepG2 and Huh7 cells) were seeded in 13-cm dishes and the cells were transfected with 12 µg p7200 alone or together with 8 µg p5451 (VSV-G). One day after transfection, the medium was exchanged with plain DMEM cell culture medium with 4 g/L D-glucose. The supernatants were harvested after 72 h.

To evaluate the fusogenic activities of different virus stocks, 2x10⁵ human primary B cells were incubated with 5 µl virus supernatants. Alternatively, to evaluate the fusogenicity of EVs equipped with CD63:Blam, 2x10⁵ PBMCs or 17 different recipient cells were incubated with 500 µl EV containing supernatants harvested from the five different donor cell lines (293T, Calu-3, Caco-2, HepG2 and Huh7 cells) for 4 h at 37 °C. To assess the fraction of Blam positive cells, primary B cells were analyzed directly but adherent cells were washed and trypsinized for further analysis. All cells were re-suspended in 100 µl of CCF4-AM staining solution in a 96-well plate. The staining solution consisted of 2 µl CCF4-AM (membrane-permeant ester forms of the negatively charged fluorescent β-lactamase substrate), 8 µl Solution B (K1095, Thermo Fisher Scientific) and 10 µl of 250 mM Probenecid (P8761, Sigma) in 1 ml CO₂-independent medium (18045-054, Thermo Fisher Scientific). After 16 h incubation in the dark at room temperature, the Blam-positive recipient cells were analyzed by flow cytometry (BD LSRFortessa™). The CCF4 FRET substrate is excited with 409 nm wavelength laser (violet). The non-cleaved substrate emits light with 520 nm wavelength (green) while the cleaved substrate emits light with a wavelength of 447 nm (blue).

Isolation and preparation of human primary B cells from adenoids

Human primary B cells were purified from adenoidal tissues, which were chopped with blades and washed with PBS. The mashed tissues were filtered with 100 µm sterile strainer (352360, Falcon®) and the cells were transferred to a sterile 50 ml tube. The volume was increased with PBS to 30 ml, 1 ml defibrinated sheep blood (SR0051D, Thermo Fisher Scientific) was added and mixed (to sediment T cells in the next step). The cell suspension was slowly layered on top of 15 ml Pancoll human (density: 1.077 g/ml) (P04-60500, PAN-Biotech) in a 50 ml tube. Samples were centrifuged at 1,900 rpm at room temperature for 30 min without brake. The interphase (white band) was collected and transferred to a new tube. The cells were washed three times with PBS and centrifuged at different speeds of 1,500, 1,400 and

1,200 rpm for 10 min.

Preparation of peripheral blood mononuclear cells (PBMCs)

20 ml freshly drawn human blood was mixed with 20 ml PBS. EDTA was added in the solution to have final concentration 2 mM to prevent coagulation. The cell suspension was added slowly on top of 10 ml Pancoll human (density: 1.077 g/ml). The two-step gradient was centrifuged at 2,000 rpm, no brake, for 30 min. The buffy coat layer (white interphase) containing monocytes, T and B cells was extracted carefully.

Physical particle concentration of formulated cell culture media

To investigate the concentration of extracellular vesicles (EVs) in fresh and spent media of different cell culture media were measured using a nanoparticle tracking analysis (NTA) instrument. The results are shown in **Figure 12A in the appendix**. Seven different formulated media and samples of cell culture media were analyzed. (i) 'RPMI⁻' was plain RPMI 1640 medium purchased from the manufacturer; (ii) 'RPMI⁺' was plain RPMI 1640 medium with all supplements for cell culture excluding fetal bovine serum (FBS). (iii) 'Common medium' consisted of 'RPMI⁺' and 10% FBS and was used to cultivate cells *in vitro*. (iv) 'Ex⁻ medium' (exosome-depleted medium) was prepared by sedimenting 35 ml of 'common medium' by ultracentrifugation in a SW32 or SW28 swing-out rotor (Beckman) at 4 °C for at least 16 h. 30 ml of the supernatant was harvested to yield 'Ex⁻ medium'. (v) 5 ml of the remaining medium was used to resuspend the 'medium pellet' that had formed during sedimentation. To quantitate particles numbers, i.e., EVs, in conditioned, spent medium, 2 ml of 'common medium' or 'ex⁻ medium' each were incubated with producer cells in 6-well cluster plates. Three days later, the media were collected and filtered using a 1.2 micron syringe filter and termed (vi) 'conditioned com' and (vii) 'conditioned ex⁻', respectively.

Using the NTA instrument, the particles contained in RPMI⁻ could not be detected and RPMI⁺ was merely above the threshold level of the instrument of 10⁷ particles per ml (**Fig. 12A**). Unexpectedly, 'ex⁻ medium' contained almost as many particles as 'common medium' (**Fig. 12A**), but particle concentration was about three-fold higher in the resuspended 'medium pellet' after ultracentrifugation of 'common medium' indicating that physical depletion of EVs contained in FBS is partially effective, at least. After three days of cell culture with 2089 EBV producer cells, conditioned common medium ('conditioned com') and 'conditioned ex⁻' medium showed small increases in particle concentration as documented in **Figure 12A**.

To analyze conditions of virus production, 2089 EBV producer cells were cultivated in 2 ml 'ex' medium' in individual wells of 6-well cluster plates for three days before physical particle concentration was measured. Different starting conditions were employed and the resulting particle concentrations are shown in **Figure 12B**. At the start of cell culture, (i) 'ex' medium', which was used to cultivate 2089 producer cells in the subsequent experiments, was used at the start of the analysis also shown in **Figure 12A** (rightmost sample); (ii) 3 μ l transfection reagent PEI Max, only, was added to 2 ml of 'ex' medium' (PEI); (iii) 0.5 μ g empty pCMV vector (p6816) was complexed with 3 μ l PEI Max and added (Vec); (iv) 0.5 μ g BALF4 (p6515) was complexed with 3 μ l PEI Max and added (BALF4). To analyze virus stocks generated after lytic induction of the 2089 EBV producer cells for three days, (v) 0.5 μ g BZLF1 (p509) was complexed with 3 μ l transfection reagent PEI Max and transfected (BZLF1); (vi) 0.25 μ g p509 and 0.25 μ g p6515 were complexed with 3 μ l PEI Max and transfected (BZLF1 + BALF4). All conditioned media were harvested three days after transfection and filtered.

The addition of 3 μ l PEI Max led to a small increase of particle counts in all three samples of PEI, Vec and BALF4 compared to 'conditioned ex' medium. In induced 2089 EBV producer cells transfection of BZLF1 alone or in combination with BALF4 led to a clear gain in particle number probably because the supernatants contained viral particles and additional debris as a consequence of virus release and production by the lytically induced cells.

Comparison of two cultivation conditions using different cell culture media

To monitor possible differences when using 'ex' medium' for cultivating cells, 2089 EBV producer cells were seeded in 6-well cluster plates. On the next day and prior to DNA transfection, the medium was exchanged with 'common medium' or 'ex' medium' (**Fig. 12A**). Under these two different conditions, cells were transfected with BALF4 (p6515), BZLF1 (p509), BZLF1 plus BALF4, or the transfection reagent PEI Max, only. The four types of conditioned media were harvested three days after transfection. The media were analyzed regarding virus titer (Raji cell infection assay; **Fig. 2**) and bioparticle concentration (Elijah cell binding assay; **Fig. 3**). The results are shown in panel A and B, respectively, of **Figure 13 in the Appendix**. No virus stocks were generated when the cells were treated with PEI Max, only, or transfected with BALF4 alone. When BZLF1 and BALF4 were co-transfected, the virus titer was clearly higher compared to cells transfected with only BZLF1 (**Fig. 13A**). Under all conditions, virus stocks generated from cells cultivated in 'ex' medium' showed slightly higher virus titer and bioparticle concentration compared with 'common medium' (**Fig. 13B**).

Flow cytometry (FACS) analysis of subpopulations of PBMC

5x10⁵ PBMCs were incubated with 1 µl antibody at 4°C for 30 min, when cells were washed with PBS and resuspended in staining buffer (1% FBS and 2 mM EDTA in PBS). The cells were analyzed by flow cytometry using a BD LSRFortessa™ instrument.

Table 3. Antibodies used for the analysis of cellular subpopulations contained in PBMCs

Antibody	Clone and catalog no.	Company
CD19-APC	HIB19, 17-0199-42	BD Biosciences
CD3-APC	SP34-2, 557597	BD Biosciences
CD11c-APC	3.9, 301613	BioLegend
CD14-PE	MEM-15, 21279144	ImmunoTools
CD303-APC	AC144, 130-097-931	MACS
CD304-PE	REA774, 130-112-045	MACS

Table 4. Medium, supplements and additional components for cell culture

Medium Supplements	Catalog No.	Company
Fetal Bovine Serum	AC-SM-0143	anprotec
Penicillin-Streptomycin (10,000 U/ml)	15140122	Gibco®
Sodium Pyruvate (100 mM)	11360070	Gibco®
Sodium Selenite (stock: 100 nM)	S5261	Sigma-Aldrich
1-Thioglycerol	M6145	Sigma-Aldrich
Bathocuproinedisulfonic acid (BCS) (stock: 43.3% α-thioglycerols (43.3 µl 1-Thioglycerol + 20 µl 10 mM BCS in 10 ml PBS))	B1125	Sigma-Aldrich
Minimum Essential Medium Non-Essential Amino Acids (MEM NEAA, 100X)	11140050	Gibco®

Hygromycin B (50 mg/ml)	10687010	Gibco®
Puromycin (stock: 2 mg/ml)	A2856.0100	Applichem
Related buffers		
Dulbecco's Phosphate Buffered Saline	D8537	Sigma-Aldrich
PEI MAX® - Polyethylenimine Hydrochloride (stock: 1 mg/ml)	24765-1	Polysciences
Pancoll human	P04-60500	PAN-Biotech

Table 5. Cell types of donor and recipient cells

Cell type	Name	Disease
B lymphocyte	BJAB	Burkitt's lymphoma
B lymphocyte	DG-75	Burkitt's lymphoma
B lymphocyte	Elijah	Burkitt's lymphoma
B lymphocyte	LCL	
B lymphocyte	Raji	Burkitt's lymphoma
Monocyte	Mono-mac-6	Acute monocytic leukemia
Monocyte	THP-1	Acute monocytic leukemia
Erythrocyte	HEL	Erythroleukemia
Epithelial cells	LN-18	Glioblastoma
Epithelial cells	U-251MG	Astrocytoma
Epithelial cells	A549	Lung carcinoma
Epithelial cells	Calu-3	Lung adenocarcinoma
Epithelial cells	HepG2	Hepatocellular carcinoma
Epithelial cells	Huh7	Hepatocellular carcinoma
Epithelial cells	MDA-MB-231	Breast adenocarcinoma
Epithelial cells	Caco-2	Colorectal adenocarcinoma

Software tools

MacVector Version 18.0.0 (55) was used for *in silico* DNA cloning. FlowJo 10.4.2 was used for analysis and visualization of flow cytometry data. The ZetaView 8.04.02

software was used for nanoparticle tracking analysis. Prism 9 for macOS Version 9.0.1 (128) and RStudio Version 1.2.5001 were used for statistical analysis and visualization. Microsoft Word for Mac Version 16.45 and Microsoft Excel for Mac Version 16.45 were used for documentation and analysis. Adobe Illustrator 25.1 was used for composing figures. The diagrams were created with BioRender.com (<https://biorender.com/>).

References

- Aiyar, A., Tyree, C., and Sugden, B. (1998). The plasmid replicon of EBV consists of multiple cis-acting elements that facilitate DNA synthesis by the cell and a viral maintenance element. *The EMBO Journal* *17*, 6394–6403.
- Albà, M.M., Das, R., Orengo, C.A., and Kellam, P. (2001). Genomewide Function Conservation and Phylogeny in the Herpesviridae. *Genome Res.* *11*, 43–54.
- Albanese, M., Chen, Y.-F.A., Hüls, C., Gärtner, K., Tagawa, T., Mejias-Perez, E., Keppler, O.T., Göbel, C., Zeidler, R., Shein, M., et al. (2020). Micro RNAs are minor constituents of extracellular vesicles and are hardly delivered to target cells. *BioRxiv* 2020.05.20.106393.
- Almohammed, R., Osborn, K., Ramasubramanyan, S., Perez-Fernandez, I.B.N., Godfrey, A., Mancini, E.J., and Sinclair, A.J. (2018). Mechanism of activation of the BNLF2a immune evasion gene of Epstein-Barr virus by Zta. *J Gen Virol* *99*, 805–817.
- Aubry, V., Mure, F., Mariamé, B., Deschamps, T., Wyrwicz, L.S., Manet, E., and Gruffat, H. (2014). Epstein-Barr Virus Late Gene Transcription Depends on the Assembly of a Virus-Specific Preinitiation Complex. *Journal of Virology* *88*, 12825–12838.
- Baker, M.P., Eliopoulos, A.G., Young, L.S., Armitage, R.J., Gregory, C.D., and Gordon, J. (1998). Prolonged Phenotypic, Functional, and Molecular Change in Group I Burkitt Lymphoma Cells on Short-Term Exposure to CD40 Ligand. *Blood* *92*, 2830–2843.
- Buschle, A., and Hammerschmidt, W. (2020). Epigenetic lifestyle of Epstein-Barr virus. *Semin Immunopathol* *42*, 131–142.
- Buschle, A., Mrozek-Gorska, P., Krebs, S., Blum, H., Cernilogar, F.M., Schotta, G., Pich, D., Straub, T., and Hammerschmidt, W. (2019). Epstein-Barr virus inactivates the transcriptome and disrupts the chromatin architecture of its host cell in the first phase of lytic reactivation. *BioRxiv* 573659.
- Busse, C., Feederle, R., Schnölzer, M., Behrends, U., Mautner, J., and Delecluse, H.-J. (2010). Epstein-Barr Viruses That Express a CD21 Antibody Provide Evidence that gp350's Functions Extend beyond B-Cell Surface Binding. *Journal of Virology* *84*, 1139–1147.

Cai, M., Liao, Z., Chen, T., Wang, P., Zou, X., Wang, Y., Xu, Z., Jiang, S., Huang, J., Chen, D., et al. (2017). Characterization of the subcellular localization of Epstein-Barr virus encoded proteins in live cells. *Oncotarget* 8, 70006–70034.

Cavrois, M., de Noronha, C., and Greene, W.C. (2002). A sensitive and specific enzyme-based assay detecting HIV-1 virion fusion in primary T lymphocytes. *Nature Biotechnology* 20, 1151–1154.

Cavrois, M., Neidleman, J., and Greene, W.C. (2014). HIV-1 Fusion Assay. *Bio Protoc* 4.

Chesnokova, L.S., Jiang, R., and Hutt-Fletcher, L.M. (2015). Viral Entry. In *Epstein Barr Virus Volume 2: One Herpes Virus: Many Diseases*, C. Münz, ed. (Cham: Springer International Publishing), pp. 221–235.

Chiu, Y.-F., Sugden, B., Chang, P.-J., Chen, L.-W., Lin, Y.-J., Lan, Y.-C., Lai, C.-H., Liou, J.-Y., Liu, S.-T., and Hung, C.-H. (2012). Characterization and Intracellular Trafficking of Epstein-Barr Virus BBLF1, a Protein Involved in Virion Maturation. *Journal of Virology* 86, 9647–9655.

Cohen, J.I. (2015). Epstein–barr virus vaccines. *Clinical & Translational Immunology* 4, e32.

Cohen, J.I., Mocarski, E.S., Raab-Traub, N., Corey, L., and Nabel, G.J. (2013). The need and challenges for development of an Epstein-Barr virus vaccine. *Vaccine* 31, B194–B196.

Dai, Y.-C., Liao, Y.-T., Juan, Y.-T., Cheng, Y.-Y., Su, M.-T., Su, Y.-Z., Liu, H.-C., Tsai, C.-H., Lee, C.-P., and Chen, M.-R. (2020). The Novel Nuclear Targeting and BFRF1-Interacting Domains of BFLF2 Are Essential for Efficient Epstein-Barr Virus Virion Release. *Journal of Virology* 94.

Davison, A.J. (2007). Overview of classification. In *Human Herpesviruses: Biology, Therapy, and Immunoprophylaxis*, A. Arvin, G. Campadelli-Fiume, E. Mocarski, P.S. Moore, B. Roizman, R. Whitley, and K. Yamanishi, eds. (Cambridge: Cambridge University Press), p.

Delecluse, H.-J., Hilsendegen, T., Pich, D., Zeidler, R., and Hammerschmidt, W. (1998). Propagation and recovery of intact, infectious Epstein–Barr virus from prokaryotic to human cells. *PNAS* 95, 8245–8250.

Delecluse, H.-J., Pich, D., Hilsendegen, T., Baum, C., and Hammerschmidt, W. (1999). A first-generation packaging cell line for Epstein–Barr virus-derived vectors. *PNAS* *96*, 5188–5193.

Delecluse, H.-J., Feederle, R., Behrends, U., and Mautner, J. (2008). Contribution of viral recombinants to the study of the immune response against the Epstein-Barr virus. *Seminars in Cancer Biology* *18*, 409–415.

Elliott, S.L., Suhrbier, A., Miles, J.J., Lawrence, G., Pye, S.J., Le, T.T., Rosenstengel, A., Nguyen, T., Allworth, A., Burrows, S.R., et al. (2008). Phase I Trial of a CD8+ T-Cell Peptide Epitope-Based Vaccine for Infectious Mononucleosis. *Journal of Virology* *82*, 1448–1457.

Epstein, M.A., Achong, B.G., and Barr, Y.M. (1964). VIRUS PARTICLES IN CULTURED LYMPHOBLASTS FROM BURKITT'S LYMPHOMA. *The Lancet* *283*, 702–703.

Epstein, M.A., Morgan, A.J., Finerty, S., Randle, B.J., and Kirkwood, J.K. (1985). Protection of cottontop tamarins against Epstein-Barr virus-induced malignant lymphoma by a prototype subunit vaccine. *Nature* *318*, 287–289.

Farina, A., Feederle, R., Raffa, S., Gonnella, R., Santarelli, R., Frati, L., Angeloni, A., Torrisi, M.R., Faggioni, A., and Delecluse, H.-J. (2005). BFRF1 of Epstein-Barr Virus Is Essential for Efficient Primary Viral Envelopment and Egress. *Journal of Virology* *79*, 3703–3712.

Faulkner, G.C., Krajewski, A.S., and Crawford, D.H. (2000). The ins and outs of EBV infection. *Trends in Microbiology* *8*, 185–189.

Feederle, R., Kost, M., Baumann, M., Janz, A., Drouet, E., Hammerschmidt, W., and Delecluse, H.-J. (2000). The Epstein–Barr virus lytic program is controlled by the cooperative functions of two transactivators. *The EMBO Journal* *19*, 3080–3089.

Feederle, R., Shannon-Lowe, C., Baldwin, G., and Delecluse, H.J. (2005). Defective Infectious Particles and Rare Packaged Genomes Produced by Cells Carrying Terminal-Repeat-Negative Epstein-Barr Virus. *Journal of Virology* *79*, 7641–7647.

Feederle, R., Bartlett, E.J., and Delecluse, H.-J. (2010). Epstein-Barr virus genetics: talking about the BAC generation. *Herpesviridae* *1*, 6.

Fixman, E.D., Hayward, G.S., and Hayward, S.D. (1992). trans-acting requirements for replication of Epstein-Barr virus ori-Lyt. *Journal of Virology* *66*, 5030–5039.

Gore, M., and Hutt-Fletcher, L.M. (2009). The BDLF2 protein of Epstein–Barr virus is a type II glycosylated envelope protein whose processing is dependent on coexpression with the BMRF2 protein. *Virology* 383, 162–167.

Granato, M., Feederle, R., Farina, A., Gonnella, R., Santarelli, R., Hub, B., Faggioni, A., and Delecluse, H.-J. (2008). Deletion of Epstein-Barr Virus BFLF2 Leads to Impaired Viral DNA Packaging and Primary Egress as Well as to the Production of Defective Viral Particles. *Journal of Virology* 82, 4042–4051.

Gruffat, H., Marchione, R., and Manet, E. (2016). Herpesvirus Late Gene Expression: A Viral-Specific Pre-initiation Complex Is Key. *Front. Microbiol.* 7.

Hammerschmidt, W., and Sugden, B. (1988). Identification and characterization of oriLyt, a lytic origin of DNA replication of Epstein-Barr virus. *Cell* 55, 427–433.

He, H.-P., Luo, M., Cao, Y.-L., Lin, Y.-X., Zhang, H., Zhang, X., Ou, J.-Y., Yu, B., Chen, X., Xu, M., et al. (2020). Structure of Epstein-Barr virus tegument protein complex BBRF2-BSRF1 reveals its potential role in viral envelopment. *Nature Communications* 11, 5405.

Hellebrand, E., Mautner, J., Reisbach, G., Nimmerjahn, F., Hallek, M., Mocikat, R., and Hammerschmidt, W. (2006). Epstein–Barr virus vector-mediated gene transfer into human B cells: potential for antitumor vaccination. *Gene Therapy* 13, 150–162.

Henson, B.W., Perkins, E.M., Cothran, J.E., and Desai, P. (2009). Self-Assembly of Epstein-Barr Virus Capsids. *Journal of Virology* 83, 3877–3890.

Herrold, R.E., Marchini, A., Fruehling, S., and Longnecker, R. (1996). Glycoprotein 110, the Epstein-Barr virus homolog of herpes simplex virus glycoprotein B, is essential for Epstein-Barr virus replication in vivo. *Journal of Virology* 70, 2049–2054.

Hettich, E., Janz, A., Zeidler, R., Pich, D., Hellebrand, E., Weissflog, B., Moosmann, A., and Hammerschmidt, W. (2006). Genetic design of an optimized packaging cell line for gene vectors transducing human B cells. *Gene Therapy* 13, 844–856.

Janz, A., Oezel, M., Kurzeder, C., Mautner, J., Pich, D., Kost, M., Hammerschmidt, W., and Delecluse, H.-J. (2000). Infectious Epstein-Barr Virus Lacking Major Glycoprotein BLLF1 (gp350/220) Demonstrates the Existence of Additional Viral Ligands. *Journal of Virology* 74, 10142–10152.

- Johannsen, E., Luftig, M., Chase, M.R., Weicksel, S., Cahir-McFarland, E., Illanes, D., Sarracino, D., and Kieff, E. (2004). Proteins of purified Epstein-Barr virus. *PNAS* *101*, 16286–16291.
- Jones, D.M., and Padilla-Parra, S. (2016). The β -Lactamase Assay: Harnessing a FRET Biosensor to Analyse Viral Fusion Mechanisms. *Sensors* *16*, 950.
- Laichalk, L.L., and Thorley-Lawson, D.A. (2005). Terminal Differentiation into Plasma Cells Initiates the Replicative Cycle of Epstein-Barr Virus In Vivo. *Journal of Virology* *79*, 1296–1307.
- Li, H., Hu, J., Luo, X., Bode, A.M., Dong, Z., and Cao, Y. (2018). Therapies based on targeting Epstein-Barr virus lytic replication for EBV-associated malignancies. *Cancer Science* *109*, 2101–2108.
- Li, J., Walsh, A., Lam, T.T., Delecluse, H.-J., and El-Guindy, A. (2019). A single phosphoacceptor residue in BGLF3 is essential for transcription of Epstein-Barr virus late genes. *PLOS Pathogens* *15*, e1007980.
- Masud, H.M.A.A., Watanabe, T., Yoshida, M., Sato, Y., Goshima, F., Kimura, H., and Murata, T. (2017). Epstein-Barr Virus BKRF4 Gene Product Is Required for Efficient Progeny Production. *Journal of Virology* *91*.
- Masud, H.M.A.A., Yanagi, Y., Watanabe, T., Sato, Y., Kimura, H., and Murata, T. (2019). Epstein-Barr Virus BBRF2 Is Required for Maximum Infectivity. *Microorganisms* *7*, 705.
- Meckes, D.G., and Raab-Traub, N. (2011). Microvesicles and Viral Infection. *Journal of Virology* *85*, 12844–12854.
- Mocarski, E.S., Post, L.E., and Roizman, B. (1980). Molecular engineering of the herpes simplex virus genome: Insertion of a second L-S junction into the genome causes additional genome inversions. *Cell* *22*, 243–255.
- Möhl, B.S., Chen, J., Sathiyamoorthy, K., Jardetzky, T.S., and Longnecker, R. (2016). Structural and Mechanistic Insights into the Tropism of Epstein-Barr Virus. *Mol Cells* *39*, 286–291.
- Moutschen, M., Léonard, P., Sokal, E.M., Smets, F., Haumont, M., Mazzu, P., Bollen, A., Denamur, F., Peeters, P., Dubin, G., et al. (2007). Phase I/II studies to evaluate safety and immunogenicity of a recombinant gp350 Epstein–Barr virus vaccine in healthy adults. *Vaccine* *25*, 4697–4705.

Murata, T., and Tsurumi, T. (2014). Switching of EBV cycles between latent and lytic states. *Reviews in Medical Virology* 24, 142–153.

Muriaux, D., and Darlix, J.-L. (2010). Properties and functions of the nucleocapsid protein in virus assembly. *RNA Biology* 7, 744–753.

Neuhierl, B., Feederle, R., Hammerschmidt, W., and Delecluse, H.J. (2002). Glycoprotein gp110 of Epstein–Barr virus determines viral tropism and efficiency of infection. *PNAS* 99, 15036–15041.

Neuhierl, B., Feederle, R., Adhikary, D., Hub, B., Geletneky, K., Mautner, J., and Delecluse, H.-J. (2009). Primary B-Cell Infection with a Δ BALF4 Epstein-Barr Virus Comes to a Halt in the Endosomal Compartment yet Still Elicits a Potent CD4-Positive Cytotoxic T-Cell Response. *Journal of Virology* 83, 4616–4623.

Pavlova, S., Feederle, R., Gärtner, K., Fuchs, W., Granzow, H., and Delecluse, H.-J. (2013). An Epstein-Barr Virus Mutant Produces Immunogenic Defective Particles Devoid of Viral DNA. *Journal of Virology* 87, 2011–2022.

Pegtel, D.M., van de Garde, M.D.B., and Middeldorp, J.M. (2011). Viral miRNAs exploiting the endosomal–exosomal pathway for intercellular cross-talk and immune evasion. *Biochimica et Biophysica Acta (BBA) - Gene Regulatory Mechanisms* 1809, 715–721.

Pelossof, R., Fairchild, L., Huang, C.-H., Widmer, C., Sreedharan, V.T., Sinha, N., Lai, D.-Y., Guan, Y., Premisrut, P.K., Tschaharganeh, D.F., et al. (2017). Prediction of potent shRNAs with a sequential classification algorithm. *Nature Biotechnology* 35, 350–353.

Pich, D., Mrozek-Gorska, P., Bouvet, M., Sugimoto, A., Akidil, E., Grundhoff, A., Hamperl, S., Ling, P.D., and Hammerschmidt, W. (2019). First Days in the Life of Naive Human B Lymphocytes Infected with Epstein-Barr Virus. *MBio* 10.

Rowe, M., Rooney, C.M., Rickinson, A.B., Lenoir, G.M., Rupani, H., Moss, D.J., Stein, H., and Epstein, M.A. (1985). Distinctions between endemic and sporadic forms of Epstein-Barr virus-positive Burkitt's lymphoma. *International Journal of Cancer* 35, 435–441.

Ruiss, R., Jochum, S., Wanner, G., Reisbach, G., Hammerschmidt, W., and Zeidler, R. (2011). A Virus-Like Particle-Based Epstein-Barr Virus Vaccine. *Journal of Virology* 85, 13105–13113.

- Russell, W.C., Graham, F.L., Smiley, J., and Nairn, R. (1977). Characteristics of a Human Cell Line Transformed by DNA from Human Adenovirus Type 5. *Journal of General Virology* 36, 59–72.
- Sathiyamoorthy, K., Hu, Y.X., Möhl, B.S., Chen, J., Longnecker, R., and Jardetzky, T.S. (2016). Structural basis for Epstein–Barr virus host cell tropism mediated by gp42 and gHgL entry glycoproteins. *Nature Communications* 7, 13557.
- Schaeffner, M., Mrozek-Gorska, P., Buschle, A., Woellmer, A., Tagawa, T., Cernilogar, F.M., Schotta, G., Krietenstein, N., Lieleg, C., Korber, P., et al. (2019). BZLF1 interacts with chromatin remodelers promoting escape from latent infections with EBV. *Life Sci Alliance* 2.
- Schepers, A., Pich, D., and Hammerschmidt, W. (1993). A transcription factor with homology to the AP-1 family links RNA transcription and DNA replication in the lytic cycle of Epstein-Barr virus. *The EMBO Journal* 12, 3921–3929.
- Sokal, E.M., Hoppenbrouwers, K., Vandermeulen, C., Moutschen, M., Léonard, P., Moreels, A., Haumont, M., Bollen, A., Smets, F., and Denis, M. (2007). Recombinant gp350 Vaccine for Infectious Mononucleosis: A Phase 2, Randomized, Double- Blind, Placebo-Controlled Trial to Evaluate the Safety, Immunogenicity, and Efficacy of an Epstein- Barr Virus Vaccine in Healthy Young Adults. *The Journal of Infectious Diseases* 196, 1749–1753.
- Sugimoto, A., Sato, Y., Kanda, T., Murata, T., Narita, Y., Kawashima, D., Kimura, H., and Tsurumi, T. (2013). Different Distributions of Epstein-Barr Virus Early and Late Gene Transcripts within Viral Replication Compartments. *Journal of Virology* 87, 6693–6699.
- Sugimoto, A., Yamashita, Y., Kanda, T., Murata, T., and Tsurumi, T. (2019). Epstein-Barr virus genome packaging factors accumulate in BMRF1-cores within viral replication compartments. *PLOS ONE* 14, e0222519.
- Taylor, G.S., Long, H.M., Brooks, J.M., Rickinson, A.B., and Hislop, A.D. (2015). The Immunology of Epstein-Barr Virus–Induced Disease. *Annual Review of Immunology* 33, 787–821.
- Visalli, R.J., Schwartz, A.M., Patel, S., and Visalli, M.A. (2019). Identification of the Epstein Barr Virus portal. *Virology* 529, 152–159.

- Wang, S., Zhao, Y., Leiby, M., and Zhu, J. (2009). A new positive/negative selection scheme for precise BAC recombineering. *Mol Biotechnol* *42*, 110–116.
- Wang, W.-H., Chang, L.-K., and Liu, S.-T. (2011). Molecular Interactions of Epstein-Barr Virus Capsid Proteins. *Journal of Virology* *85*, 1615–1624.
- Wang, W.-H., Kuo, C.-W., Chang, L.-K., Hung, C.-C., Chang, T.-H., and Liu, S.-T. (2015). Assembly of Epstein-Barr Virus Capsid in Promyelocytic Leukemia Nuclear Bodies. *Journal of Virology* *89*, 8922–8931.
- Warming, S., Costantino, N., Court, D.L., Jenkins, N.A., and Copeland, N.G. (2005). Simple and highly efficient BAC recombineering using galK selection. *Nucleic Acids Research* *33*, e36–e36.
- Watanabe, C., Cuellar, T.L., and Haley, B. (2016). Quantitative evaluation of first, second, and third generation hairpin systems reveals the limit of mammalian vector-based RNAi. *RNA Biology* *13*, 25–33.
- Wyrwicz, L.S., and Rychlewski, L. (2007). Identification of Herpes TATT-binding protein. *Antiviral Research* *75*, 167–172.
- Xiao, J., Palefsky, J.M., Herrera, R., and Tugizov, S.M. (2007). Characterization of the Epstein-Barr virus glycoprotein BMRF-2. *Virology* *359*, 382–396.
- Xiao, J., Palefsky, J.M., Herrera, R., Berline, J., and Tugizov, S.M. (2008). The Epstein-Barr virus BMRF-2 protein facilitates virus attachment to oral epithelial cells. *Virology* *370*, 430–442.
- Yanagi, Y., Masud, H.M.A.A., Watanabe, T., Sato, Y., Goshima, F., Kimura, H., and Murata, T. (2019). Initial Characterization of the Epstein-Barr Virus BSRF1 Gene Product. *Viruses* *11*, 285.
- Yetming, K.D., Lupey-Green, L.N., Biryukov, S., Hughes, D.J., Marendy, E.M., Miranda, J.L., and Sample, J.T. (2020). The BHLF1 Locus of Epstein-Barr Virus Contributes to Viral Latency and B-Cell Immortalization. *Journal of Virology* *94*.
- Young, L.S., Arrand, J.R., and Murray, P.G. (2007). EBV gene expression and regulation. In *Human Herpesviruses: Biology, Therapy, and Immunoprophylaxis*, A. Arvin, G. Campadelli-Fiume, E. Mocarski, P.S. Moore, B. Roizman, R. Whitley, and K. Yamanishi, eds. (Cambridge: Cambridge University Press), p.

Zaret, K.S., and Mango, S.E. (2016). Pioneer transcription factors, chromatin dynamics, and cell fate control. *Current Opinion in Genetics & Development* 37, 76–81.

Zyl, D.G. van, Tsai, M.-H., Shumilov, A., Schneidt, V., Poirey, R., Schlehe, B., Fluhr, H., Mautner, J., and Delecluse, H.-J. (2018). Immunogenic particles with a broad antigenic spectrum stimulate cytolytic T cells and offer increased protection against EBV infection ex vivo and in mice. *PLOS Pathogens* 14, e1007464.

van Zyl, D.G., Mautner, J., and Delecluse, H.-J. (2019). Progress in EBV Vaccines. *Front. Oncol.* 9.

Appendix

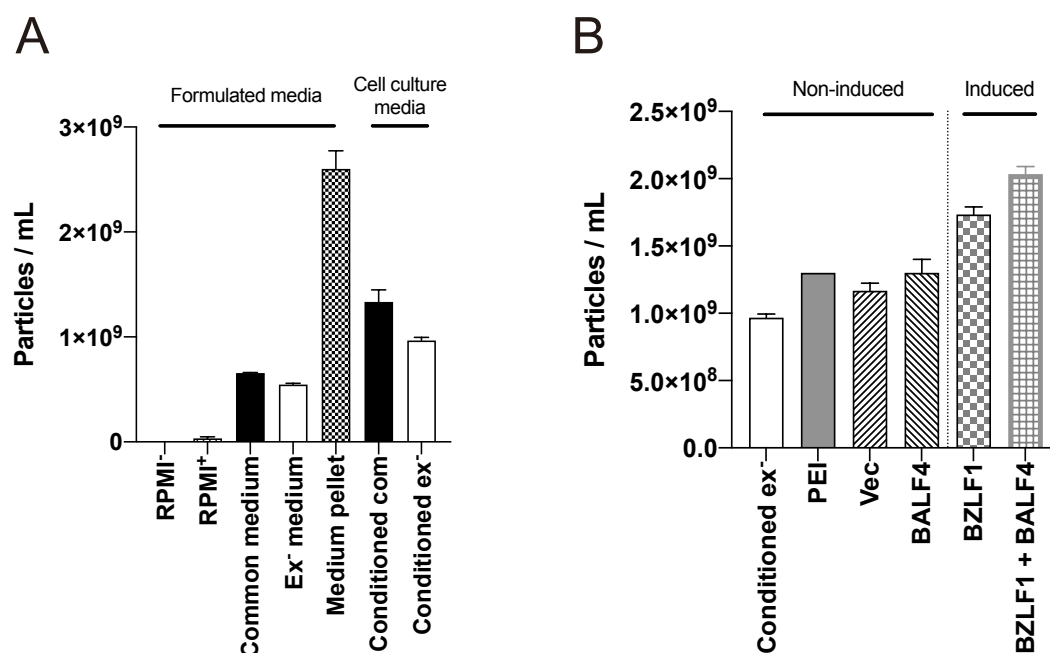


Fig. 12 Concentration of physical particles in different cell culture media and in supernatants from induced 2089 EBV producer cells generated under various conditions.

Concentrations of physical particles were determined with the aid of the nanoparticle tracking analysis (NTA) using the ZetaView PMX110 instrument. Mean and standard deviation of three replicates are shown.

(A) Different cell culture medium preparations based on standard RPMI1640 medium were analyzed as follows:

RPMI⁻: plain, non-supplemented commercial RPMI 1640 medium (Gibco).

RPMI⁺: commercial RPMI1640 medium supplemented with 5 ml penicillin-streptomycin stock (10,000 U/ml), 5 ml sodium pyruvate (100 mM), 500 μ l of 10 nM sodium selenite, and 500 μ l of 43.3% α -thioglycerols.

Common medium: RPMI⁺ with 10% fetal bovine serum (Bio&Sell) and the supplements listed above.

Ex⁻ medium (exosome-depleted medium): common medium with 10% fetal bovine serum (final concentration) after ultracentrifugation (100,000 g, 4 °C for more than 16 hours) and prepared as described in Materials and Methods.

Medium pellet: Common medium was concentrated 7-fold by ultracentrifugation and analyzed. Technically, 35 ml common medium was ultracentrifuged (100,000 g, 4 °C for 16 hours) and 30 ml supernatant was removed and the pellet was resuspended.

Conditioned com: Supernatant from non-induced 2089 EBV producer cells cultured in common medium for three days.

Conditioned ex⁻: Supernatant from the non-induced 2089 EBV producer cell line cultured in exosome-

depleted medium (ex⁻ medium) for three days.

(B) Analysis of supernatants from non-induced and induced 2089 EBV producer cells including controls. Conditioned ex⁻: The conditioned ex⁻ medium in panel A is used here to cultivate the cells.

PEI: Non-induced 2089 EBV producer cells were cultured in exosome-depleted medium (ex⁻ medium) for three days. 3 µl PEI MAX was added at the start of cell culture to mimic DNA transfection conditions.

Vec: 2089 EBV producer cells were transfected with pCMV control plasmid DNA (0.5 µg; p6815) using 3 µl PEI MAX and kept in exosome-depleted medium (ex⁻ medium) for three days when the supernatant was harvested and analyzed.

BALF4: same as above (Vec) but the cells were transfected with 0.5 µg of the BALF4 expression plasmid p6515.

BZLF1: same as above (Vec), but the cells were transfected with 0.5 µg of the BZLF1 expression plasmid p509 to induce EBV production.

BZLF1 + BALF4: same as above (Vec), but the cells were co-transfected with 0.25 µg each of the expression plasmids p509 and p6515 coding for BZLF1 and BALF4, respectively.

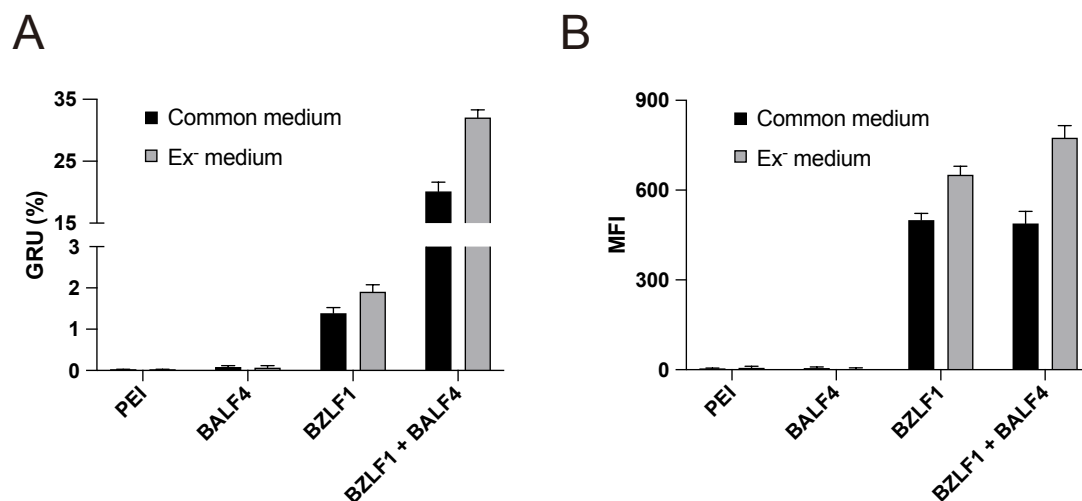


Fig. 13 Comparison of virus production from 2089 EBV producer cells using common cell culture medium versus exosome-depleted medium (ex⁻ medium).

The 2089 EBV producer cell line was seeded in 6-well cluster plates (6.5×10^5 cells per well) and the medium was exchanged after overnight incubation with 2 ml common cell culture medium (fully supplemented RPMI1640 medium with 10% fetal bovine serum) or exosome-depleted (ex⁻ medium). As a reference, cells were mock transfected with PEI MAX but no plasmid DNA was added (PEI). Alternatively, the EBV producer cell line 2089 was transfected with only the BALF4 encoding plasmid p6516 (0.5 µg), with the BZLF1 encoding plasmid p509 (0.5 µg) or with both BALF4 and BZLF1 plasmids (0.25 µg each) as indicated. Supernatants were harvested after three days and filtered (1.2 µm mesh size). **(A)** 1×10^5 Raji cells were infected with 10 µl of the different supernatants and analyzed by flow cytometry after three days. The percentage of GFP-positive cells is provided as 'green Raji units' (GRU). **(B)** 2×10^5 Elijah cells were incubated with 20 µl of the different supernatants following the protocol of

the Elijah cell binding assay (see Materials and Methods). Mean fluorescence intensity (MFI) values of the cells were analyzed by flow cytometry.

Table 6. Synthetic oligonucleotides used to remove epitope tags from 76 expression plasmids to restore their open reading frames

Gene (plasmid #)	Primer/oligonucleotide
BBRF3 (p6534)	6534_Top (Bgl2) 5': GATCTTCCCCTAAAGTAACAGC 6534_Bottom (Not1) 5': GGCCGCTGTTACTTTAGGGGAA
BDLF3 (p6535)	6535_Forward (Bsp1) 5': CCAATGCCACAAAAACAACACTGC 6535_Reverse (Not1) 5': TTTTGC GGCCGCTACACCAGTCCCTTGTAAGC
BILF2 (p6536)	6536_Forward (Esp31) 5': GTAAATGACTCCAACACCTCC 6536_Reverse (Not1) 5': TTTTGC GGCCGCTCAGAGGGTATCCAGCCCTT
BKRF2 (p6537)	6537_Top (Aju1) 5': CTCAGTGGAAGACCTGTTTGGTGCCAACCTAAACAGATACGCATGGCAT CGCGGGGGCTAGGC 6537_Bottom (Not1) 5': GGCCGCTAGCCCCCGCATGCCATGCGTATCTGTTAAGTTGGCACCAAACAGGTCTTCCACTGAGAATGA
BLRF1 (p6538)	6538_Top (Bpu10I) 5': TCAGCCATCTACCTGATGTACGTCTGCTTTAACAAGTTTGTGAACACGCTGCTGACGGATTAGGC 6538_Bottom (Not1) 5': GGCCGCTAATCCGTCAGCAGCGTGTTCACAACTTGTAAAGCAGACGTACATCAGGTAGATGGC
BMRF2 (p6539)	6539_Forward (Bpu10I) 5': TTACTTTAGCGGGGTAGCGG 6539_Reverse (Not1) 5': TTTTGC GGCCGCTTAGGATTTAATGAATGTCAC
BXLF2 (p6540)	6540_Forward (Bsp1) 5': TGACCTCACACGAGACAAGC 6540_Reverse (Not1) 5': TTTTGC GGCCGCTAAAGGAAAAACATAACAATCTTG
BZLF2 (p6541)	6541_Forward (BamH1) 5': CAAACCAATGTAGAGGTCTGG 6541_Reverse (Xba1) 5': TTTTCTAGATTAGCTATTTGATCTTTGACT
BBLF1 (p6557)	6557_Forward (Nco1) 5': AACAACTCCGCCCCATTGAC 6557_Reverse (Not1) 5': GGGGGCGGCCGCTTAGTTTGTTTTTTATTGGC
BDLF2 (p6558)	6558_Top (Xho1) 5': TCGAGGAGGTCATGTATGTGATGGTTCAGTAGGC 6558_Bot (Not1) 5': GGCCGCTACTGAACCATCACATACATGACCTCC
BGLF1 (p6559)	6559_Top (Mun1, Mfe1) 5': AATTGGCACTACCCCCGAGGAGAGGGGATATATTCTGGCACGTCATGGCATCCGCCGGAACAGTAGGC 6559_Bot (Not1) 5': GGCCGCTACTGTTCGCGGCGGATGCCATGACGTGCCAGAATATATCCCCTCTCCTCGGGGGTGAGTGCC
BGLF2 (p6560)	6560_Top (Mun1, Mfe1) 5': AATTGCCAAGTACTGAAACGTCAGGTCTTACATTCTTATTGAGC 6560_Bot (Not1) 5': GGCCGCTCAATAAGAATGTAAGACCTGACGTTTCAGTACTTGCC
BGLF4 (p6561)	6561_Forward (Pst1) 5': GCTCTATCGCCTCTATTGCC 6561_Reverse (Not1) 5': TTTTGC GGCCGCTCATCCACGTCGGCCATCTGGACC
BKRF4 (p6562)	6562_Top (Mun1, Mfe1) 5': AATTGGCCATGGCTGTAAGC 6562_Bot (Not1) 5': GGCCGCTTACAGCCATGGCC
BLRF2 (p6563)	6563_Forward (Bpu10I) 5': TGTTCTTCTGCTCCAGTGC

Gene (plasmid #)	Primer/oligonucleotide
	6563_Reverse (Not1) 5': TTTTGC GGCCGCTTAATCAGAAATTTGCACTTTCTTTGC
BNRF1 (p6564)	6564_Forward (BsrG1) 5': TCATCTGGCTCTCCTGTGTG 6564_Reverse (Not1) 5': TTTTGC GGCCGCTCACTCGGAGGGGCGACCGTGCCTG
BOLF1 (p6565)	6565_Forward (EcoR5) 5': AGGAGGAGAAGGAGCATAACG 6565_Reverse (Xba1) 5': TTTTCTAGATTACTCATCTTCGGCGGTGGGGCGGGG 6565C_Top (Pml1) 5': GTGACCATGGCGTCCGCTATGGAGAGTGACAGCAGCGGCGGTAGCGGAGGGGCGAGACGCCAGCCACCCCT GGCAGAGGTGGACGGGGGGCTCGCCCGCTGA 6565C_Bot (Mlu1) 5': CGCGTCACGCGGGCGAGCCCCCGTCCACCTCTGCCAGGGGTGGCTGGGCGTCTGCCCTCCGCTACCGCCGC TGCTGTCACTCTCCATAGCGGACGCCATGGTCAC
BORF2 (p6566)	6566_Forward (Blp1) 5': AACAGAATGAGCGGAGTCC 6566_Reverse (Not1) 5': TTTTGC GGCCGCTTATTGGCAAGATTCACAGGCTCG
BPLF1 (p6567)	6567_Top (Nhe1) 5': CTAGCCGAGTACTGTCTCGTTCGTGAGCCAGCTTCGCCGCAAGCTGGAGCGTTCACCCACCGCCTCATCGCA GACCTCGAGAGACTCAAGTTTTTGTATCTGTAAT 6567_Bot (Xba1) 5': CTAGATTACAGATACAAAACTTGAGTCTCTCGAGGTCTGCGATGAGGCGGTGGGTGGAACGCTCCAGCTTGC GGCGAAGCTGGCTCACGAAGCGAGACAGTACTCGG
BRRF2 (p6568)	6568_Forward (Bpu101) 5': TACCGTCCAGCAAAAAGGG 6568_Reverse (Not1) 5': TTTTGC GGCCGCTTAGACGACGCTCAGTGAATACAG
BSRF1 (p6569)	6569_Forward (Age1) 5': CGCTCAGTCATCTGGAATAC 6569_Reverse (Not1) 5': TTTTGC GGCCGCTACGTTAACGCGAGCTCCGTGGG
BVRF1 (p6570)	6570_Forward (Hind3) 5': TCATCTCACCAGTGAACC 6570_Reverse (Not1) 5': GGGGGCGGCCGCTCAGCTTGGGGCCACCGGGGAGG
BXLF1 (p6571)	6571_Forward (Nhe1) 5': TTTGTCTTGC GTTCAACC 6571_Reverse (Not1) 5': CCCC GCGCCGCTAGTCCCGATTTCCCTCTCAAATC
BBRF1 (p6593)	6593_Forward (Age1) 5': ATAATCAGGGGCAGCGTCTC 6593_Reverse (Not1) 5': TTTTGC GGCCGCTTA ACTTCCAGCACCAGGCGGGG
BcLF1 (p6594)	6594_Forward (Cla1) 5': AGTTTGTAGTGATTGCTGGC 6594_Reverse (Not1) 5': TTTTGC GGCCGCTCAAAAAACCACTTATTTCCAAA
BDLF1 (p6595)	6595_Forward (Pst1) 5': TGTGGACATTGTTTTCCCC 6595_Reverse (Not1) 5': TTTTGC GGCCGCTTATCTTAACCAGCAAGTGGCCGT
BdRF1 (p6596)	6596_Forward (BspE1) 5': TGAATGAGTTACAGCACACG 6596_Reverse (Not1) 5': TTTTGC GGCCGCTCAAGCCACGCTTATTACAGCAA
BFRF3 (p6597)	6597_Forward (Bpu101) 5': CCATAGACAAGAGGCAGAGAG 6597_Reverse (Not1) 5': TTTTGC GGCCGCTACTGTTTCTTACGTGCCCGCG

Gene (plasmid #)	Primer/oligonucleotide
BORF1 (p6598)	6598_Foward (Pst1) 5': CAACTTCATCACCCCTGTG 6598_Reverse (EcoR5) 5': TTTTGATATCCTAGAGAATCACCTCCCAGTCAGA
BALF1 (p6632)	6632_Foward (Pml1) 5': TTTTCACGTGGCGATGAACCTGGCCATTG 6632_Reverse (Not1) 5': TTTTGCGGCCGCTTACAAAGATTTTCAGGAAGTCAGT
BALF3 (p6633)	6633_Foward (BsiW1) 5': CGTGTCCTCTACAACAAG 6633_Reverse (Not1) 5': TTTTGCGGCCGCTACGCCGAGTCATCTCTCATTG
BALF5 (p6634)	6634_Foward (Nco1) 5': GCTACCTGTGGGCTTTTTG 6634_Reverse (Xba1) 5': GGGGTCTAGATTAGAATGGTGGCCGGGCTGTAAA
BARF1 (p6635)	6635_Foward (Bpu101) 5': CCTTTCAGGGGCTTCTTTG 6635_Reverse (Not1) 5': AAAAGCGGCCGCTTATTGCGACAAGTATCCAGAAAC
BaRF1 (p6636)	6636_Foward (BamH1) 5': TGGCACCAAAATCAACGG 6636_Reverse (Xba1) 5': TTTTCTAGATCAAAGGTCATCTACCACCAGCAT
BBLF2/BBLF3 (p6637)	6637_Top (EcoRV) 5': ATCGGCCCTCCACCCCGGCTACACCATTCTATGGAAATCACGCGAGAGACAGATTTACTGATGACTGTTCTCAG TTTATTCTAGT 6637_Bot (Xba1) 5': CTAGACTAGAATAAACTGAGAACAGTCATCAGTAAATCTGTCTCTCGCGTGATTTCCATAGGAATGGTGTAGCCG GGGTGGAGGGCCGAT
BBLF4 (p6638)	6638_Foward (Pst1) 5': GCTGCCTGGAACACAATAC 6638_Reverse (Not1) 5': TTTTGCGGCCGCTCAGTAAACCAGTAGTGCGCGTGA
BBRF2 (p6639)	6639_Foward (Bsg1) 5': GCAACAATCTGGACTCTCTG 6639_Reverse (Not1) 5': TTTTGCGGCCGCTAGGGAATTATTTTTGAGACCGT
BCRF1 (p6640)	6640_Foward (Nco1) 5': CGGGACTTTCCAAAATGTCG 6640_Reverse (Not1) 5': TTTTGCGGCCGCTCACCTGGCTTTAATTGTCATGTA
BcRF1 (p6641)	6641_Foward (Xho1) 5': TACCAACTTTCCCTCGGTG 6641_Reverse (Not1) 5': TTTTGCGGCCGCTTACACTTGAGCATCACGGCAGTG
BDLF4 (p6642)	6642_Foward (BamH1) 5': CGGGACTTTCCAAAATGTCG 6642_Reverse (Not1) 5': TTTTGCGGCCGCTCAACACTTGGTTGTCAATGTGGA
BFLF1 (p6643)	6643_Foward (Bpu101) 5': CCTCATCAAGACCCAAAACAC 6643_Reverse (Not1) 5': TTTTGCGGCCGCTCACACGTAGACCTGGGAAGTTTG
BFLF2 (p6644)	6644_Foward (Bsg1) 5': TGTGCCTCAGGAGTTTAGC 6644_Reverse (Not1) 5': TTTGCGGCCGCTACTGTTTATTTCCAAAATGAG
BFRF1 (p6645)	6645_Foward (Blp1) 5': CGGATGTTGACCTACCAAAG 6645_Reverse (Not1) 5': TTTTGCGGCCGCTCAGGTCCACCTCAGAAACATCAG
BFRF1A (p6646)	6646_Foward (Xho1) 5': CGGGACTTTCCAAAATGTCG 6646_Reverse (Not1) 5': TTTTGCGGCCGCTTATTGAGCTCGTCTAGGAGCCTC
BFRF2 (p6647)	6647_Foward (Blp1) 5': CGGTTACTGCTTGAACCTTGG

Gene (plasmid #)	Primer/oligonucleotide
	6647_Reverse (Not1) 5': TTTTGC GGCCGCTTAGGAAGCAGGGGACTGTCTGGA
BGLF3 (p6648)	6648_Forward (Xho1) 5': CGGGACTTTCCAAAATGTCG 6648_Reverse (Not1) 5': TTTTGC GGCCGCTACTCATCTTCATAAGTCACCAT
BGLF5 (p6649)	6649_Forward (Bsg1) 5': GGGTGGAGTCTATGCTCTAC 6649_Reverse (Not1) 5': TTTTGC GGCCGCTATGGAGTTGACTCGTCGTCGGC
BGRF1/BDRF1 (p6650)	6650_Top (Asp7181) 5': GTACCTACACCTACACCGCAAGCAGCGCAACCTCTCTGACGACGTGCTGGTTGCGCTAGTCATGGCTCATTTT CTCGCAACAACACAGAAGCACACGTTCAAGAAAGTTCATTAAGC 6650_Bottom (Not1) 5': GGCCGCTTAATGAACCTTCTTGAACGTGTGCTTCTGTGTTGTTGCGAGAAAATGAGCCATGACTAGCGCAACCA GCACGTCGTCAGAGAGGTTGCGCTGCTTGCCGGTGTAGGTGTAG
BHRF1 (p6651)	6651_Top (BamH1) 5': GATCCAGAAGGTTTAGCTGGACTTTGTTTCTTGCTGGACTGACTTTGAGTCTGTTAGTTATATGTAGTTATTTATT TATCTCCAGAGGAAGACACTAAGC 6651_Bottom (Not1) 5': GGCCGCTTAGTGTCTTCTCTGGAGATAAATAAATAACTACATATAACTAACAGACTCAAAGTCAGTCCAGCAAG AAACAAAGTCCAGCTAAACCTTCTG
BILF1 (p6833)	6833_Forward (Bsg1) 5': TGATGGGCGTGTTTTGTC 6833_Reverse (Not1) 5': TTTTGC GGCCGCTCAGGTGGACTGGCTAGGCACCCT 6833C_Top (Pml1) 5': GTGACCATGCTCTCCACCATGGCCCCGGGTCCACCGTGGGGACCCCTGGTGGCCAACATGACTCCGTC AATGC AACGGAAGATGCGTGCACTAAATCCTACAGCGCCTTCC 6833C_Bot (BbvC1) 5': TGAGGAAGGCGCTGTAGGATTTAGTGACGCATCTTCCGTTGATTGACGGAAGTCATGTTGGCCACCAGGGT CCCCACGGTGGACCCGGGGCCATGGTGGAGAGCATGGTCAC
BKRF3 (p6834)	6834_Forward (Bsg1) 5': GCATACGGCTTTCCAGTTC 6834_Reverse (Not1) 5': TTTTGC GGCCGCTACAGCCTCCAATCTATCTCACC
BLLF2 (p6835)	6835_Forward (Pml1) 5': GAGAACCCACTGCTTACTG 6835_Reverse (Not1) 5': TTTTGC GGCCGCTAGCATGGAGAGGTTTGAGAATC
BLLF3 (p6836)	6836_Forward (Cla1) 5': CCGATGAAGACCACA ACTG 6836_Reverse (Not1) 5': AAAAGCGGCCGCTCATTGACCCGAGGATCCAAACCC
BLRF3 (p6837)	6837_Top (Bgl2) 5': GATCTAAGAACACTTCTTCAAGCGATTGGAGCCGCGGCTACGGTGAGCATCCCTATGGCCTAAGC 6837_Bottom (Not1) 5': GGCCGCTTAGGCCATAGGGATGCTCACCGTAGCCGCGGCTCCAATCGCTTGAAGAAGTGTCTTA
BMLF1 (p6838)	6838_Forward (Bpu101) 5': TCTACATCACCTGTGCCACG 6838_Reverse (Not1) 5': AAAAGCGGCCGCTTATTGATTTAATCCAGGAACAAA

Gene (plasmid #)	Primer/oligonucleotide
BNLF2a (p6839)	6839_Forward (Nco1) 5': CGGGACTTTCCAAAATGTCG 6839_Reverse (Not1) 5': AAAAGCGGCCGCTTAGATGAGGAGCAGGCATAAAAAG
BNLF2b (p6840)	6840_Forward (Mlu1) 5': CCAAAGGTCAAAGAACAAGGC 6840_Reverse (Not1) 5': TTTTGC GGCCGCTTATCCACACCATCCCAATTCACA
BRLF1 (p6841)	6841_Forward (Age1) 5': TATGTTCTGCCAAAGCCG 6841_Reverse (Not1) 5': AAAAGCGGCCGCCTAAAATAAGCTGGTGTCAAAAAT
BRRF1 (p6842)	6842_Forward (Xho1) 5': GGTATGAGGAAGGTAATCGC 6842_Reverse (Not1) 5': TTTTGC GGCCGCTTATTTGTATTGCATGGCAGAACA
BSLF1 (p6843)	6843_Top (Nhe1) 5': CTAGCCCGTCGTAGAGACAGACAAGATGGTTCCTTCTCAGAGACTCTCCCGAACTAGGC 6843_Bottom (Not1) 5': GGCCGCCTAGTTCGGGAGAGTCTCTGAGAAGGAACCATCTTGTCTGTCTCTACGACGGG
BSLF2/BMLF1 (p6844)	6844_Forward (Bpu101) 5': CTTCTACATCACCTGTGCC 6844_Reverse (Not1) 5': AAAAGCGGCCGCTTATTGATTTAATCCAGGAACAAA
BTRF1 (p6845)	6845_Top (Blp1) 5': TGAGCTTGGCACCATGGCACAGTTTCTAGGAAAGTACATCAAGGTCAAGAAGGAACTGGAATGTACACACTG GTCAAGCTTTATTACCTGCTGCGCATCTAAGC 6845_Bottom (Not1) 5': GGCCGCTTAGATGCGCAGCAGGTAATAAAGCTTGACCAGTGTGTACATTCCAGTTTCCTTCTTGACCTTGATGTA CTTTCTAGAACTGTGCCATGGTGCCAAGC
BVLF1 (p6846)	6846_Top (Blp1) 5': TCAGCTTGGGGCCACCGGGGAGGCCAGGTAGGC 6846_Bottom (Not1) 5': GGCCGCCTACCTGGCCTCCCCGGTGGCCCCAAGC
BVRF2 (p6847)	6847_Forward (BbvC1) 5': TACGAAGTGCCAGATACG 6847_Reverse (Not1) 5': TTTTGC GGCCGCTCAAGCCACGCGTTTATTAGCAA
BXRF1 (p6848)	6848_Top (Xho1) 5': TCGAGCTGGCAGAGCGGGAGGCCGAAAGGGCCAGGTCCGAGCGGTGGGACAGGTGTGCCAGGTGCTCAA AAATAGGC 6848_Bottom (Not1) 5': GGCCGCCTATTTTTGAGCACCTGGGCACACCTGTCCCACCGCTCCGACCTGGCCCTTTCGGCCTCCCGCTCTGC CAGC
BALF2 (p6927)	6927_Top (PspX1) 5': TCGAGGTCTAGTCGATATCGCGGCCGCT 6927_Bot (Xba1) 5': CTAGAGCGGCCGCGATATCGACTAGACCTCGA
BLLF1 (p7050)	7050_Forward (Bsu361) 5': AAATGCCACCAACCACAC 7050_Reverse (Not1) 5': TTTTGC GGCCGCTTATACATAGGTCTCGGCGTCATC
BDLF3.5 (p7078)	7078_Top (Bsg1) 5': GCACCCTCCTGGACCTGGCCGGGTGGAATGTCAGACCAAGGCCGATTGAAT 7078_Bot (Xba1) 5': CTAGATTCAATCGGCCTTGGTCTGACATTCCACCCGGCCAGGTCCAGGAGGGTGCAA
BGLF3.5 (p7079)	7079_Forward (Bgl2) 5': CGGGACTTTCCAAAATGTCG

Gene (plasmid #)	Primer/oligonucleotide
	7079_Reverse (Xba1) 5': AAAATCTAGATT <u>CA</u> ATGACAGTCACCTTCCCCAAA
BHLF1 (p7080)	The sequence was restored with a PCR product using p2089 DNA as template
BLLF2 (p7081)	7081_Top (Bsp1201) 5': GGCCCACCGGCTGCCCCAGCCCAAACCACCTTGCCAGAGCCGCCAGCGCCCCAGCCCTGACAGCCAGACC AGCCCTGCT <u>AA</u> AT 7081_Bot (Xba1) 5': CTAGATT <u>TT</u> AGCAGGGGCTGGTCTGGCTGTCAGGGCTGGGGCGCTGGCGGCTCTGGCAAGGTGGTTTGGG CTGGGGCAGCCGGTG
LF1 (p7082)	7082_Forward (EcoR5) 5': AGAGGAGATGTGGCACTCAG 7082_Reverse (Xba1) 5': TTTTCTAGATT <u>CA</u> GTGCTGCATGGGCTCTTC
LF2 (p7083)	7083_Forward (BspE1) 5': ACAACAACACCTACGAGGC 7083_Reverse (EcoR5) 5': TTTTGATATCG <u>ATT</u> ACAGAGTGCCCTCGGAGG
sLF3 (p7084)	7084_Forward (BstE2) 5': ATCGGGGTGACCATCAACTG 7084_Reverse (Xho1) 5': TTTTCTCGAGT <u>CA</u> GAAAGAGGAGGGGCAGCAG
A73 (p7085)	7085_Forward (Bsp1201, BsrG1) 5': TGAACAAGCCCCAACAGTG 7085_Reverse (Xba1) 5': TTTTCTAGATT <u>AC</u> AGCTCCTCAGGGCTGG
RPMS1 (p7086)	7086_insert (codon optimized): CCATGGCAGGAGCAAGAAGACGGGCAAGGTGTCCAGCAAGCGCAGGATGTGCGTATTCAGCTCGGCCACCC CCTCTCTACACGCGGTAGGCGAATTAGCGCAGGCTCAGGACAACCGCGGTGGTGGCCCTGGGGATCACCT CCTCCACCGGATACGCGTTATAGACGTCCCGGACCGGGACGTCGTGCACGTTCTTGTCTCCATGCTGGACCTA GGGGAAGACCCTCATAGTAGGACACGCGCCCGGAGAACCAGCCCCGGAGCAGGCGGGCGGGATGGAG AGGCGGAAGTTGTACAAGTCAAAGAT <u>GAG</u> CGGCCGC

To restore the original genes of the EBV gene expression plasmid contained in the library provided by Dr. Josef Mautner, the EBNA1 and 6xHis tags were removed by conventional molecular cloning. The table lists primers designed for restoring the open reading frame of individual genes. Underlined sequences mark the stop codon of the open reading frame. The sequence of BHLF1 (p7080) was replaced with the sequence derived from B95-8 strain EBV genome. The entire sequence of RPMS1 (p7086) was replaced with codon-optimized synthetic oligonucleotides purchased from Twist Bioscience (USA).

Table 7. Overview of synthetic oligonucleotides cloned into the basic lentiviral shRNA expression vector plasmid p6924 to be stably introduced into 2089 EBV producer cells

Target gene (plasmid #)	Oligonucleotide
GFP	shRNA 7272 top CTAGGTTTATGTTTGGATGAACTGACATACGCGTATCCGTC <u>TTGAAGTTCACCTTGATGCCGT</u> GTAGTGAAATAT ATATTAAAC <u>ACGGCATCAAGGTGAACTTCAT</u> TACGGTAACGCGG
	shRNA 7272 bot AATCCGCGTTACCGTA <u>ATGAAGTTCACCTTGATGCCGT</u> GTTTAATATATATTTCACTAC <u>ACGGCATCAAGGTGA ACTTCAA</u> GACGGATACGCGTATGTCAGTTCATCCAAACATAAAC
	shRNA 7273top CTAGGTTTATGTTTGGATGAACTGACATACGCGTATCCGTC <u>TTACTTGTACAGCTCGTCCATG</u> GTAGTGAAATAT ATATTAAAC <u>CATGGACGAGCTGTACAAGTAT</u> TACGGTAACGCGG
	shRNA 7273 bot AATCCGCGTTACCGTA <u>ATACTTGTACAGCTCGTCCATG</u> GTTTAATATATATTTCACTAC <u>CATGGACGAGCTGTAC AAGTAA</u> GACGGATACGCGTATGTCAGTTCATCCAAACATAAAC
	shRNA 7274 top CTAGGTTTATGTTTGGATGAACTGACATACGCGTATCCGTC <u>TGTAGTTGTACTCCAGCTTGTG</u> GTAGTGAAATAT ATATTAAAC <u>CACAAGCTGGAGTACA</u> ACTACTTACGGTAACGCGG
	shRNA 7274 bot AATCCGCGTTACCGTA <u>AGTAGTTGTACTCCAGCTTGTG</u> GTTTAATATATATTTCACTAC <u>CACAAGCTGGAGTAC AACTACA</u> GACGGATACGCGTATGTCAGTTCATCCAAACATAAAC
BALF4 (p6515)	shRNA 6954 for CTAGGTTTATGTTTGGATGAACTGACATACGCGTATCCGTC <u>TAATGTTGTCTTTAAACACCCAT</u> GTAGTGAAATATA TATTAAAC <u>ATGGTGTTTAAAGACA</u> ACATTTTACGGTAACGCGG
	shRNA 6954 rev AATCCGCGTTACCGTA <u>AAATGTTGTCTTTAAACACCCAT</u> GTTTAATATATATTTCACTAC <u>ATGGTGTTTAAAGACA ACATTA</u> GACGGATACGCGTATGTCAGTTCATCCAAACATAAAC
	shRNA 6955 for CTAGGTTTATGTTTGGATGAACTGACATACGCGTATCCGTC <u>TTTAGTGAGATGAAGGTCTGCA</u> GTAGTGAAATA TATTAAAC <u>TGCAGACCTTCATCTCA</u> TAATACGGTAACGCGG
	shRNA 6955 rev AATCCGCGTTACCGTA <u>ATTAGTGAGATGAAGGTCTGCA</u> GTTTAATATATATTTCACTAC <u>TGCAGACCTTCATCTC ACTAAA</u> GACGGATACGCGTATGTCAGTTCATCCAAACATAAAC
	shRNA 6956 for CTAGGTTTATGTTTGGATGAACTGACATACGCGTATCCGTC <u>TTATAAAATATGTAATGGCTTC</u> GTAGTGAAATATA TATTAAAC <u>GAAGCCATTACATATTTTATAT</u> TACGGTAACGCGG
	shRNA 6956 rev

Target gene (plasmid #)	Oligonucleotide
	AATTCCGCGTTACCGTAATATAAAATATGTAATGGCTTCGTTAATATATATTTCACTACGAAGCCATTACATATTTTATAAGACGGATACGCGTATGTCAGTTCATCCAAACATAAAC
BKRF4 (p6562)	shRNA 7296 top CTAGGTTTATGTTTGGATGAACTGACATACGCGTATCCGTCGTGTGTTTATTGTATGTATTGGGGTAGTGAAATATA TATTAAACCCCAATACATACAATAAACACTTACGGTAACGCGG
	shRNA 7296 bot AATTCCGCGTTACCGTAAGTGTGTTTATTGTATGTATTGGGGTTAATATATATTTCACTACCCCAATACATACAATAAACACAGACGGATACGCGTATGTCAGTTCATCCAAACATAAAC
	shRNA 7297 top CTAGGTTTATGTTTGGATGAACTGACATACGCGTATCCGTCCTTTATTGTATGTATTGGGACTTGTAGTGAAATATA TATTAAACAAGTCCCAATACATACAATAATTACGGTAACGCGG
	shRNA 7297 bot AATTCCGCGTTACCGTAATTATTGTATGTATTGGGACTTGTTTAATATATATTTCACTACAAGTCCCAATACATACAATAAAGACGGATACGCGTATGTCAGTTCATCCAAACATAAAC
	shRNA 7298 top CTAGGTTTATGTTTGGATGAACTGACATACGCGTATCCGTCATTGTATGTATTGGGACTTGAAGTAGTGAAATATA TATTAAACTCAAGTCCCAATACATACAATTACGGTAACGCGG
	shRNA 7298 bot AATTCCGCGTTACCGTAATTGTATGTATTGGGACTTGAAGTTAATATATATTTCACTACTCAAGTCCCAATACATACAATAAGACGGATACGCGTATGTCAGTTCATCCAAACATAAAC
BVLF1 (p6846)	shRNA 7299 top CTAGGTTTATGTTTGGATGAACTGACATACGCGTATCCGTCATAATAAACTCATCGCACGGGGGTAGTGAAATAT ATATTAAACCCCGTGCGATGAGTTTATTTTACGGTAACGCGG
	shRNA 7299 bot AATTCCGCGTTACCGTAATAATAAACTCATCGCACGGGGTTAATATATATTTCACTACCCCGTGCGATGAGTTTATTTAGACGGATACGCGTATGTCAGTTCATCCAAACATAAAC
	shRNA 7300 top CTAGGTTTATGTTTGGATGAACTGACATACGCGTATCCGTCCTCTTTAGCATCTTCAGGAGGAGTAGTGAAATAT ATATTAAACTCCTCCTGAAGATGCTAAAGATTACGGTAACGCGG
	shRNA 7300 bot AATTCCGCGTTACCGTAATCTTTAGCATCTTCAGGAGGAGTTAATATATATTTCACTACTCCTCCTGAAGATGCTAAAGAAAGACGGATACGCGTATGTCAGTTCATCCAAACATAAAC
	shRNA 7301 top CTAGGTTTATGTTTGGATGAACTGACATACGCGTATCCGTCATAAAGTTAACTTAGGGTCAAGTAGTGAAATAT ATATTAAACTGACCCTAAGTGTTAACTTTTTTACGGTAACGCGG
	shRNA 7301 bot

Target gene (plasmid #)	Oligonucleotide
	AATTCCGCGTTACCGTA <u>AAAAAGTTAACACTTAGGGTCA</u> GTTTAATATATATTTCACTAC <u>TGACCCTAAGTGTTA</u> <u>ACTTTTA</u> GACGGATACGCGTATGTCAGTTCATCCAAACATAAAC
BNLF2a (p6839)	shRNA 7302 top CTAGGTTTATGTTTGGATGAACTGACATACGCGTATCCGTC <u>TTTATTATTGCATCACAAGTC</u> GTAGTGAAATATA TATTAAAC <u>GACTTGTGATGCAATAAATAAT</u> TACGGTAACGCGG
	shRNA 7302 bot AATTCCGCGTTACCGTA <u>ATTATTATTGCATCACAAGTC</u> GTTTAATATATATTTCACTAC <u>GACTTGTGATGCAATAA</u> <u>ATAAA</u> GACGGATACGCGTATGTCAGTTCATCCAAACATAAAC
	shRNA 7303 top CTAGGTTTATGTTTGGATGAACTGACATACGCGTATCCGTC <u>TTATTATTGCATCACAAGTCA</u> GTAGTGAAATATA TATTAAAC <u>TGACTTGTGATGCAATAAATAI</u> TACGGTAACGCGG
	shRNA 7303 bot AATTCCGCGTTACCGTA <u>ATATTATTGCATCACAAGTCA</u> GTTTAATATATATTTCACTAC <u>TGACTTGTGATGCAATA</u> <u>AATAA</u> GACGGATACGCGTATGTCAGTTCATCCAAACATAAAC
	shRNA 7304 top CTAGGTTTATGTTTGGATGAACTGACATACGCGTATCCGTC <u>TTTATTGCATCACAAGTCACAT</u> GTAGTGAAATATA TATTAAAC <u>ATGTGACTTGTGATGCAATAAT</u> TACGGTAACGCGG
	shRNA 7304 bot AATTCCGCGTTACCGTA <u>ATTATTGCATCACAAGTCACAT</u> GTTTAATATATATTTCACTAC <u>ATGTGACTTGTGATGCA</u> <u>ATAAA</u> GACGGATACGCGTATGTCAGTTCATCCAAACATAAAC
BXRF1 (p6848)	shRNA 7305 top CTAGGTTTATGTTTGGATGAACTGACATACGCGTATCCGTC <u>TTGTAAATCTTATTGTCCGCGA</u> GTAGTGAAATATA TATTAAAC <u>TCGCGGACAATAAGATTACAT</u> TACGGTAACGCGG
	shRNA 7305 bot AATTCCGCGTTACCGTA <u>ATGTAAATCTTATTGTCCGCGA</u> GTTTAATATATATTTCACTAC <u>TCGCGGACAATAAGAT</u> <u>TTACAA</u> GACGGATACGCGTATGTCAGTTCATCCAAACATAAAC
	shRNA 7306 top CTAGGTTTATGTTTGGATGAACTGACATACGCGTATCCGTC <u>TTAAATTCTACAATATAACACC</u> GTAGTGAAATATA TATTAAAC <u>GGTGTTATATTGTAGAATTTAT</u> TACGGTAACGCGG
	shRNA 7306 bot AATTCCGCGTTACCGTA <u>ATAAATTCTACAATATAACACC</u> GTTTAATATATATTTCACTAC <u>GGTGTTATATTGTAGAAT</u> <u>TTAA</u> GACGGATACGCGTATGTCAGTTCATCCAAACATAAAC
	shRNA 7307 top CTAGGTTTATGTTTGGATGAACTGACATACGCGTATCCGTC <u>TTGATAATCTCAAAGAGGGTGT</u> GTAGTGAAATAT ATATTAAAC <u>ACACCCTCTTTGAGATTATCAT</u> TACGGTAACGCGG
	shRNA 7307 bot

Target gene (plasmid #)	Oligonucleotide
	AATTCCGCGTTACCGTAATGATAATCTCAAAGAGGGTGTGTTAATATATATTTCACTACACACCCTCTTTGAGAT TATCAA GACGGATACGCGTATGTCAGTTCATCCAAACATAAAC
BFLF2 (p6644)	shRNA 7308 top CTAGGTTTATGTTTGGATGAACTGACATACGCGTATCCGTC TTATTTTCCAAAATGAGCTGGG GTAGTGAAATAT ATATTAAACCCAGCTCATTGAAATATACGGTAACGCGG
	shRNA 7308 bot AATTCCGCGTTACCGTAATATTTTCCAAAATGAGCTGGG GTTAATATATATTTCACTACCCAGCTCATTGGA AATAAGACGGATACGCGTATGTCAGTTCATCCAAACATAAAC
	shRNA 7309 top CTAGGTTTATGTTTGGATGAACTGACATACGCGTATCCGTC TTTATTTTCCAAAATGAGCTGG GTAGTGAAATAT ATATTAAACCCAGCTCATTGAAATAATTACGGTAACGCGG
	shRNA 7309 bot AATTCCGCGTTACCGTAATATTTTCCAAAATGAGCTGG GTTAATATATATTTCACTACCCAGCTCATTGGA AATAAGACGGATACGCGTATGTCAGTTCATCCAAACATAAAC
	shRNA 7310 top CTAGGTTTATGTTTGGATGAACTGACATACGCGTATCCGTC TTTGATAGGACTGTACCAGGTC GTAGTGAAATAT ATATTAAACGACCTGGTACAGTCCTATCAATTACGGTAACGCGG
	shRNA 7310 bot AATTCCGCGTTACCGTAATTGATAGGACTGTACCAGGTC GTTAATATATATTTCACTACGACCTGGTACAGTCCT ATCAAGACGGATACGCGTATGTCAGTTCATCCAAACATAAAC
BMRF1 (p5106)	shRNA 7311 top (same as 6963 for) CTAGGTTTATGTTTGGATGAACTGACATACGCGTATCCGTC TAGGATTTAATGAATGTCACCA GTAGTGAAATAT ATATTAAACTGGTGACATTCATTAATCCTTACGGTAACGCGG
	shRNA 7311 bot (same as 6963 rev) AATTCCGCGTTACCGTA AAGGATTTAATGAATGTCACCA GTTAATATATATTTCACTACTGGTGACATTCATTA ATCCTAGACGGATACGCGTATGTCAGTTCATCCAAACATAAAC
	shRNA 7312 top CTAGGTTTATGTTTGGATGAACTGACATACGCGTATCCGTC TAAAATAACACTAAGATCCAAC GTAGTGAAATAT ATATTAAACGTTGGATCTTAGTGTTATTTTACGGTAACGCGG
	shRNA 7312 bot AATTCCGCGTTACCGTA AAAAATAACACTAAGATCCAAC GTTAATATATATTTCACTACGTTGGATCTTAGTGTT ATTTAGACGGATACGCGTATGTCAGTTCATCCAAACATAAAC
	shRNA 7313 top CTAGGTTTATGTTTGGATGAACTGACATACGCGTATCCGTC TTATCATCATATCCATAGTGA GTAGTGAAATATAT ATTAAACTCACTATGGAATATGATGATATACGGTAACGCGG
	shRNA 7313 bot

Target gene (plasmid #)	Oligonucleotide
	AATTCCGCGTTACCGTAATATCATCATATTCCATAGTGAAGTTTAATATATATTTCACTACTCACTATGGAATATGATGATAAGACGGGATACGCGTATGTCAGTTCATCCAAACATAAAC
BHLF1 (p7080)	shRNA 7314 top CTAGGTTTATGTTTGGATGAACTGACATACGCGTATCCGTCCTAAACAGTTTATTGATAGGTGGTAGTGAAATATATATTAACACCTATCAATAAACTGTTTATACGGTAACGCGG
	shRNA 7314 bot AATTCCGCGTTACCGTAATAAACAGTTTATTGATAGGTGGTTTAATATATATTTCACTACACCTATCAATAAACTGTTTAAAGACGGGATACGCGTATGTCAGTTCATCCAAACATAAAC
	shRNA 7315 top CTAGGTTTATGTTTGGATGAACTGACATACGCGTATCCGTCCTGACATGTAGGTGAGTAGTGTGTAGTGAAATATATATTAACACACTACTCACCTACATGTCATACGGTAACGCGG
	shRNA 7315 bot AATTCCGCGTTACCGTAATGACATGTAGGTGAGTAGTGTGTGTTAATATATATTTCACTACACACTACTCACCTACATGTCATAGACGGGATACGCGTATGTCAGTTCATCCAAACATAAAC
	shRNA 7316 top CTAGGTTTATGTTTGGATGAACTGACATACGCGTATCCGTCCTACTTTTAGAGTGTAGTGTACGTAGTGAAATATATATTAACGTACTACTACTCTAAAAGTATACGGTAACGCGG
	shRNA 7316 bot AATTCCGCGTTACCGTAATACTTTTAGAGTGTAGTGTACGTGTTAATATATATTTCACTACGTACTACTACTCTAAAAGTAAAGACGGGATACGCGTATGTCAGTTCATCCAAACATAAAC
BXLF1 (p6571)	shRNA 7320 top CTAGGTTTATGTTTGGATGAACTGACATACGCGTATCCGTCCTAAGTACACTAAAGATGCTGTGTAGTGAAATATATATTAACACAGCATCTTTAGTGTACTTATACGGTAACGCGG
	shRNA 7320 bot AATTCCGCGTTACCGTAATAAGTACACTAAAGATGCTGTGTGTTAATATATATTTCACTACACAGCATCTTTAGTGTACTTAAAGACGGGATACGCGTATGTCAGTTCATCCAAACATAAAC
	shRNA 7321 top CTAGGTTTATGTTTGGATGAACTGACATACGCGTATCCGTCCTGTAAATTAAGTGTAGCGGTGTAGTGAAATATATATTAACACCGCTACAAGTTAATTACATACGGTAACGCGG
	shRNA 7321 bot AATTCCGCGTTACCGTAATGTAAATTAAGTGTAGCGGTGTGTTAATATATATTTCACTACACCGCTACAAGTTAATTACATTTACAAAGACGGGATACGCGTATGTCAGTTCATCCAAACATAAAC
	shRNA 7322 top CTAGGTTTATGTTTGGATGAACTGACATACGCGTATCCGTCCTAACTACTAACTCGCGCCCAAGTAGTGAAATATATATTAACCTGGCGCGAGTTTAGTAAGTTTACGGTAACGCGG
	shRNA 7322 bot

Target gene (plasmid #)	Oligonucleotide
	AATTCCGCGTTACCGTA <u>AAACTTACTAAACTCGCGCCA</u> GTTTAATATATATTTCACTAC <u>TGGGCGCGAGTTTAG</u> <u>TAAGTTA</u> GACGGATACGCGTATGTCAGTTCATCCAAACATAAAC
BVRF2 (p6847)	shRNA 7264 top CTAGGTTTATGTTTGGATGAACTGACATACGCGTATCCGTC <u>TTTAAATACGACTCGGCTGGGA</u> GTAGTGAAATAT ATATTAAAC <u>TCCAGCCGAGTCGTATTTAAT</u> TACGGTAACGCGG
	shRNA 7264 bot AATTCCGCGTTACCGTA <u>ATTAAATACGACTCGGCTGGGA</u> GTTTAATATATATTTCACTAC <u>TCCAGCCGAGTCGT</u> <u>ATTTAA</u> GACGGATACGCGTATGTCAGTTCATCCAAACATAAAC
	shRNA 7265top CTAGGTTTATGTTTGGATGAACTGACATACGCGTATCCGTC <u>TAAGTGTTAACTTTTACCTGTG</u> GTAGTGAAATAT ATATTAAAC <u>CACAGGTAAAAGTTAACACTTI</u> TACGGTAACGCGG
	shRNA 7265 bot AATTCCGCGTTACCGTA <u>AAAGTGTTAACTTTTACCTGTG</u> GTTTAATATATATTTCACTAC <u>CACAGGTAAAAGTTAA</u> <u>CACTTA</u> GACGGATACGCGTATGTCAGTTCATCCAAACATAAAC
	shRNA 7266 top CTAGGTTTATGTTTGGATGAACTGACATACGCGTATCCGTC <u>TTTGATGAGGCTGAAATCCGTA</u> GTAGTGAAATAT ATATTAAAC <u>TACGGATTTTACGCTCATCAAT</u> TACGGTAACGCGG
	shRNA 7266 bot AATTCCGCGTTACCGTA <u>ATTGATGAGGCTGAAATCCGTA</u> GTTTAATATATATTTCACTAC <u>TACGGATTTTACGCTC</u> <u>ATCAAA</u> GACGGATACGCGTATGTCAGTTCATCCAAACATAAAC
BALF2 (p6927)	shRNA 7323 top CTAGGTTTATGTTTGGATGAACTGACATACGCGTATCCGTC <u>TTCTCAATCTCATATGTGGTCG</u> GTAGTGAAATATA TATTAAAC <u>CGACCACATATGAGATTGAGAT</u> TACGGTAACGCGG
	shRNA 7323 bot AATTCCGCGTTACCGTA <u>ATCTCAATCTCATATGTGGTCG</u> GTTTAATATATATTTCACTAC <u>CGACCACATATGAGATT</u> <u>GAGAA</u> GACGGATACGCGTATGTCAGTTCATCCAAACATAAAC
	shRNA 7324 top CTAGGTTTATGTTTGGATGAACTGACATACGCGTATCCGTC <u>TTCTTGATCTTGATGTTCTCTGG</u> GTAGTGAAATATA TATTAAAC <u>CCAGGAACATCAAGATCAAGAT</u> TACGGTAACGCGG
	shRNA 7324 bot AATTCCGCGTTACCGTA <u>ATCTTGATCTTGATGTTCTCTGG</u> GTTTAATATATATTTCACTAC <u>CCAGGAACATCAAGAT</u> <u>CAAGAA</u> GACGGATACGCGTATGTCAGTTCATCCAAACATAAAC
	shRNA 7325 top CTAGGTTTATGTTTGGATGAACTGACATACGCGTATCCGTC <u>TTCATAACTGGACCACTTCGG</u> GTAGTGAAATAT ATATTAAAC <u>CCGAAGTGGTCCAGTTTATGAT</u> TACGGTAACGCGG
	shRNA 7325 bot

Target gene (plasmid #)	Oligonucleotide
	AATTCCGCGTTACCGTAATCATAAACTGGACCACTTCGGGTTTAATATATATTTCACTACCCGAAGTGGTCCAGT TTATGAA GACGGATACGCGTATGTCAGTTCATCCAAACATAAAC
BPLF1 (p6567)	shRNA 6975 top CTAGGTTTATGTTTGGATGAACTGACATACGCGTATCCGTC TTAATAAACAATTACAGATACA GTAGTGAAATATA TATTAAACTGTATCTGTAATTGTTATTAT TACGGTAACGCGG
	shRNA 6975 bot AATTCCGCGTTACCGTAATAATAAACAATTACAGATACA GTTTAATATATATTTCACTACTGTATCTGTAATTGTTTA TTAA GACGGATACGCGTATGTCAGTTCATCCAAACATAAAC
	shRNA 6976 top CTAGGTTTATGTTTGGATGAACTGACATACGCGTATCCGTC TTTATTAATAAACAATTACAGA GTAGTGAAATATA TATTAAACTCTGTAATTGTTTATTAATAAT TACGGTAACGCGG
	shRNA 6976 bot AATTCCGCGTTACCGTAATTATTAATAAACAATTACAGA GTTTAATATATATTTCACTACTCTGTAATTGTTTATTAA TAAA GACGGATACGCGTATGTCAGTTCATCCAAACATAAAC
	shRNA 6977 top CTAGGTTTATGTTTGGATGAACTGACATACGCGTATCCGTC TTCATAGACAGAAATTGGGTG GTAGTGAAATA TATATTAAAC CACCCAATTTCTGTCTATTGATTACGGTAACGCGG
	shRNA 6977 bot AATTCCGCGTTACCGTAATCAATAGACAGAAATTGGGTG GTTTAATATATATTTCACTACCACCCAATTTCTGTCT ATTGAA GACGGATACGCGTATGTCAGTTCATCCAAACATAAAC
BBRF1 (p6593)	shRNA 6978 for CTAGGTTTATGTTTGGATGAACTGACATACGCGTATCCGTC TAAAGAATCTTGATAAAACAGG GTAGTGAAATAT ATATTAAAC CCTGTTTTATCAAGATTCTTTT TACGGTAACGCGG
	shRNA 6978 rev AATTCCGCGTTACCGTA AAAAGAATCTTGATAAAACAGG GTTTAATATATATTTCACTACCCTGTTTTATCAAGAT TCTTTA GACGGATACGCGTATGTCAGTTCATCCAAACATAAAC
	shRNA 6979 for CTAGGTTTATGTTTGGATGAACTGACATACGCGTATCCGTC TTGGCATTCTCAATCATCGAGA GTAGTGAAATAT ATATTAAAC TCTCGATGATTGAGAATGCCAT TACGGTAACGCGG
	shRNA 6979 rev AATTCCGCGTTACCGTA ATGGCATTCTCAATCATCGAGA GTTTAATATATATTTCACTACTCTCGATGATTGAGAA TGCCAA GACGGATACGCGTATGTCAGTTCATCCAAACATAAAC
	shRNA 6980 for CTAGGTTTATGTTTGGATGAACTGACATACGCGTATCCGTC TTCATGTTGAACATGACCTCAGG GTAGTGAAATAT ATATTAAAC CTGAGGTCATGTTCAACATGAT TACGGTAACGCGG
	shRNA 6980 rev

Target gene (plasmid #)	Oligonucleotide
	AATTCCGCGTTACCGTAATCATGTTGAACATGACCTCAGTTTAATATATATTTCACTACCTGAGGTCATGTTCAA CATGAAAGACGGATACGCGTATGTCAGTTCATCCAAACATAAAC
BGLF4 (p6561)	shRNA 6969 top (same as 6966 top) CTAGGTTTATGTTTGGATGAACTGACATACGCGTATCCGTC TTGATGAAGATGTTGACTGGGA GTAGTGAAATA TATATTAAACTCCAGTCAACATCTTCATCAT TACGGTAACGCGG
	shRNA 6969 bot (same as 6966 bot) AATTCCGCGTTACCGTAATGATGAAGATGTTGACTGGGAGTTTAATATATATTTCACTACTCCAGTCAACATCTT CATCAAAGACGGATACGCGTATGTCAGTTCATCCAAACATAAAC
	shRNA 6970 top CTAGGTTTATGTTTGGATGAACTGACATACGCGTATCCGTC TAAATCTGATAAATGACCTCTT GTAGTGAAATATA TATTAAAC AAGAGGTCATTATCAGATTTT TACGGTAACGCGG
	shRNA 6970 bot AATTCCGCGTTACCGTA AAAATCTGATAAATGACCTCTT GTTTAATATATATTTCACTAC AAGAGGTCATTATCA GATTTAGACGGATACGCGTATGTCAGTTCATCCAAACATAAAC
	shRNA 6971 top CTAGGTTTATGTTTGGATGAACTGACATACGCGTATCCGTC TGAAGTAATCAATGACAGTCAC GTAGTGAAATAT ATATTAAAC GTGACTGTCATTGATTACTTCT TACGGTAACGCGG
	shRNA 6971 bot AATTCCGCGTTACCGTA AGAAGTAATCAATGACAGTCAC GTTTAATATATATTTCACTAC GTGACTGTCATTGATT ACTTCA GACGGATACGCGTATGTCAGTTCATCCAAACATAAAC
BFRF1 (p6645)	shRNA 6992 top CTAGGTTTATGTTTGGATGAACTGACATACGCGTATCCGTC TTTATTAATAAAGTGCATACAC GTAGTGAAATATA TATTAAAC GTGTATGCACTTTATTAATAAT TACGGTAACGCGG
	shRNA 6992 bot AATTCCGCGTTACCGTA ATTATTAATAAAGTGCATACAC GTTTAATATATATTTCACTAC GTGTATGCACTTTATTAA TAAAGACGGATACGCGTATGTCAGTTCATCCAAACATAAAC
	shRNA 6993 top CTAGGTTTATGTTTGGATGAACTGACATACGCGTATCCGTC TTGGATATCACAAACACGGGCG GTAGTGAAATA TATATTAAAC CGCCCGTGTGTTGTGATATCCAT TACGGTAACGCGG
	shRNA 6993 bot AATTCCGCGTTACCGTA ATGGATATCACAAACACGGGCG GTTTAATATATATTTCACTAC CGCCCGTGTGTTGTGA TATCCAA GACGGATACGCGTATGTCAGTTCATCCAAACATAAAC
	shRNA 6994 top CTAGGTTTATGTTTGGATGAACTGACATACGCGTATCCGTC TTGAAATTTAGGAAGCAGGGGA GTAGTGAAATA TATATTAAACTCCCTGCTTCTAAATTTCAIT TACGGTAACGCGG
	shRNA 6994 bot

Target gene (plasmid #)	Oligonucleotide
	AATTCCGCGTTACCGTAATGAAATTTAGGAAGCAGGGGAGTTTAATATATATTTCACTACTCCCCTGCTTCCTAA ATTTCAA GACGGATACGCGTATGTCAGTTCATCCAAACATAAAC
BSLF1 (p6843)	shRNA 7001 top CTAGGTTTATGTTTGGATGAACTGACATACGCGTATCCGTC TGATTTGAAAAAATAGACTGGG GTAGTGAAATA TATATTAAACCCAGTCTATTTTTTCAAATCTTACGGTAACGCGG
	shRNA 7001 bot AATTCCGCGTTACCGTAAGATTTGAAAAAATAGACTGGG GTTTAATATATATTTCACTACCCAGTCTATTTTTTC AAATCA GACGGATACGCGTATGTCAGTTCATCCAAACATAAAC
	shRNA 7002 top CTAGGTTTATGTTTGGATGAACTGACATACGCGTATCCGTC TTCTGTGAATAGTACTGGGG GTAGTGAAATAT ATATTAAACCCCAGTGTACTATTACAGAT TACGGTAACGCGG
	shRNA 7002 bot AATTCCGCGTTACCGTAATCTGTGAATAGTACTGGGG GTTTAATATATATTTCACTACCCCAGTGTACTATTTC ACAGAA GACGGATACGCGTATGTCAGTTCATCCAAACATAAAC
	shRNA 7003 top CTAGGTTTATGTTTGGATGAACTGACATACGCGTATCCGTC TGTCATTACAAAGTAGTGCTG GTAGTGAAATAT ATATTAAACCAGGCACTACTTTGTAATGACT TACGGTAACGCGG
	shRNA 7003 bot AATTCCGCGTTACCGTAAGTCATTACAAAGTAGTGCTG GTTTAATATATATTTCACTACCAGGCACTACTTTGTA ATGACA GACGGATACGCGTATGTCAGTTCATCCAAACATAAAC
BTRF1 (p6845)	shRNA 7004 top CTAGGTTTATGTTTGGATGAACTGACATACGCGTATCCGTC TGACATTTCTCATAATGGTGCC GTAGTGAAATATA TATTAAACGGCACCATTATGAGAAATGTCT TACGGTAACGCGG
	shRNA 7004 bot AATTCCGCGTTACCGTAAGACATTTCTCATAATGGTGCC GTTTAATATATATTTCACTACGGCACCATTATGAGAA ATGTCA GACGGATACGCGTATGTCAGTTCATCCAAACATAAAC
	shRNA 7005 top CTAGGTTTATGTTTGGATGAACTGACATACGCGTATCCGTC TTTCTAGAAACTGTGCCATGG GTAGTGAAATAT ATATTAAACCCATGGCACAGTTTCTAGGAAT TACGGTAACGCGG
	shRNA 7005 bot AATTCCGCGTTACCGTAATTCTAGAAACTGTGCCATGG GTTTAATATATATTTCACTACCCATGGCACAGTTTCT AGGAAA GACGGATACGCGTATGTCAGTTCATCCAAACATAAAC
	shRNA 7006 top CTAGGTTTATGTTTGGATGAACTGACATACGCGTATCCGTC TGTGGAAGACAATCTGTCCCGA GTAGTGAAATA TATATTAAACTCGGGACAGATTGTCTTCCACT TACGGTAACGCGG
	shRNA 7006 bot

Target gene (plasmid #)	Oligonucleotide
	AATTCCGCGTTACCGTA <u>AGTGGGAAGACAATCTGTCCCGA</u> GTTTAATATATATTTCACTAC <u>TCGGGACAGATTGTC</u> <u>TTCCACA</u> GACGGATACGCGTATGTCAGTTCATCCAAACATAAAC
BMR2 (p6539)	shRNA 6963 for CTAGGTTTATGTTTGGATGAACTGACATACGCGTATCCGTC <u>TAGGATTTAATGAATGTCACCA</u> GTAGTGAAATAT ATATTAAACT <u>TGGTGACATTCATTAATCCTT</u> TACGGTAACGCGG
	shRNA 6963 rev AATTCCGCGTTACCGTA <u>AAGGATTTAATGAATGTCACCA</u> GTTTAATATATATTTCACTAC <u>TGGTGACATTCATTAA</u> <u>ATCCTA</u> GACGGATACGCGTATGTCAGTTCATCCAAACATAAAC
	shRNA 6964 for CTAGGTTTATGTTTGGATGAACTGACATACGCGTATCCGTC <u>TTCACAAACTTCTTAAGCTTGT</u> GTAGTGAAATAT ATATTAAAC <u>ACAAGCTTAAGAAGTTTGTGAT</u> TACGGTAACGCGG
	shRNA 6964 rev AATTCCGCGTTACCGTA <u>ATCACAAACTTCTTAAGCTTGT</u> GTTTAATATATATTTCACTAC <u>ACAAGCTTAAGAAGTT</u> <u>TGTGA</u> GACGGATACGCGTATGTCAGTTCATCCAAACATAAAC
	shRNA 6965 for CTAGGTTTATGTTTGGATGAACTGACATACGCGTATCCGTC <u>TCACAAACTTCTTAAGCTTGT</u> GTAGTGAAATAT ATATTAAACT <u>TACAAGCTTAAGAAGTTTGTGAT</u> TACGGTAACGCGG
	shRNA 6965 rev AATTCCGCGTTACCGTA <u>ACACAAACTTCTTAAGCTTGT</u> GTTTAATATATATTTCACTAC <u>TACAAGCTTAAGAAGT</u> <u>TTGTGA</u> GACGGATACGCGTATGTCAGTTCATCCAAACATAAAC
BBRF3 (p6534)	shRNA 6960 for CTAGGTTTATGTTTGGATGAACTGACATACGCGTATCCGTC <u>TAAAGTAAAAGCTGTTGCCAG</u> GTAGTGAAATA TATTAAAC <u>CTGGGCAACAGCTTTTACTTTT</u> TACGGTAACGCGG
	shRNA 6960 rev AATTCCGCGTTACCGTA <u>AAAAGTAAAAGCTGTTGCCAG</u> GTTTAATATATATTTCACTAC <u>CTGGGCAACAGCTTT</u> <u>TACTTTA</u> GACGGATACGCGTATGTCAGTTCATCCAAACATAAAC
	shRNA 6961 for CTAGGTTTATGTTTGGATGAACTGACATACGCGTATCCGTC <u>TAAATAATTTGCAAAGGGCGTG</u> GTAGTGAAATAT ATATTAAAC <u>CACGCCCTTTGCAAATTATTTT</u> TACGGTAACGCGG
	shRNA 6961 rev AATTCCGCGTTACCGTA <u>AAAATAATTTGCAAAGGGCGTG</u> GTTTAATATATATTTCACTAC <u>CACGCCCTTTGCAAA</u> <u>TTATTTA</u> GACGGATACGCGTATGTCAGTTCATCCAAACATAAAC
	shRNA 6962 for CTAGGTTTATGTTTGGATGAACTGACATACGCGTATCCGTC <u>TTTTAAATAATTTGCAAAGGGC</u> GTAGTGAAATAT ATATTAAAC <u>GCCCTTTGCAAATTATTTAAAT</u> TACGGTAACGCGG
	shRNA 6962 rev

Target gene (plasmid #)	Oligonucleotide
	AATTCCGCGTTACCGTA <u>ATTTAAATAATTTGCAAAGGGC</u> GTTTAATATATATTTCACTAC <u>GCCCTTTGCAAATTATT</u> <u>TAAAA</u> GACGGATACGCGTATGTCAGTTCATCCAAACATAAAC
BNRF1 (p6564)	shRNA 6972 top CTAGGTTTATGTTTGGATGAACTGACATACGCGTATCCGTC <u>TTCAGTGTATGCATAGTCTGGA</u> GTAGTGAAATAT ATATTAAACT <u>TCCAGACTATGCATACACTGAT</u> TACGGTAACGCGG
	shRNA 6972 bot AATTCCGCGTTACCGTA <u>ATCAGTGTATGCATAGTCTGGA</u> GTTTAATATATATTTCACTAC <u>TCCAGACTATGCATACA</u> <u>CTGAA</u> GACGGATACGCGTATGTCAGTTCATCCAAACATAAAC
	shRNA 6973 top CTAGGTTTATGTTTGGATGAACTGACATACGCGTATCCGTC <u>TTTGTAATACAGCACACAGGT</u> GTAGTGAAATAT ATATTAAAC <u>ACCTGTGTGCTGTATTACAAT</u> TACGGTAACGCGG
	shRNA 6973 bot AATTCCGCGTTACCGTA <u>ATTGTAATACAGCACACAGGT</u> GTTTAATATATATTTCACTAC <u>ACCTGTGTGCTGTATT</u> <u>TACAAA</u> GACGGATACGCGTATGTCAGTTCATCCAAACATAAAC
	shRNA 6974 top CTAGGTTTATGTTTGGATGAACTGACATACGCGTATCCGTC <u>TGCTATTGCATTAACGAAGGGA</u> GTAGTGAAATAT ATATTAAACT <u>TCCTTCGTTAATGCAATAGCT</u> TACGGTAACGCGG
	shRNA 6974 bot AATTCCGCGTTACCGTA <u>AGCTATTGCATTAACGAAGGGA</u> GTTTAATATATATTTCACTAC <u>TCCTTCGTTAATGCA</u> <u>ATAGCA</u> GACGGATACGCGTATGTCAGTTCATCCAAACATAAAC
BBLF1 (p6557)	shRNA 6966 for CTAGGTTTATGTTTGGATGAACTGACATACGCGTATCCGTC <u>TTGATGAAGATGTTGACTGGGA</u> GTAGTGAAATA TATTAAACT <u>TCCAGTCAACATCTTCATCAT</u> TACGGTAACGCGG
	shRNA 6966 rev AATTCCGCGTTACCGTA <u>ATGATGAAGATGTTGACTGGGA</u> GTTTAATATATATTTCACTAC <u>TCCAGTCAACATCTT</u> <u>CATCAA</u> GACGGATACGCGTATGTCAGTTCATCCAAACATAAAC
	shRNA 6967 for CTAGGTTTATGTTTGGATGAACTGACATACGCGTATCCGTC <u>TTCATCATTTTCAGAGTCTCTCA</u> GTAGTGAAATATA TATTAAACT <u>TGAGGACTCTGAAAATGATGAT</u> TACGGTAACGCGG
	shRNA 6967 rev AATTCCGCGTTACCGTA <u>ATCATCATTTTCAGAGTCTCTCA</u> GTTTAATATATATTTCACTAC <u>TGAGGACTCTGAAAAT</u> <u>GATGAA</u> GACGGATACGCGTATGTCAGTTCATCCAAACATAAAC
	shRNA 6968 for CTAGGTTTATGTTTGGATGAACTGACATACGCGTATCCGTC <u>TGTCAAAGTATTGTCTGCGTA</u> GTAGTGAAATAT ATATTAAACT <u>TACGCAGACAATACTTTGACT</u> TACGGTAACGCGG
	shRNA 6968 rev

Target gene (plasmid #)	Oligonucleotide
	AATTCCGCGTTACCGTA <u>AGTCAAAGTATTGTCTGCGTA</u> GTTTAATATATATTTCACTAC <u>TACGCAGACAATACTT</u> <u>TTGACA</u> GACGGATACGCGTATGTCAGTTCATCCAAACATAAAC
BRLF1 (p6841)	shRNA 6998 top CTAGGTTTATGTTTGGATGAACTGACATACGCGTATCCGTC <u>TTTACTATAACTACATTTCAGGG</u> GTAGTGAAATATA TATTAAAC <u>CCCTGAATGTAGTTATAGTAAT</u> TACGGTAACGCGG
	shRNA 6998 bot AATTCCGCGTTACCGTA <u>ATTACTATAACTACATTTCAGGG</u> GTTTAATATATATTTCACTAC <u>CCCTGAATGTAGTTATA</u> <u>GTAAG</u> GACGGATACGCGTATGTCAGTTCATCCAAACATAAAC
	shRNA 6999 top CTAGGTTTATGTTTGGATGAACTGACATACGCGTATCCGTC <u>TCATCATTAGAAATGTATCCA</u> GTAGTGAAATATA TATTAAAC <u>TGGATACATTTCTAAATGATGT</u> TACGGTAACGCGG
	shRNA 6999 bot AATTCCGCGTTACCGTA <u>ACATCATTAGAAATGTATCCA</u> GTTTAATATATATTTCACTAC <u>TGGATACATTTCTAAAT</u> <u>GATGA</u> GACGGATACGCGTATGTCAGTTCATCCAAACATAAAC
	shRNA 7000 top CTAGGTTTATGTTTGGATGAACTGACATACGCGTATCCGTC <u>TACTATAACTACATTTCAGGGAT</u> GTAGTGAAATATA TATTAAAC <u>ATCCCTGAATGTAGTTATAGTT</u> TACGGTAACGCGG
	shRNA 7000 bot AATTCCGCGTTACCGTA <u>AACTATAACTACATTTCAGGGAT</u> GTTTAATATATATTTCACTAC <u>ATCCCTGAATGTAGTTA</u> <u>TAGTA</u> GACGGATACGCGTATGTCAGTTCATCCAAACATAAAC
BALF1 (p6632)	shRNA 6986 top CTAGGTTTATGTTTGGATGAACTGACATACGCGTATCCGTC <u>TTCATTTACAAAGATTTTCAGGA</u> GTAGTGAAATAT ATATTAAAC <u>TCTGAAATCTTTGTAAATGAT</u> TACGGTAACGCGG
	shRNA 6986 bot AATTCCGCGTTACCGTA <u>ATCATTACAAAGATTTTCAGGA</u> GTTTAATATATATTTCACTAC <u>TCTGAAATCTTTGTAA</u> <u>ATGAA</u> GACGGATACGCGTATGTCAGTTCATCCAAACATAAAC
	shRNA 6987 top CTAGGTTTATGTTTGGATGAACTGACATACGCGTATCCGTC <u>TATTCATTACAAAGATTTTCAG</u> GTAGTGAAATATA TATTAAAC <u>CTGAAATCTTTGTAAATGAATT</u> TACGGTAACGCGG
	shRNA 6987 bot AATTCCGCGTTACCGTA <u>AATTCATTACAAAGATTTTCAG</u> GTTTAATATATATTTCACTAC <u>CTGAAATCTTTGTAAAT</u> <u>GAATA</u> GACGGATACGCGTATGTCAGTTCATCCAAACATAAAC
	shRNA 6988 top CTAGGTTTATGTTTGGATGAACTGACATACGCGTATCCGTC <u>TTTACAAAGATTTTCAGGAAGTC</u> GTAGTGAAATAT ATATTAAAC <u>GACTTCTGAAATCTTTGTAAT</u> TACGGTAACGCGG
	shRNA 6988 bot

Target gene (plasmid #)	Oligonucleotide
	AATTCCGCGTTACCGTAATTACAAAGATTTTCAGGAAGTCGTTTAATATATATTTCACTACGACTTCCTGAAATCTT TGTAAGACGGATACGCGTATGTCAGTTCATCCAAACATAAAC
BBRF2 (p6639)	shRNA 6989 top (same as 6978 top) CTAGGTTTATGTTTGGATGAACTGACATACGCGTATCCGTC TAAAGAATCTTGATAAAACAGG GTAGTGAAATAT ATATTA AAC CCTGTTTTATCAAGATTCTTTT TACGGTAACGCGG
	shRNA 6989 bot (same as 6978 bot) AATTCCGCGTTACCGTA AAAAGAATCTTGATAAAACAGG GTTTAATATATATTTCACTAC CCTGTTTTATCAAGAT TCTTTA GACGGATACGCGTATGTCAGTTCATCCAAACATAAAC
	shRNA 6990 top (same as 6979 top) CTAGGTTTATGTTTGGATGAACTGACATACGCGTATCCGTC TTGGCATTCTCAATCATCGAGA GTAGTGAAATAT ATATTA AAC TCTCGATGATTGAGAATGCCATTACGGTAACGCGG
	shRNA 6990 bot (same as 6979 bot) AATTCCGCGTTACCGTA ATGGCATTCTCAATCATCGAGA GTTTAATATATATTTCACTAC TCTCGATGATTGAGAA TGCCAA GACGGATACGCGTATGTCAGTTCATCCAAACATAAAC
	shRNA 6991 top CTAGGTTTATGTTTGGATGAACTGACATACGCGTATCCGTC TTGGTCAATAAAGAATCTTGAT GTAGTGAAATAT ATATTA AAC ATCAAGATTCTTTATTGACCAI TACGGTAACGCGG
	shRNA 6991 bot AATTCCGCGTTACCGTA ATGGTCAATAAAGAATCTTGAT GTTTAATATATATTTCACTAC ATCAAGATTCTTTATTG ACCAA GACGGATACGCGTATGTCAGTTCATCCAAACATAAAC
BMLF1 (p6838)	shRNA 6995 top CTAGGTTTATGTTTGGATGAACTGACATACGCGTATCCGTC TTGTAATTCTTGATGTAGTGCC GTAGTGAAATAT ATATTA AAC GCCACTACATCAAGAATTACAT TACGGTAACGCGG
	shRNA 6995 bot AATTCCGCGTTACCGTA ATGTAATTCTTGATGTAGTGCC GTTTAATATATATTTCACTAC GCCACTACATCAAGAA TTACAA GACGGATACGCGTATGTCAGTTCATCCAAACATAAAC
	shRNA 6996 top CTAGGTTTATGTTTGGATGAACTGACATACGCGTATCCGTC TTTATTGATTTAATCCAGGAAC GTAGTGAAATATA TATTA AAC GTTCCTGGATTAAATCAATAAT TACGGTAACGCGG
	shRNA 6996 bot AATTCCGCGTTACCGTA ATTATTGATTTAATCCAGGAAC GTTTAATATATATTTCACTAC GTTCCTGGATTAAATCA ATAAA GACGGATACGCGTATGTCAGTTCATCCAAACATAAAC
	shRNA 6997 top CTAGGTTTATGTTTGGATGAACTGACATACGCGTATCCGTC TTCACAAAGTTGTAGTCTCGCG GTAGTGAAATAT ATATTA AAC CGCGAGACTACAAC TTTGTGAT TACGGTAACGCGG
	shRNA 6997 bot

Target gene (plasmid #)	Oligonucleotide
	AATCCGCGTTACCGTAATCACAAAGTTGTAGTCTCGCGTTTAATATATATTTCACTACCGCGAGACTACAACCTT TGTGAAGACGGATACGCGTATGTCAGTTCATCCAAACATAAAC
	Antisense/target: red-colored (top, for) and brown-colored (bot, rev) Sense/passenger: green-colored (top, for) and blue-colored (bot, rev)

Each shRNA sequence consists of a pair of oligonucleotides, encoding the forward and reverse strand. The antisense shRNA sequences are colored in red (forward) and brown (reverse) and the sense sequences are colored in green (forward) and blue (reverse). Additionally, the last nucleotide of oligonucleotide sequences in sense orientation was replaced with thymine (T) to increase the knockdown efficiency of shRNAs (Watanabe et al., 2016).

Table 8. Synthetic pairs of oligonucleotides used for the construction of luciferase reporter plasmids

Target gene (plasmid #)	Oligonucleotide
GFP (p7275)	7275 for (shGFP) TCGAG <u>ACGGCATCAAGGTGAACTTCAA</u> AATT <u>CATGGACGAGCTGTACAAGTAA</u> AATT <u>CACAAGCTGGAGTCAACTACA</u> GC
	7275 rev (shGFP) GGCCGC <u>TGTAGTTGTACTCCAGCTTGTG</u> AATTT <u>TACTTGTACAGCTCGTCCATG</u> AATTT <u>TGAAGTTCACCTTGATGCCGTC</u>
BALF4 (p7204)	7204 for (sh6515-2, BALF4) TCGAG <u>ATGGTGTTTAAAGACAACATTA</u> AATTT <u>GCAGACCTTCATCTCACTAAA</u> AATT <u>GAAGCCATTACATATTTATAA</u> GC
	7204 rev (sh6515-2, BALF4) GGCCGC <u>TTATAAAATATGTAATGGCTTCA</u> AATTT <u>TTAGTGAGATGAAGGTCTGCA</u> AATTT <u>TAATGTTGTCTTTAAACACCATC</u>
BKRF4 (p7329)	7329 top (sh6562, BKRF4) TCGAG <u>CCCAATACATACAATAAACACA</u> AATT <u>AAGTCCCAATACATACAATAAAA</u> AATTT <u>TCAAGTCCCAATACATACAATA</u> GC
	7329 bot (sh6562, BKRF4) GGCCGC <u>TATTGTATGTATTGGGACTTGA</u> AATTT <u>TTATTGTATGTATTGGGACTT</u> AATTT <u>TGTGTTTATTGTATGTATTGGGC</u>
BVLF1 (p7330)	7330 top (sh6846, BVLF1) TCGAG <u>CCCCGTGCGATGAGTTTATTTA</u> AATTT <u>TCCTCCTGAAGATGCTAAAGAA</u> AATTT <u>TGACCCTAAGTGTTAACTTTT</u> AGC
	7330 bot (sh6846, BVLF1) GGCCGC <u>AAAAAGTTAACTTAGGGTCA</u> AATTT <u>TTCTTTAGCATCTTCAGGAGGA</u> AATTT <u>TAAATAAACTCATCGCACGGGGC</u>
BNLF2a (p7331)	7331 top (sh6839, BNLF2a) TCGAG <u>GACTTGTGATGCAATAAATAAAA</u> AATTT <u>TGACTTGTGATGCAATAAATAA</u> AATTT <u>ATGTGACTTGTGATGCAATAA</u> GC
	7331 bot (sh6839, BNLF2a) GGCCGC <u>TTTATTGCATCACAAGTCACAT</u> AATTT <u>TTATTATTGCATCACAAGTCA</u> AATTT <u>TTTATTATTGCATCACAAAGTCC</u>
BXRF1 (p7332)	7332 top (sh6848, BXRF1) TCGAG <u>TCGCGGACAATAAGATTTACAA</u> AATTT <u>GGTGTTATATTGTAGAATTTAA</u> AATTT <u>ACACCCTCTTTGAGATTATCAA</u> GC
	7332 bot (sh6848, BXRF1) GGCCGC <u>TTGATAATCTCAAAGAGGGTGT</u> AATTT <u>TTAAATTCTACAATATAACACCA</u> AATTT <u>TGTAAATCTTATTGTC</u>

Target gene (plasmid #)	Oligonucleotide
	<u>CGCGAC</u>
BFLF2 (p7333)	7333 top (sh6644, BFLF2) TCGAG <u>CCCAGCTCATT</u> <u>TTGGAAAATAA</u> AATT <u>CCAGCTCATT</u> <u>TTGGAAAATAA</u> AATT <u>GACCTGGTACAGTCT</u> <u>ATCAAAGC</u>
	7333 bot (sh6644, BFLF2) GGCCGC <u>TTTGATAGGACTGTACCAGGTC</u> AATT <u>TTTATTTCCAAAATGAGCTGGA</u> AATT <u>TTATTTCCAAAATG</u> <u>AGCTGGG</u> C
BMRF1 (p7334)	7334 top (sh5106, BMRF1) TCGAG <u>TGGTGACATT</u> <u>CATTAATCCTA</u> AATT <u>GTTGGATCTTAGTGTTATTTA</u> AATT <u>TCACTATGGAATATGATG</u> <u>ATAAGC</u>
	7334 bot (sh5106, BMRF1) GGCCGC <u>TTATCATCATATTCCATAGTGAA</u> AATT <u>TAAAATAACACTAAGATCCAACA</u> AATT <u>TAGGATTTAATGAATGT</u> <u>CACCAC</u>
BHLF1 (p7335)	7335 top (sh7080, BHLF1) TCGAG <u>CACCTATCAATAAACTGTTAA</u> AATT <u>ACACTACTCACCTACATGTCAA</u> AATT <u>GTACACTACACTCTAAA</u> <u>AGTAA</u> GC
	7335 bot (sh7080, BHLF1) GGCCGC <u>TTACTTTTAGAGTGTAGTGTACA</u> AATT <u>TTGACATGTAGGTGAGTAGTGTAA</u> AATT <u>TTAAACAGTTTATTG</u> <u>ATAGGTGC</u>
BXLF1 (p7337)	7337 top (sh6571, BXLF1) TCGAG <u>ACAGCATCTTTAGTGTACTTAA</u> AATT <u>ACCGCTACAAGTTAATTTACAA</u> AATT <u>TGGGCGCGAGTTTAGT</u> <u>AAGTTA</u> GC
	7337 bot (sh6571, BXLF1) GGCCGC <u>TAACTTACTAAACTCGCGCCCA</u> AATT <u>TTGTAAATTA</u> ACTTGTAGCGGTAAATT <u>TTAAGTACACTAAAG</u> <u>ATGCTGT</u> C
BVRF2 (p7267)	7267 for (sh6847, BVRF2) TCGAG <u>TCCCAGCCGAGTCGTATTTAAA</u> AATT <u>CACAGGTA</u> AAAGTTAACTTAAATT <u>TACGGATTT</u> CAGCCTC <u>ATCAAAGC</u>
	7267 rev (sh6847, BVRF2) GGCCGC <u>TTTGATGAGGCTGAAATCCGTA</u> AATT <u>TAAGTGTTAACTTTTACCTGTGA</u> AATT <u>TTTAAATACGACTCG</u> <u>GCTGGGAC</u>
BALF2 (p7338)	7338 top (sh6927, BALF2) TCGAG <u>CGACCACATATGAGATTGAGAA</u> AATT <u>CCAGGAACATCAAGATCAAGAA</u> AATT <u>CCGAAGTGGTCCAG</u> <u>TTTATGAA</u> GC
	7338 bot (sh6927, BALF2) GGCCGC <u>TCATAAACTGGACCACTTCGG</u> AATT <u>TTCTTGATCTTGATGTTCTGGA</u> AATT <u>TTCTCAATCTCATATG</u>

Target gene (plasmid #)	Oligonucleotide
	<u>TGGTCGC</u>
BPLF1 (p7211)	7211 for (sh6567-2, BPLF1) TCGAG <u>TGTATCTGTAATTGTTTATTAA</u> AATT <u>TCTGTAATTGTTTATTAATAAA</u> AATT <u>CACCCAATTTCTGTCTATT</u> <u>GAA</u> GC
	7211 rev (sh6567-2, BPLF1) GGCCGC <u>TTCAATAGACAGAAATTGGGTGA</u> AATT <u>TTTATTAATAAACAATTACAGAA</u> AATT <u>TTAATAAACAATTACA</u> <u>GATACAC</u>
BBRF1 (p7212)	7212 for (sh6593-4, BRRF1) TCGAG <u>CCTGTTTTATCAAGATTCTTTA</u> AATT <u>TCTCGATGATTGAGAATGCCAA</u> AATT <u>CTGAGGTCATGTTCAAC</u> <u>ATGAA</u> GC
	7212 rev (sh6593-4, BRRF1) GGCCGC <u>TTCATGTTGAACATGACCTCAGA</u> AATT <u>TTGGCATTCTCAATCATCGAGA</u> AATT <u>TAAAGAATCTTGATA</u> <u>AAACAGG</u> C
BGLF4 (p7209)	7209 for (sh6561-2, BGLF4) TCGAG <u>TCCAGTCAACATCTTCATCAA</u> AATT <u>AAGAGGTCATTTATCAGATTTA</u> AATT <u>GTGACTGTCATTGATTA</u> <u>CTTCA</u> GC
	7209 rev (sh6561-2, BGLF4) GGCCGC <u>TGAAGTAATCAATGACAGTCACA</u> AATT <u>TAAATCTGATAAATGACCTCTT</u> AATT <u>TTGATGAAGATGTTG</u> <u>ACTGGG</u> AC
BFRF1 (p7215)	7215 for (sh6645-2, BFRF1) TCGAG <u>GTGTATGCACTTTATTAATAAAA</u> AATT <u>CGCCCGTGTTTGTGATATCCAA</u> AATT <u>TCCCCTGCTCCTAAATT</u> <u>TCAA</u> GC
	7215 rev (sh6645-2, BFRF1) GGCCGC <u>TTGAAATTTAGGAAGCAGGGGA</u> AATT <u>TTGGATATCACAAACACGGGCGA</u> AATT <u>TTTATTAATAAAGT</u> <u>GCATACAC</u> C
BSLF1 (p7218)	7218 for (sh6843-2, BSLF1) TCGAG <u>CCCAGTCTATTTTTCAAATCA</u> AATT <u>CCCCAGTGTACTATTCACAGAA</u> AATT <u>CAGGCACTACTTTGTAA</u> <u>TGACA</u> GC
	7218 rev (sh6843-2, BSLF1) GGCCGC <u>TGTCATTACAAAGTAGTGCTGA</u> AATT <u>TTCTGTGAATAGTACACTGGGGA</u> AATT <u>TGATTTGAAAAATA</u> <u>GA</u> CTGGGC
BTRF1 (p7219)	7219 for (sh6845-2, BTRF1) TCGAG <u>GGCACCATTATGAGAAATGTCA</u> AATT <u>CCATGGCACAGTTTCTAGGAAA</u> AATT <u>TCGGGACAGATTGTC</u> <u>TTCCACA</u> GC
	7219 rev (sh6845-2, BTRF1) GGCCGC <u>TGTGGAAGACAATCTGTCCCGA</u> AATT <u>TTTCTAGAACTGTGCCATGGA</u> AATT <u>TGACATTTCTCATAA</u>

Target gene (plasmid #)	Oligonucleotide
	<u>TGGTGCCC</u>
BMR2 (p7207)	7207 for (sh6539-2, BMR2) TCGAG <u>TGGTGACATTCATTAATCCTA</u> AATT <u>ACAAGCTTAAGAAGTTTGTGAA</u> AATT <u>TACAAGCTTAAGAAGT</u> <u>TTGTGAGC</u>
	7207 rev (sh6539-2, BMR2) GGCCGC <u>TCACAAACTTCTTAAGCTTGTA</u> AATT <u>TCACAAACTTCTTAAGCTTGT</u> AATT <u>TAGGATTTAATGAATG</u> <u>TCACCAC</u>
BBRF3 (p7206)	7206 for (sh6534-4, BRRF3) TCGAG <u>CTGGGCAACAGCTTTTACTTTA</u> AATT <u>CACGCCCTTTGCAAATTATTTA</u> AATT <u>GCCCTTTGCAAATTAT</u> <u>TAAAAGC</u>
	7206 rev (sh6534-4, BRRF3) GGCCGC <u>TTTTAAATAATTTGCAAAGGGCA</u> AATT <u>TAAATAATTTGCAAAGGGCGTG</u> AATT <u>TAAAGTAAAAGCTG</u> <u>TTGCCCAGC</u>
BNRF1 (p7210)	7210 for (sh6564-2, BNRF1) TCGAG <u>TCCAGACTATGCATACACTGAA</u> AATT <u>ACCTGTGTGCTGTATTTACAAA</u> AATT <u>TCCCTTCGTTAATGCAA</u> <u>TAGCAGC</u>
	7210 rev (sh6564-2, BNRF1) GGCCGC <u>TGCTATTGCATTAACGAAGGGAA</u> AATT <u>TTTGTAATACAGCACACAGGT</u> AATT <u>TTCAGTGTATGCATA</u> <u>GTCTGGAC</u>
BBLF1 (p7208)	7208 for (sh6557-2, BBLF1) TCGAG <u>TCCAGTCAACATCTTCATCAA</u> AATT <u>TGAGGACTCTGAAAATGATGAA</u> AATT <u>TACGCAGACAATACTT</u> <u>TTGACAGC</u>
	7208 rev (sh6557-2, BBLF1) GGCCGC <u>TGTCAAAGTATTGTCTGCGTA</u> AATT <u>TTTCATCATTTCAGAGTCTCAA</u> AATT <u>TTGATGAAGATGTTG</u> <u>ACTGGGAC</u>
BRLF1 (p7217)	7217 for (sh6841-2, BRLF1) TCGAG <u>CCCTGAATGTAGTTATAGTAAA</u> AATT <u>TGGATACATTTCTAAATGATGA</u> AATT <u>ATCCCTGAATGTAGTTAT</u> <u>AGTAGC</u>
	7217 rev (sh6841-2, BRLF1) GGCCGC <u>TACTATAACTACATTCAGGGATA</u> AATT <u>TCATCATTTAGAAATGTATCCA</u> AATT <u>TTTACTATAACTACATTC</u> <u>AGGGC</u>
BALF1 (p7213)	7213 for (sh6632-2, BALF1) TCGAG <u>TCCTGAAATCTTTGTAAATGAA</u> AATT <u>CTGAAATCTTTGTAAATGAATA</u> AATT <u>GACTTCCTGAAATCTTT</u> <u>GTAAAAGC</u>
	7213 rev (sh6632-2, BALF1) GGCCGC <u>TTTACAAAGATTTTCAGGAAGTCA</u> AATT <u>TATTCATTTACAAAGATTTTCAGA</u> AATT <u>TTTACATTTACAAAGATT</u>

Target gene (plasmid #)	Oligonucleotide
	<u>TCAGGAC</u>
BBRF2 (p7214)	7214 for (sh6639-2, BBRF2) TCGAG <u>CCTGTTTTATCAAGATTCTTTA</u> AATT <u>TCTCGATGATTGAGAATGCCAA</u> AATT <u>ATCAAGATTCTTTATTGA</u> <u>CCAAGC</u>
	7214 rev (sh6639-2, BBRF2) GGCCGC <u>TTGGTCAATAAAGAATCTTGATA</u> AATT <u>TTGGCATTCTCAATCATCGAGA</u> AATT <u>TAAAGAATCTTGATAA</u> <u>AACAGGC</u>
BMLF1 (p7216)	7216 for (sh6838-2, BMLF1) TCGAG <u>GCCACTACATCAAGAATTACAA</u> AATT <u>GTTCTGGATTAAATCAATAAA</u> AATT <u>CGCGAGACTACAACCTT</u> <u>TGTGAA</u> GC
	7216 rev (sh6838-2, BMLF1) GGCCGC <u>TCACAAAGTTGTAGTCTCGCG</u> AATT <u>TTTATTGATTTAATCCAGGAAC</u> AATT <u>TTGTAATTCTTGATGT</u> <u>AGTGGCC</u>
	Sense/target: three individual red-colored sequences Antisense: three individual brown-colored sequences

Each luciferase reporter contains a pair (sense and antisense orientation) of oligonucleotides, which encompass three corresponding perfect-match target sequences corresponding to each of the three shRNAs per viral transcript as listed in **Table 7**. The shRNA target sequences are colored in red (forward, sense orientation) or brown (reverse orientation).

Curriculum Vitae

Yen-Fu Adam Chen

Nationality: Taiwanese

E-Mail: yen-fu.chen@helmholtz-muenchen.de

Current Position

PhD student

Wolfgang Hammerschmidt's research group,

Helmholtz Zentrum München –

German Research Center for Environmental Health

AGV Research Unit Gene Vectors

Feodor-Lynen-Str. 21

81377 München

Education

2016- Ph.D study, Faculty of Biology, Ludwig-Maximilians-Universität
München, Munich, Germany

2010-2012 M.Sc., Department of Biotechnology and Laboratory Science in
Medicine, National Yang-Ming University, Taipei, Taiwan

2006-2010 B.Sc., Department of Biological Science and Technology,
China Medical University, Taichung, Taiwan

Experiences

2014-2016 Research Assistant, Center for Infectious Disease and Cancer Research
(CICAR), Kaohsiung Medical University (KMU), Taiwan

2012-2013 Military Police, Compulsory Military Service, Taiwan

Master thesis

2012 Metformin activates p53 via ribosomal stress in A549 lung cancer cells

Acknowledgements

I would like to express my thanks to all people who ever supported me during my studies in Munich while working on my PhD project, especially ...

Wolfgang: Thank you for giving me this opportunity of starting and finishing my PhD study. It is my honor to join your research group and learn from you. Thank you for your patience leading me into the EBV field. You are always open to questions and you give me priceless advices, no matter whether the problem is of scientific or practical or general nature. Although research work can be sometimes industrious, your encouragements are always helpful and motivating.

Bettina: Thank you for your valuable suggestions for my thesis, TAC meetings and arranging my thesis committee. You always pointed out critical questions but also helped me solve the problems.

Barbara: Thank you for being a member of my TA committee. Your expertise helped me deal with difficult questions and provided new insights to me as well.

Josef: Thank you for providing the EBV gene expression plasmid library. It was the start of my thesis. I always asked you for solving technical and addressing experimental problems. Your knowledge about EBV answered my questions every time. Thank you for your patience regarding my relentless questions.

I would like to thank my lab members in Hammerschmidt's group. **Dagmar** – Your iconic laughter provides a very good atmosphere in the lab! I would also like to thank you for your expertise. You really helped me a lot to master flow cytometry.

Christine – You are always nice and help me with annoying obstacles in my daily life and, also, you encouraged me to improve my German. **Takanobu** – You helped me know the environment, inside and outside the labs, when I began my study. Your suggestions were always direct and useful to me. Even when you left the group, you are still supportive. **Manuel** – You are surely one of the nicest people who I have ever met. It is great to work and complete the project together with you. I constantly learn from you. I would also thank you for your meal recipes. Congratulations to your new position in Milano, I wish you all the best. **Paulina** – Thank you for your advice about experiments. Occasional chats with you are relaxing. Both in the laboratory and geographically, you are a very good neighbor. **Alex** – Your

accomplishment of bioinformatics impressed me so much. It is nice working with you and chatting about FC Bayern. **Mickaël** – It was a great experience working with you and I wish I can be as confident as you are. **Ezgi** – Thank you for your suggestions every time when I finished my presentations, which let me understand my strengths and weaknesses. Besides, I am thankful for you snacks, refueling me all the time. **Bianca** – Thank you for your knowledge helping me clarify and solve the statistical problems. I wish I could be as talkative as you are. **Roswitha** – Thank you for taking care of everything beyond my research life. You are so essential and reliable such that one can concentrate on research work.

I would like to thank my family. Thanks to mom, you always support me whatever I do. Thanks to my brothers for taking care of the family, when I am away from home. Finally, this thesis is dedicated to my beloved father. I wish you could see me finish my PhD. Although you already left us, your legacy and contributes are still with us.

我想要感謝一路上陪伴與支持我的家人朋友，沒有你們的幫忙我無法獨自一人完成博士學位。謝謝我的家人，感謝老媽，謝謝妳一直支持我無論我做了什麼決定。謝謝哥哥們，感謝你們照顧老媽和這個家，當我不在台灣的時候。最後，這篇論文要獻給我摯愛的老爸。我多希望你可以看到我完成博士學位。我可以想像你會有多開心。雖然你已經不在，但是我們會把你一直記在心裡。

Epilogue

Here, I would like to take the opportunity to remind myself about my life in Germany.

If I have the chance to read these lines in the future, currently (Feb, 2021, during coronavirus time), I am writing my PhD thesis. Looking back to the past few years, I stepped out of my comfort zone in Taiwan and moved to Munich, a completely different environment. It was so challenging that I lived on my own in the beginning. Perseverance, resilience and endurance, they are not synonyms of cleverness, but they are my style and strength conquering obstacles. It includes a bit of stubbornness as well. Time flies, I may think I did not accomplish or learn anything. However, I actually have learned a lot and gained much experience when I recapitulate the four years that have gone by - they made me much more mature. Unfortunately, in my age, some relatives and friends have left me already, which is very sad but inevitable. But, I have also found good friends from all of the world at the same time. The culture shock might have scared me, but it also has improved my personality. Don't be shy, but be open-minded! I will not know how my future will look like, but I wish I can value what I have achieved and I wish that I will always look at the bright side of life.

後記：僅此回顧我過去這幾年在德國的生活。假如你有機會再看這篇論文，你現在（2021的2月）正在寫著博士論文。回顧過去幾年，你踏出舒適圈來到慕尼黑，一個全新的環境，全新的挑戰。堅持與毅力不等同於聰明，但是這是你的長處與面對問題一貫的態度。儘管有時候顯得固執。時光飛逝，你總以為你沒學到什麼，其實，當你回顧以前，你已經不知不覺學到很多也變得更加成熟。你這個年紀開始會失去一些親人朋友，但同樣地你也會交到更多的朋友。文化衝擊在所難免，你也可以從中學習。不要畏縮，練習敞開心胸。雖然現在的我不知道未來會如何，但是我希望你能珍惜你擁有的並且保持樂觀。